Elsevier Editorial System(tm) for Journal of Chemical Neuroanatomy
Manuscript Draft

Manuscript Number: CHENEU-D-11-00020R1

Title: A half century of experimental neuroanatomical tracing

Article Type: Review Article

Keywords: Tract-tracing; Fluoro-Gold; Cholera toxin; Biotinylated dextran amine; Phaseolus vulgaris-leucoagglutinin

Corresponding Author: Dr. Jose Luis Lanciego, MD, PhD

Corresponding Author's Institution: Center for Applied Medical Research

First Author: Jose Luis Lanciego, MD, PhD

Order of Authors: Jose Luis Lanciego, MD, PhD; Floris G Wouterlood, PhD

Abstract: Most of our current understanding of brain function and dysfunction has its firm base in what is so elegantly called the 'anatomical substrate', i.e. the anatomical, histological, and histochemical domains within the large knowledge envelope called 'neuroscience' that further includes physiological, pharmacological, neurochemical, behavioral, genetical and clinical domains. This review focuses mainly on the anatomical domain in neuroscience. To a large degree neuroanatomical tract-tracing methods have paved the way in this domain. Over the past few decades, a great number of neuroanatomical tracers have been added to the technical arsenal to fulfill almost any experimental demand. Despite this sophisticated arsenal, the decision which tracer is best suited for a given tracing experiment still represents a difficult choice. Although this review is obviously not intended to provide the last word in the tract-tracing field, we provide a survey of the available tracing methods including some of their roots. We further summarize our experience with neuroanatomical tracers, in an attempt to provide the novice user with some advice to help this person to select the most appropriate criteria to choose a tracer that best applies to a given experimental design.

Cover Letter

cima
CENTER FOR APPLIED MEDICAL RESEARCH
UNIVERSITY OF NAVARRA

NEUROSCIENCE DIVISION
Laboratory of Basal Ganglia Neuromorphology
José L. Lanciego MD, PhD

Dear Harry,

Please find enclosed a revised version of the review manuscript entitled ***"A half century of experimental neuroanatomical tracing"*** by José L. Lanciego and Floris G. Wouterlood, resubmitted for consideration in the Journal of Chemical Neuroanatomy.

All suggestions raised by reviewers have been taking into consideration when preparing the renewed version of the manuscript. We acknowledge the reviewers for their valuable input as well as for the efforts taken in revising the manuscript.

We look forward to hearing from you in due course.

Best regards and have a nice day,

José L. Lanciego & Floris G. Wouterlood

Avda. Pío XII, 55 E-31008 Pamplona **T** +34 948 194 700 **ext.** 2002 **F** +34 948 194 715 jlanciego@unav.es www.cima.es

***Research Highlights**

Overview of neuroanatomical tracers currently available. > Neuroanatomical tract-tracing methods to delineate brain circuits. >The complexity of brain circuits often requires multiple tracing paradigms. > Which tracers are better suited for their combined use. > Colorimetric vs. fluorescent detection.

J. Chemical Neuroanatomy – review –

A half century of experimental neuroanatomical tracing

by

José L. Lanciego and Floris G. Wouterlood*

Basal Ganglia Laboratory, Center for Applied Medical Research (CIMA and CIBERNED), University of Navarra, Pamplona, Spain, and *Department of Anatomy and Neurosciences, Vrije University Medical Center, Amsterdam, The Netherlands

statistics:

text pages: 69

cartoons: 3

figures: 13

text boxes: 4

authors:

José L. Lanciego, M.D., Ph.D.
Center for Applied Medical Research (CIMA and CIBERNED)
Neurosciences, Basal Ganglia Laboratory
University of Navarra
Pio XII Ave 55 Edificio CIMA
31008 Pamplona Navarra
Spain

(*) Corresponding author:
Floris G. Wouterlood , Ph.D
Department of Anatomy and Neurosciences
Vrije University
University Medical Center, MF-G-136
P.O. Box 7057
1007 MB Amsterdam
The Netherlands

Table of contents

Abstract

Most of our current understanding of brain function and dysfunction has its firm base in what is so elegantly called the ‘anatomical substrate’, i.e. the anatomical, histological, and histochemical domains within the large knowledge envelope called ‘neuroscience’ that further includes physiological, pharmacological, neurochemical, behavioral, genetical and clinical domains. This review focuses mainly on the anatomical domain in neuroscience. To a large degree neuroanatomical tract-tracing methods have paved the way in this domain. Over the past few decades, a great number of neuroanatomical tracers have been added to the technical arsenal to fulfill almost any experimental demand. Despite this sophisticated arsenal, the decision which tracer is best suited for a given tracing experiment still represents a difficult choice. Although this review is obviously not intended to provide the last word in the tract-tracing field, we provide a survey of the available tracing methods including some of their roots. We further summarize our experience with neuroanatomical tracers, in an attempt to provide the novice user with some advice to help this person to select the most appropriate criteria to choose a tracer that best applies to a given experimental design.

1. Introduction

Even the brain of the most diminutive vertebrate appears to us from a strictly anatomical point of view as an incomprehensibly large collection of neurons with sets of equally incomprehensibly complicated interactions. Special about this remarkable central organ is that large groups of neurons act together to collect and analyze sensory and visceral information arriving from the periphery via cranial and spinal nerves. These neurons process the information, integrate and take care of storing the outcome for later use. Simultaneously they formulate an appropriate response, for instance a motor act, autonomous response or, as is so essentially human, a thought, logical reasoning or a creative idea.

Attempts to unravel the anatomy of the brain, spinal cord and peripheral nerves have resulted so far in huge amounts of descriptive and experimental data and a wealth of creative integrative ideas. Von Waldeyer (1891) was the first to propagate the idea that the nervous system is made up of discrete individual cells, and together with Foster and Sherrington's (1897) notion of the synapse as the physiological site of information transfer the intellectual framework had been established that supports neuroanatomical tracing as we know it today. Giant steps in unraveling neuronal connectivity were made by Santiago Ramón y Cajal who pioneered the art of neuronal network visualization with the then newly discovered Golgi silver impregnation technique. Techniques like these create light absorbing inorganic deposits, 'dyes' that accumulate inside neurons or diffuse through cell processes in post mortem tissue, such in contrast to labels that are taken up and transported in living neurons. In this review we keep this distinction between purely physical diffusion of dyes in essentially fixed material and the spread of label in living cells via active physiological transport processes. Ramón y Cajal was the first who described neuron types in the brain systematically, based on the morphological features of their cell bodies, dendrites and axons (although he considered dendritic spines as artifacts). His great scientific legacy was published in the two-volume 'Système nerveux de l 'Homme et des Vertébrés in 1909-1911. In Ramón y Cajal's age, experimental lesioning of large myelinated tracts was already an established yet coarse method of tract-tracing (Waller, 1850). Building upon Waller's legacy a whole subdiscipline blossomed in experimental neuroanatomical tract tracing, supported in its heyday by a most powerful tool, the selective silver staining method originally developed by Nauta (1952) and refined by Fink and Heimer (1967). Only in the second half of the 20th century techniques became available, starting with the groundbreaking discovery by Kristensson and Olsson (1971a,b) that intrinsic cellular transport mechanisms in the live subject can be used to deliver original labels that identify the origin, course and termination of axons of groups or individual neurons. Combined with

immunohistochemical, genetic and neurophysiological techniques, our knowledge about the wiring of neuron populations thus exploded. A picture of 'brain' is emerging in which the neurons maintain a multitude of synaptic and nonsynaptic relationships in order to fulfill incredibly complex and dynamic tasks. We consider the brain with awe: an incomprehensibly large collection of neurons with sets of incomprehensibly complicated anatomical and chemicophysiological interactions. This review tries to provide an oversight of the main categories of techniques in neuroanatomical tracing and the state of the art after the first ten years of the 21st century.

2. Tracing based on transport in living neurons

In the living subject, macromolecules are continuously manufactured by the cellular molecular machinery, transported inside cells or sent packed or unpacked across cell membranes into the extracellular space. Macromolecules can be taken up from the extracellular space, transported to the cell body and metabolized there, or stored for later use. As this happens everywhere in the body the nervous system is no exception to this rule. Thus, neurons may take up small or big macromolecules anywhere along their outer membrane, for instance at or close to their peripheral axon terminals or their motor end plates. Molecules may enter the cell's interior via receptor-mediated uptake, or in a 'mass process' by vesicular endocytosis. Following internalization these molecules are transported to the perikaryon for further metabolic processing, storage or disposal. The transport from the periphery back to the cell body is called *retrograde* transport. Tracing methods that employ this class of transport are called retrograde tracing methods. Conversely, macromolecules can be taken up by the perikaryon and dendrites and transported centrifugally, along their axon towards the periphery. This kind of transport is called *anterograde* transport, and it forms the basis of so-called anterograde tracing techniques. We will keep this distinction throughout this review, although most tracers are to a certain degree transported bidirectionally with one direction of transport prevailing.

2.1. Anterograde tracing with biotinylated dextran amine (BDA)

Glover and coworkers (1986) introduced dextran amine conjugated with selected fluorescent dyes, fluorescein and rhodamine, as new neuroanatomical tract tracing macromolecules. Previously, dextrans conjugated to fluorescein isothiocyanate (dextran-FITC), had been applied to study vascular permeability in the peripheral nervous system (Olsson et al., 1975; Hultström et al., 1983). Glover et al. (1986) portrayed the fluorescing dextrans basically as retrograde tracers in the CNS. Their novel application generated a wave of interest in the use of dextran-based fluorescent tracers, several of which appeared to be transported predominantly in the anterograde direction

(Nance and Burns, 1990; Schmued et al., 1990; Fritszch and Wilm, 1990; Chang, 1991). The first to report on the superior quality of biotinylated dextran amine (BDA) as an anterograde neuroanatomical tracer were Veenman et al. (1992). Dextran molecules, dextran amines and their conjugates are taken up via an unknown mechanism by dendrites and neuronal cell bodies and mainly transported in the anterograde direction (Reiner et al., 2000; Reiner and Honig, 2006). We will deal here further with BDA 10 kD which is the most outspoken anterograde tracer of the family and maybe for this reason overwhelmingly applied. BDA 3 kD represents another member of the family of dextran amines and is better suited for retrograde tracing purposes (for review on dextran amines, please see Reiner et al., 2000).

Biotinylated dextran amine conjugated to lysine (MW 10 kD, Invitrogen-Molecular Probes, Eugene, OR) is dissolved in 10 mM phosphate buffer, pH 7.25 (5%-10%, rodents; 10% primates) and injected under stereotaxic guidance into the brain. Both iontophoretic and mechanical injections have been reported (Reiner et al., 2000). Typical iontophoretic application into rat brain is through a 5 μA positive pulsed direct current (7 s on/off) on a micropipette filled with BDA solution, inner tip diameter 20-40 μm (Wouterlood and Jorritsma-Byham, 1993; Gonzalo et al., 2001). Survival time is in proportion to the length of the projection under study. Transport is estimated to span 15-20 mm of tract in one week (Reiner et al., 1993). In rats a survival time of one week is usually in the safe range. BDA remains stable in the rodent brain up to 4 weeks post injection while in primates it may remain detectable up to 7 weeks after application. BDA tolerates a wide variety of fixatives. Sections of aldehyde-fixed brain, cut on a freezing microtome, vibrating microtome or cryostat are incubated with streptavidin-HRP followed by incubation in 3-3'-diaminobenzidine/H_2O_2 according to one of the many recipes available (e.g. Vectastain kit, Vector, Burlingame, CA; see section 8) or, for fluorescence microscopy, incubated for one hour with streptavidin conjugated to one of a repertoire of fluorescent tags, e.g. streptavidin-Alexa Fluor™ 488, streptavidin-Alexa Fluor™ 543 (Invitrogen-Molecular Probes), streptavidin-Cy3™ (Amersham Life Science, Inc), etcetera.

As BDA 'fills' the neuronal cytoplasm within the limiting membranes the staining product forms a homogeneous label inside neurons against a perfectly clear background, and in this way resembles classical Golgi silver impregnation. All the details of the labeled neurons in the injection sites, e.g. dendritic spines, are available for inspection. Most important is that the tracer appears equally homogeneously distributed along the entire trajectories of the fibers, from the labeled parent neurons all the way downstream to the location where the fibers form their terminal arborizations and synapse with the processes or cell bodies of the target neurons. This characteristic allows extremely precise mapping of fiber tracts, the analysis of the

compartmentation of large fascicles and association bundles and the study of terminal projection patterns. Quantitative estimation of the numbers and densities of labeled axon terminals can be attempted (Wouterlood et al., 2007, 2008). In the electron microscope the label generated by BDA-processing can be seen inside the nuclei of neurons and throughout the cytoplasmic compartments including that of the main dendrites and their branches down to the most distal branchlets (at least when dealing with BDA-filled neurons in the vicinity of the injection sites) and in fibers with their varicosities and axon terminals. Detail in the electron microscope is preserved so well that the pre- and postsynaptic membrane densities of labeled axon terminals can be appreciated (Wouterlood and Jorritsma-Byham, 1993). Retrograde transport of BDA may occur, resulting sometimes in a granular deposit of the tracer in a limited number of neuronal perikarya, while infrequently complete or 'dense' labeling is present of cell bodies and dendrites in areas known to project to the site of injection (Reiner et al., 1993). When the latter occurs the investigator should be aware of the possibility of 'false' anterograde labeling of collateral fibers belonging to these initially retrogradely labeled neurons (Chen and Aston-Jones, 1997). Although the labeling of collateral fibers is often regarded as a limitation of BDA, it is also worth noting that one can take advantage of this property to analyze reciprocal connections between closely related brain regions. An example of such application is clearly depicted in the study of Shink et al. (1996) who took advantage of these unique properties of BDA to elucidate tight relationships between functionally related groups of neurons in the subthalamic nucleus and the globus pallidus of monkeys. The retrograde transport component of BDA derivatives was also exploited by Bácskai et al. (2010) through application of fluorescent conjugates of dextran amine (tertrametylrhodamine dextran amine (RDA) and fluorescein dextran amine (FDA), contralateral to each other to the cut end of the hypoglossal nerve in the frog, *Rana esculenta*. The aim of this particular experiment was to study cellular aspects of the relationships of hypoglossal motoneurons across the midline of the brain stem.

As the label is located in the neuron's interior, the detection reporter molecule (streptavidin-HRP) must, in the conventional procedure of free-floating incubation, penetrate into the sections and cross cellular membranes to bind to its target. This penetration process takes some time to happen. However, the detection of transported BDA does not require antibodies. Because a molecule of streptavidin conjugated to a fluorochrome has a modest molecular weight compared with an antibody it does not suffer from poor penetration to the degree encountered with, for example, lectin tracing immunohistochemistry. The addition of a detergent to enhance the penetration of reagents into tissue sections (e.g. 0.3-0.5% Triton X-100) is not always necessary and can be replaced for electron microscopy purposes by a freeze-thaw procedure, or can even

be omitted completely. The property that the detection of biotin does not require antibodies while this compound is very tolerant to fixatives and in no sense interacts with immunohistochemical treatment, renders this tracer highly efficient for combination with other tracing methods, immunohistochemical staining procedures and with intracellular injection of neurons in slices of fixed material (see 7.4). BDA is also well suited for double-label electron microscopic purposes. This wide versatility, together with the ease of application and the reliability of the tracer, has made BDA a widely applied and successful neuroanatomical tracer. At present, BDA undoubtedly represents the first choice anterograde tracer. Besides the broadly used BDA 10 kD, it is also worth noting that a lower molecular weight form of BDA (BDA 3 kD) is also available and has its own advantages, particularly when considering the retrograde transport of the tracer. Indeed, BDA 3 kD can be regarded as an excellent retrograde tracer that results in Golgi-like retrograde labeling of striatofugal neurons in rats and monkeys. Illustrative examples can be found elsewhere (Reiner et al., 2000; Lei et al., 2004; Sidibé and Smith, 1996).

BDA is compatible with a wide range of fixatives which implies that the choice for a particular fixative in multilabel experiments depends on the most demanding marker. In rodents, we prefer a fixative that allows additional immunohistochemistry: buffered 4% formaldehyde, 0.1% glutaraldehyde and 0.25% of a saturated picric acid solution. After fixation, the brain can be cut with any of the available sectioning methods. Brain sections whose thickness ranges between 40 and 400 µm can be processed. Thinner sections may be required when a second or third marker is (immunohistochemically) visualized in addition to transported BDA.

2.2. Anterograde tracing with *Phaseolus vulgaris*–Leucoagglutinin (PHA-L)

The common kidney bean, *Phaseolus vulgaris*, contains a lectin whose subunits exhibit either leucocyte agglutinating (L-subunit) or erythrocyte agglutinating (E-subunit) activity. Combination of four L subunits produces a stable lectin that, after focal deposition into the CNS, appears to be taken up nearly exclusively by neuronal cell bodies. Transport occurs in the anterograde direction towards the axon terminals (Gerfen and Sawchenko, 1984). Uptake is thought to be receptor-mediated. Detection is via an antibody raised in rabbit or goat against the lectin, and this detection results in the visualization of the most exquisite details of the entire neuron, most importantly the fibers and axon collaterals including the terminal branches of the axon down to and including the terminal boutons. The researchers who developed the tracing method immediately understood that detection based on an immunohistochemical procedure would open the door widely for combinations with parallel procedures, e.g., multiple immunostaining (Gerfen and Sawchenko 1985) and with other tracing methods, for instance retrograde transport of a fluorescent tracer or

even anterograde tracing with a non-competitive tracer substance. Such combinations of PHA-L tracing with various types of immunohistochemistry and retrograde tracing have indeed become reality. BDA (which was introduced as a tracer some years after PHA-L) comes here into focus. The good compatibility of PHA-L and BDA, because they rely on completely independent detection systems, makes it possible to study in one and the same experimental animal questions dealing with convergence or divergence of projections to certain brain areas (Lanciego and Wouterlood, 1994; Lanciego et al., 1997). In double-tracing experiments in which BDA and PHA-L are combined, the detection of the first label (usually BDA) can be achieved via a blue-black Ni-enhanced diaminobenzidine reaction product while the detection of the second tracer can be finalized with a classical brown diaminobenzidine reaction, thus creating sections in which each tracer has its own specific identifying color (Herrera et al., 1994; Lanciego and Wouterlood, 1994). The availability of robust multichannel confocal microscopes has made it even possible to create three-label preparations, e.g. the two tracers, BDA and PHA-L plus one additional marker pinpointing a neurotransmitter or other neuroactive substance. Some of these combined methods are being discussed elsewhere in this review (section 4). The combined injection of an anterograde tracer (either PHA-L or BDA) and a retrograde tracer opens ways to study in detail the anatomical connectivity of chains of neurons (Wouterlood et al., 1992; for review, see Lanciego and Wouterlood 2006).

2.3 Other anterograde transport-tracers: neurobiotin, biocytin, tritiated amino acids, cobalt-lysine

2.3.1. Neurobiotin and biocytin

The N-(2-aminoethyl)biotinamide derivative of biotin, ‘Neurobiotin’ (trade mark of Vector, Burlingame, CA), was introduced by Kita and Armstrong (1991) as an alternative for HRP, Procion yellow, and Lucifer yellow to mark neurons subject to intracellular neurophysiological recording. After the neurophysiology session the morphological features of the recorded cells can thus be documented. In this particular application, Neurobiotin has enjoyed throughout the years a steady popularity. It is being applied both in mammals (rat, rabbit; as exemplified recently by Ruigrok et al., 2011), amphibians (Zhang et al., 2006), and invertebrates (Fan et al., 2005) (see section 5). Although Neurobiotin can be used as a neuroanatomical tracer (see below), most publications about its use deal with combined electrophysiological recording/identification of single cells. Biocytin, i.e., biotin conjugated to lysine, was also introduced as a physiological recording-compatible dye to label intracellularly recorded ‘live’ neurons (Horikawa and Armstrong, 1988), but

within one year after its introduction, King et al. (1989) reported a useful additional characteristic, notably that after extracellular injection the compound appears to be taken up and transported. Transport occurs mostly in the anterograde direction, especially when the injection spots are small. King and coworkers reported some injection track labeling and also retrograde transport following large, mechanical injections (up to 1.3 µl with a Hamilton syringe). An extensive comparison between the characteristics of Neurobiotin and Biocytin was published by Lapper and Bolam (1991). These authors confirmed King et al.'s (1989) observation that both neurobiotin and biocytin show a tendency of being transported retrogradely. Even more important in Lapper and Bolam's 1991 article is their description of the good properties of neurobiotin and biocytin in preparations for electron microscopy. Survival times after biocytin or neurobiotin injections need to be relatively short because both compounds are metabolized quickly. Both substances therefore are being used exclusively for short-distance tracing and for the visualization via intracellular injection of single neurons or, as has been demonstrated elegantly by Pinault (1996), via juxtacellular injection. The latter procedure results in the labeling of single or very small groups of neurons and can be combined with electrophysiological recording (Taverna et al., 2004; see also section 5). Li et al. (1990) reported successful application of biocytin as an intracellular-injection marker in neurons in slices of fixed brain. Delivering the colorless biocytin into cells in fixed brain slices offers quite a challenge (Li et al. (1990) used micropipettes loaded with biocytin mixed with Lucifer yellow). This challenge can be addressed by using a fluorescent derivative of biocytin, named biotin-dextran miniruby (Liu et al., 1993). Because biocytin and neurobiotin are taken up and transported rapidly, survival time can be kept short (1-4 days). They can easily be applied in electron microscopy procedures methods (Cowan et al., 1994; Szabadics et al., 2010). In order to generate a second electron dense label, biocytin tracing has been combined with the anterograde degeneration method that also requires short post surgery survival times (2-3 days in rat) (Wouterlood et al., 2004). A special application of Neurobiotin has been neuroanatomical tracing in slices of post mortem human brain (Dai et al., 1998a,b).

2.3.2. Tritiated amino acids

In the first chapter of the book 'Cytochemical Methods in Neuroanatomy' (1982) a pioneer, Anita Hendrickson, vividly describes her decision to exploit *in vivo* axonal transport processes for the tracing of fiber connectivity of striate cortex via autoradiography (Hendrickson, 1982). In the 1960's and 1970's, before the ascent of the immunofluorescence methods, various autoradiographical methods enjoyed their heyday. Neurons, like cells everywhere in the body, take up amino acids, incorporate these in polypeptide macromolecules and subsequently transport some of these

products through their axons to the axon terminals. The introduction of a tracing method based on this principle led to superiority, in terms of both concept and sensitivity, compared to the existing, Nauta-Gygax enhanced silver tracing method (Nauta, 1952). The latter method is based on a pathological condition, i.e., a changed affinity for silver staining of myelinated nerve fibers traumatically separated from their parent cell bodies. The separation is experimentally inflicted via surgical, thermoelectric or chemical means. Uptake and incorporation of amino acids like ^{3}H leucine and ^{3}H proline into proteins had been introduced in the 1950's and early 1960's for the study of uptake and transport mechanisms in the peripheral and central nervous system (e.g. Droz and Leblond, 1962, 1963). However it was Hendrickson, together with Maxwell Cowan and collaborators (Cowan et al., 1972), who took the method systematically to neuroanatomical tracing. In the 1980's the much faster, direct and equally reliable tracing methods like BDA- and PHA-L tracing rapidly overtook autoradiographic tracing methods. Also the cumbersome and time consuming nature of the autoradiographic method has contributed to a drastic reduction of the number of practitioners. Finally, it should be taken into consideration that the product of autoradiographic tracing, i.e., silver grains in an emulsion overlying preparations, is an indirect label located *outside* the labeled neurons while an immunohistochemical applied label is much more appropriately located, namely *inside* the labeled neurons. In addition, restrictions and measures associated with the short-term and long-term management of radioactive isotopes and radioactive waste have continuously dampened the enthusiasm. Nevertheless, the impact on neuroscience of this method has been so immense that it deserves mentioning in the present review. Orthograde axoplasmic transport autoradiographic tracing (OOAT, to re-use an abbreviation introduced by Hendrickson in her 1982 chapter) utilizes the above mentioned uptake by cell bodies of amino acids. The ribosomes in the cell bodies' rough endoplasmic reticulum assemble proteins. As axons and axon terminals do not possess ribosomes, protein synthesis is centralized in the cell body and the subsequent transport of the manufactured proteins strictly anterograde. It is important to note that the axoplasmic transport is a naturally occurring, physiological process. Two technical 'tricks' govern OOAT, first the application of amino acids that contain radioisotopes, second the application of radioisotopes with short (^{32}P, ^{35}S) or long (^{3}H, ^{14}C) decay times. Because the sensitivity and resolution of the detection in a photographic emulsion of the radiation emitted by decaying radioisotopes depends on the type of particle released and its energy, the low-energy beta particle-emitter ^{3}H became the isotope of choice. However, detection is indirect because beta particles inevitably travel several microns from their origin through the tissue section and the emulsion layer before hitting a silver bromide molecule. As a consequence, the resolution of the detection depends on the point spread function of beta particles emitted by

the decaying isotope, analogous to the point spread function of photons emitted from fluorochromes in modern confocal microscopes. Thus the pinpointing of the tracer bears down to calculating from positions of silver grains in the photographic emulsion overlying a section the statistically confident location of the 'invisible' radioactive protein molecules inside the tissue section from which the radiation has originated (Bachmann and Salpeter, 1969). The procedures involved in the OOAT method are explained at length by Cowan and Cuénod (1975). A thorough discussion of the advantages and caveats of the OOAT method was published by Swanson (1981).

2.3.3. Cobalt and nickel compounds

Tracing with heavy metal atoms can be considered as an extension of intracellular filling. In 1972, Pitman et al. (1972) reported about intracellular filling of neurons in whole-mount insect ganglion preparations with cobalt chloride. Fuller and Prior (1975) extended cobalt-tracing to in vitro vertebrate whole-brain preparations. The property of spreading into neuronal processes of cobalt ions in living animals was further explored by Lázár (1978) who traced retinotectal connectivity with a cobalt-lysine complex in a chronically anesthetized frog preparation. Bazer and Ebbesson (1984) further simplified the cobalt-lysine tracing technique. Although cobalt-lysine tracing has been superseded by the techniques that utilize transport of macromolecules or lectins, it is still being used, in vertebrates exclusively in cold-blooded species (e.g., Rooney et al., 1992; Tóth et al., 1994; Matesz, 1994) and, more frequently, in invertebrate brains (Hackney and Altman, 1982; Chase and Tolloczko, 1993; Baba, 2000). Baba (2000) reported on tracing with NiCl next to cobalt ions.

2.4. Retrograde changes in neuronal perikarya after a lesion downstream

Retrograde post traumatic morphological changes in specific neuronal systems were already noticed more than a century ago. The Russian-born Swiss psychiatrist, Constantin von Monakow is regarded as one of the great pioneers in descriptive and experimental neuroanatomical tracing in the late 19th century (Wiesendanger, 2006). One of the illustrations of von Monakow's (1897) book, 'Gehirnpathologie' shows a case of unilateral hypertrophy of the inferior olivary nucleus in a clinical case. Von Monakow was the first to describe primary, secondary and tertiary retrograde hypertrophic neurodegenerative events (Becker, 1952). Chromatolysis of neuronal perikarya and its causes were reviewed by Cragg (1970). Observations like those by von Monakow can be conceived as metabolic adaptations of neurons that start in the periphery and have effect in a retrograde sense on the parent cell bodies (Cragg, 1970; Boesten and Voogd, 1985). A nice

modern synthesis of the old notion of morphological retrograde changes is an experiment by Ferreira-Gomes et al. (2010) who in a rat model of osteoarthritis analyzed dorsal root ganglion cells identified as receiving fibers from arthritic joints via retrograde fluorescence tracing.
Thus the infliction of a lesion or the deposition of a tracer substance in the periphery can have an effect on the parent cell body that in some systems, e.g., the olivocerebellar system, results in hypertrophy. The principle of an effect in the CNS following a challenge in the periphery forms the basis of retrograde tracing.

2.5. Retrograde tracing with enzyme markers: the HRP-family

The first report exploiting retrograde axonal transport of an enzymatic protein marker in a neuroanatomical tracing experiment came from the lab of Krister Kristensson in Göteborg, Sweden. Here, Kristensson and Olsson (1971a,b) deposited the enzyme, horseradish peroxidase (HRP) in the gastrocnemius muscle of rats, waited a few days and next detected HRP-activity in motoneurons in the spinal cord with Karnovsky's diaminobenzidine (DAB) substrate staining method (Graham and Karnovsky, 1965). In the very same year, Kristensson et al. (1971) repeated the tracing experiment, but they now deposited HRP into the tongue of a rat and found labeled motoneurons in the hypoglossal nucleus (Kristensson et at, 1971). Finally, LaVail and LaVail (1972) demonstrated uptake and retrograde transport of HRP in the CNS itself. Internalization of HRP occurs in all the neuron's processes as well as the cell body via fluid endocytosis. Thus, pressure-injected HRP is prone to being taken up by damaged fibers of passage at the injection site, a feature observed only infrequently with anterograde tracers such as BDA and PHA-L, at least when the latter were injected by iontophoresis. In the interior of the neuron the HRP remains membrane-packaged in so-called endosomes that are finally transported to the perikaryon for subsequent metabolic degradation in lysosomes. Endosomes typically show an oval or tubular shape.
A classical approach employing retrograde transport to study connectivity of the CNS is via the injection of 0.1-0.5µl of a 20-50% solution of HRP in saline through a Hamilton microsyringe. Alternative vehicles for HRP application include foam or gel drenched in HRP solution, HRP crystals, pellets, and plain HRP-gel. As foams, gels and pellets are hard to inject, these 'hard' vehicles are often implanted, or they are brought in close contact with the proximal stump of a cut cranial or peripheral nerve (Barbas-Henry and Wouterlood, 1986). The most common types of HRP used are Sigma Type VI (Sigma-Aldrich, St. Louis, MO) and Boehringer (Boehringer-Ingelheim). Large mechanical injections must be carried out carefully to avoid mechanical damage to the brain tissue at the syringe tip which may cause local necrosis. For this

reason, administration must be slow, over a 10-20 minute period. After the injection is completed the syringe is left in situ for a short period time to avoid back-filling of the syringe track with HRP. As reduction of the enzymatic activity of transported HRP is a function of time, and as transport is related to distance and typically differs between fiber systems, the optimal survival period following injection of HRP varies from two to five days, after which the histochemical staining begins to produce less dense deposit. Boosting the enzymatic reaction under such conditions by adding peroxide substrate may help, but is usually of limited value since background has a tendency to build up extra fast when too much substrate is available.

The typical fixative for HRP tracing includes a mixture of 0.5-1.5% glutaraldehyde with 4% buffered formaldehyde (Mesulam, 1982). Tissue sections obtained by cutting the brain on a freezing microtome are first treated for 1-2 minutes with a phosphate-buffered 1-2% peroxide solution to suppress endogenous peroxidase activity (ubiquitously present in erythrocytes; endogenous peroxidase will compete with, and outperform HRP-activity if perfusion fixation has been suboptimal and erythrocytes are still clogging capillaries - also vascular endothelium and choroid plexus cells are notorious sources of peroxidase activity). The bleached sections are carefully rinsed in 50 mM Tris-HCl, pH 7.6, pre-incubated for 30 minutes in 5 mg 3-3' diaminobenzidine in 10 ml Tris-HCl whereafter the reaction is started by adding 3.3 µl of 30% H_2O_2 per 10 ml of preincubation solution. The peroxidase catalyzes electron transfer from the diaminobenzidine donor molecule to oxygen ions in the peroxide oxidizer. As a result, a brown diaminobenzidine precipitate is formed, with molecular oxygen as a byproduct. When the peroxidase reaction is too strong, the formed oxygen may become gaseous and form gas bubbles that damage the histological detail. In lieu of diaminobenzidine other electron donors can be used, e.g. tetramethylbenzidine (TMB), o-dianisidine, benzidine dihydrochloride (BDHC; Lakos and Basbaum, 1986), p-phenylendiamine (PPD-PC), 1-naphthol/azur B (Mauro et al., 1985), alkaline phosphatase (purple reaction product, Wouterlood et al., 1987), the magenta chromogen, Vector-VIP (Zhou and Grofova, 1995), and HistoGreen (Thomas and Lemmer, 2005). Contrast of the formed precipitate versus background can be enhanced by the addition of nickel-ammonium sulphate to the incubation medium (Ni-enhancement; Hancock, 1986). Sensitivity can be increased considerably by using wheat germ agglutinin-conjugated HRP as tracer instead of native HRP (Gonatas et al., 1979; see section 2.9).

Application of multiple retrograde tracers can be attractive when the aim is to study axon collateralization. Hayes and Rustioni developed in 1979 a method based on the combined use of enzymatically active HRP and inactive HRP containing ^3H radioisotopes. Transported enzymatic

active HRP was detected via standard HRP-histochemistry while the enzymatically inactive yet radioactive HRP was detected via autoradiography.

2.6. Retrograde tracing with fluorescent inorganic compounds

One year before publishing his landmark paper about retrograde transport of HRP, Kristensson reported on experiments in which a conjugate of albumin and the fluorescent dye, Evans Blue, had been injected into the gastrocnemius muscle of rats. After apparent retrograde transport a fluorescence signal was detected in spinal motoneurons (Kristensson, 1970). Thus, retrograde fluorescent tracing had been conceived and made operational for the first time. Next, Kuypers and collaborators (Bentivoglio et al., 1979; Kuypers et al., 1979; Skirboll et al., 1984) were the first to demonstrate that unconjugated anorganic fluorescent dyes injected focally into the CNS 'behaved' similarly to HRP, that is, these dyes are taken up by nerve terminals and transported retrogradely to the cell bodies of the involved projection neurons where they accumulate in the cytoplasm, nucleus or in specific organelles. Within a few years, Kuypers and collaborators identified a great number of fluorescent retrograde tracers including Bisbenzimide, Dapi-primuline, Propidium Iodide (Kuypers et al., 1979), True Blue, Granular Blue (Bentivoglio et al., 1979; Skirboll et al., 1984), Nuclear yellow, Fast Blue (FB; Kuypers et al., 1980; Bentivoglio et al., 1980) and Diamidino Yellow (DY; Keizer et al., 1983). These dyes bind to adenine-thymine rich nucleic acids. One main advantage of retrograde fluorescence tracing is that the labeled perikarya are directly visible in a fluorescence microscope, without any histochemical treatment. Another advantage is that these tracers can be considered reliable in the tracing of extremely long fiber tracts, e.g. corticospinal and bulbospinal projections (e.g. Rice et al., 2010), a feature shared with anterograde autoradiographic tracers (e.g. Holstege and Kuypers, 1987). Several retrograde tracers, e.g. Fluoro-Gold (FG), survive immunofluorescence procedures. Because of their spectral characteristics, fluorescent retrograde markers serve as near-ideal tracers to study axon collateralization in double-labeling experiments and, in combination with immunofluorescence, to study the neurochemical identity of traced fiber projections (pioneered by van der Kooy and Steinbusch, 1980; see also Skirboll et al., 1984); reviewed by Huisman et al.,1984; Wessendorf, 1990). Since FB and DY label different features of the cell, i.e. the cytoplasm in blue for FB and the nucleus in yellow for DY at UV excitation, double labeled neurons can be easily distinguished and differentiated from single-labeled neurons. Furthermore, it is also possible to use these tracers in combination with a third fluorescent marker in multiple labeling paradigms (e.g., Godschalk et al., 1984). Richmond et al. (1994) systematically compared results with seven different retrograde

tracers in a cat peripheral motor nerve model: FB, FG, fluorescein-dextran, rhodamine-dextran, fluorescent latex microspheres, HRP and DiI.

To this day, FB and DY are the most commonly used tracers for single or double retrograde fluorescent labeling. Because the initial manufacturer of FB (Dr. Ihling, Germany) terminated production of this compound, FB is becoming scarce and is being replaced by FG (see below). Application of all these tracers is mostly via mechanical injection devices though a few studies report microiontophoretical delivery (e.g., Schmued and Heimer 1990). Most fluorescent tracers, including FB (4-7%), can be dissolved in water. DY is difficult to dissolve and is typically suspended at 2-3% in 200 mM phosphate buffer, pH 7.2 (Keizer et al., 1983), and sonicated just before use. DY produces smaller injection sites than FB, which may be an advantage depending on the system that is being investigated. Transport times for long distance fiber connections in primates range between one and five weeks, depending on the distance involved in the projection (e.g., 5 weeks for strong labeling of corticospinal and corticobulbar neurons in macaque monkeys after injection of DY into the cervical spinal cord and FB into the lower medulla, Keizer and Kuypers, 1989). The tissue is commonly fixed by perfusion-fixation with phosphate-buffered 4% paraformaldehyde (or 10% formalin). Higher concentrations of formalin (30%) can also be used to enhance FB fiber labeling (Ugolini and Kuypers, 1986). A trace of glutaraldehyde (0.05%) is allowed to improve fixation although care must be exerted since this chemical strongly contributes to green background signal under UV fluorescence illumination. After fixation the tissue is cryoprotected in graded concentrations of phosphate buffered sucrose (10% to 30%), equilibrated and cut at 40-60 µm thickness on a freezing microtome. Sections are immediately mounted on glass slides within 6 hours of cutting to avoid in vitro diffusion of the tracer from labeled neurons (Keizer et al., 1983), air-dried and stored in the dark at 4°C. Coverslipping requires a special non-fluorescing, fade retarding mounting medium.

Another fluorescent tracer, Fluoro-Gold (FG; hydroxystilbamidine), introduced by Schmued and Fallon in 1986 as a “retrograde tracer with unique properties”, is also widely employed (Cartoon 1). FG can be used either alone or in combination with other fluorescent tracers, and it can be applied in combination with immunofluorescence detection of additional markers. The dye accumulates in small punctate structures in the cytoplasmic compartment of neuronal cell bodies. At higher concentration FG may fill neurons completely with intense white/yellow fluorescence under mercury lamp UV illumination. This fluorescence is extremely resistant to bleaching. In a living animal FG may resist metabolic breakdown up to a year post injection. Its intense and bleach-resistant labeling has contributed to raising FG to the level of ‘gold standard’ for fluorescent labeling in rodents, particularly for multiple labeling in combination with other tracers. Due to its

wide emission spectrum that causes cross bleed problems, FG is however less ideal in combination with other fluorescent tracers in retrograde double labeling procedures intended to demonstrate collateralization, because it tends to mask the presence of the second fluorescent tracer in the same cell (see Schmued and Fallon, 1986). FG is less favored in confocal laser scanning studies, since it possesses a wide excitation spectrum while, because of its excitation peak at 323 nm (Schmued and Fallon, 1986), it requires an expensive ultraviolet laser that is offered for most instruments as an option beyond the standard configuration. The availability of an antibody against FG (Chang et al., 1990) has two advantages. First, via immunohistochemistry the FG is 'replaced' by a fluorochrome of choice with the proper spectral characteristics with respect to the researcher's confocal laser scanning microscope (although the FG itself will remain visible in standard fluorescence mode). Second, peroxidase immunohistochemistry makes it possible to take material studied previously in the fluorescence microscope to the electron microscope (see Deller et al., 2000). FG is marketed by Fluorochrome, Inc. (Denver, CO) and its application is via mechanical injection or iontophoresis. The powder can be dissolved in a range of buffers (e.g., 5 mM acetate buffer, pH 5.0, 100 mM phosphate buffer, pH 7.4) of which 100 mM cacodylate buffer, pH 7.3 is common for either a mechanical application via a Hamilton syringe or by means of microiontophoresis (Schmued and Heimer, 1990). Survival periods range from one week up to one year, and tissue fixation and sectioning can be conducted according to standard neuroscience laboratory procedures. With long survival periods (more than one week), the retrogradely labeled neurons stand out with high contrast to the background. Some examples are provided in Figure 1.

2.7. Retrograde tracing with bacterial toxins: the CTB family

In a search for a more sensitive tracer than native HRP, Trojanowski et al. (1981, 1982) proposed the use of a conjugate of the non-toxic B fragment of cholera toxin (choleragenoid) (CTB-HRP) as a tracer. While HRP apparently is taken up indiscriminately by fibers of passage, undamaged axons of passage have only a limited capacity to internalize a probe like CTB-HRP. Because of the immunohistochemical detection rather than histochemical assay such a conjugate is detected with higher sensitivity than native HRP. The retrograde transport of CTB-HRP labels a greater number of neurons and reveals the dendritic arbors of labeled neurons better than native HRP. The superior sensitivity of CTB-HRP is especially due to the fact that its uptake is receptor-mediated, i.e., it reflects binding of CTB to specific receptors on neuronal membranes, which is not affected by conjugation of the toxin fragment with HRP (reviewed by Trojanowski, 1983). Such binding results in uptake of the CTB-HRP conjugate by adsorptive endocytosis, a process that is more efficient than the uptake of native HRP by fluid phase endocytosis. Another fact that

contributes to its greater sensitivity is that CTB-HRP is less rapidly eliminated from retrogradely labeled neurons than native HRP (e.g., Wan et al., 1982), probably because the CTB-HRP is transported along a different intracellular pathway than that utilized by native HRP (Trojanowski, 1983). Both WGA-HRP and CTB-HRP are transported bidirectionally, and this may be an advantage or a disadvantage depending on the system under investigation. Anterograde axonal transport occurs at fast rate, e.g., in rat about 108 mm/day for WGA-HRP (Trojanowski, 1983) . A further development along the line of CTB-HRP tracing was to eliminate the HRP conjugate altogether and experiment with CTB in its unconjugated form and detect transported label immunohistochemically (Luppi et al., 1990). A big advantage of unconjugated CTB with respect to HRP is that peroxidase, next to being a tracer, is also present intrinsically in neurons in peroxisomes and lysosomes. This requires measures in HRP histochemical procedures to suppress endogenous peroxidase-associated background staining. Using the 'exotic' CTB and immunohistochemical detection potentially eliminates background. Today, most CTB applications include either immunoperoxidase or immunofluorescence detection, via an intermediary step of incubation with an antibody against CTB, although direct tracing with fluorescent CTB-rhodamine and CTB-fluoresceine conjugates has been reported, e.g. in the visual system of mice (Lyckman et al., 2005). Conjugates of CTB with a wide variety of Alexa™ fluorochromes have recently become available from Invitrogen-Molecular Probes (see Conte et al., 2009a,b). These compounds are directly visible in a fluorescence microscope. Because of their photostability they are particularly well suited for inspection in the confocal laser scanning microscope.

As with any methodology there are both advantages and limitations to the application of these markers in neuroanatomical studies. The nature of the experiments determines which tracers and methods are most suitable in a given situation. Some of the potential drawbacks of their use are the same as those associated with other tracers. For instance, the visualization of the injection site produced by WGA-HRP and CTB-HRP appears similar to that produced by native HRP. The extent of the apparent injection site depends upon the sensitivity of the substrate used for histochemical visualization of HRP activity (i.e., the injection site appears smaller when detected with DAB as substrate than with the more sensitive TMB). Determining the effective area of uptake within the injection sites is a problem common with all these markers (see Mesulam, 1982). Differences have been observed in the efficiency of uptake in given pathways, which are related to differences in availability of receptors for WGA or CTB on neuronal membranes. This is particularly the case in the peripheral nervous system, where important differences have been observed in the uptake and anterograde transganglionic transport of WGA-HRP and CTB-HRP in primary sensory neurons. For instance, a preferential uptake occurs by small primary sensory neurons in case of

WGA-HRP and by large primary sensory neurons in case of CTB-HRP (Robertson and Arvidsson 1985; Robertson and Grant 1985).

2.8. Retrograde tracing with micro- and nanoparticles

The idea of using small particles composed of an indifferent, label-coated material instead of inorganic dyes or organic macromolecules was first implemented by Katz and coworkers in 1984. One big advantage of particles versus fluorescence is that results seen with the light microscope may in principle be carried over to the electron microscope without much complex additional histochemical wizardry. Fluorescent, rhodamine carrying latex beads, with diameters between 20 and 200 nm, applied via a mechanical delivery system, appeared to be taken up and transported retrogradely (Katz et al., 1984). Apart from the above conceptual advantage it can be argued that particles are not cytotoxic, they diffuse only minimally at the site of injection, persist for long and that their particulate nature makes them not only in concept but also in practice suitable for combined light-electron microscopic examination (as demonstrated by Egensperger and Holländer, 1988). Fluorescent latex microbeads can be taken up and transported by damaged fibers of passage (Katz et al., 1984). Katz and coworkers observed that small particles are not internalized indiscriminately but that they have to fulfill certain physical and chemical conditions. Physical size and chemical ‘attractiveness’ for membranes apparently does matter. Thus, gold nanoparticles 10-12nm) coated with wheat-germ conjugated apoHRP (WGAapoHRP; Basbaum and Menetrey, 1987) are taken up by axon terminals and retrogradely transported to the cell body where they can be made visible for light microscopic viewing through a silver enhancement step. In the electron microscope they can be viewed directly. Compatibility of nanogold coated with WGA-apoHRP exists with other neuroanatomical tracing methods (Basbaum and Menetrey, 1987) and also with non-tracing histochemical procedures, e.g., in situ-hybridization (Jongen-Rêlo and Amaral, 2000). Because of their distinct geometry and electron absorptive characteristics the gold particles are particularly suitable markers in electron microscopy applications. A quite new development is the combination of retrograde tracing with fluorescent latex microbeads followed with diOlistic labeling with DiI of target neurons whose cell bodies have accumulated the transported microbeads (Neely et al., 2009). The future of nanoparticles seems assured since they have been used successfully as non-cytotoxic vehicles to deliver viral vectors into neurons (Bharali et al., 2005; 30 nm size silica particles). While delivery via injection succeeded it remained doubtful whether the nanoparticles had actually been transported over significant distances inside neuronal processes of the transfected neurons. Further development of this branch of nanoparticle delivery technology is necessary to obtain nanopartices that bridge distances inside axons via coupling to

internal transport systems and then deliver their payload. The payload itself could be anything interesting to neuroscientists, cell biologists and clinicians alike, e.g. drugs or photosensitive dyes for photodynamic cancer treatment (Roy et al., 2003).

2.9. Bidirectional tracing

Tracers from the neuroscientist's arsenal may be transported either strictly anterogradely (OAAT, section 2.3.2) or retrogradely (nanoparticles, section 2.8), but usually their transport characteristics are mixed, with the balance in favor of either anterograde or retrograde transport. A tracer that is transported equally well in both directions might be interesting for some niches in neuroscience.
As spin-off in the search in the 1980's for reliable and sensitive one-way retrograde tracers and more sensitive chromogens it was discovered that several lectins and toxins are in fact transported bidirectionally. For instance, the lectin, wheat germ agglutinin (WGA) was introduced as a highly sensitive retrograde tracer by Schwab et al. (1978). In these initial studies, WGA was radiolabeled, but it was soon found that WGA could be conjugated with HRP (Gonatas et al., 1979; Schwab and Agid, 1979), which made it possible to detect the transported tracer using the same enzymatic reactions and substrates as those existing for native HRP (see section 2.5) but with a considerably increased sensitivity (up to 40 times as sensitive as the detection of transported native, unconjugated HRP; Gonatas et al, 1979). The increased sensitivity of the detection revealed the anterograde component in the transport of WGA-HRP. Next it as shown with hight-sensitivity detection that even native HRP can be transported anterogradely under certain circumstances (Mesulam and Mufson, 1980). The WGA-HRP story continued in 1987 with the addition to the repertoire of nanogold particles coated with wheat-germ conjugated apoHRP (Basbaum and Menetrey, 1987, see section 2.8). However, this 'captured' WGA-HRP is only transported in the retrograde direction. The uptake of the gold particles may be triggered by their WGA-apoHRP coat while, once internalized, their size causes them to being coupled to a retrograde transport system capable of hauling big particles back to the cell body for disposal. The high sensitivity of the procedure has been instrumental in the popularity of WGA-HRP. Today, native HRP as a tracer has moved to the background. WGA-HRP is, strangely enough, still regarded by a majority of workers as basically a retrograde tracer.
Bidirectional tracing can be achieved indirectly, that is via the application of an anterograde tracer simultaneously with the application of a second, retrograde tracer. Examples are anterograde autoradiographic tracing combined in one experiment with retrograde tracing trough injection of FG (Reep et al., 1988), and anterograde PHA-L tracing in combination with retrograde FB tracing

(Wouterlood et al., 1992). The conditions that govern successful combinations of multiple tracing paradigms are listed in the next section.

2.10. Multitracing experiments with various anterograde and retrograde tracers

Immediately following the introduction of peroxidase- and fluorescence-based tracing methods, pioneers in the neuroscience community started to experiment with combinations of tracing and neurotransmitter immunohistochemistry (Ljungdahl et al., 1975; Björklund and Skagerberg, 1979; van der Kooy and Steinbusch, 1980). After these exciting early days, combination of tracing and immunohistochemistry in a single experiment have become mainstream activity. In a complex experiment, Morecraft et al. (2002) succeeded in injecting up to five anterograde tracers in motor cortex of the rhesus monkeys: PHA-L, BDA, Lucifer yellow-dextran, fluorescein-dextran, and Fluoro Ruby (tetramethylrhodamine-dextran). The complexity of this experiment mostly concerned the processing of sections to reveal all tracers. A solution was obtained by double-staining BDA and one of the complementary tracers in adjacent sections instead of having all tracers visualized simultaneously in each section. This staining strategy, through pairs of sections, worked out quite well because BDA tracer detection acted as a landmark topographical reference in all other sections.

In addition to combining two anterograde tracers a third, retrograde tracer can be added for the purpose of mapping or to determine whether the projection neurons in a zone of interest are specifically being targeted by incoming projections. Experiments in which two anterograde tracers (BDA, PHA-L) were applied, combined with retrograde FG labeling of neurons projecting out of the region, and where all three markers were subsequently visualized simultaneously in one-and-the-same section, were first reported by Lanciego et al. (1998a). The same research group developed a similar triple-tracing paradigm combining anterograde tracing with BDA together with dual retrograde tracing using FG and CTB as labels (Lanciego et al., 1998b; see also Figures 2, 3 and 4). Combination of two anterograde tracers (BDA, PHA-L) with intracellular injection of presumed target neurons (Kajiwara et al., 2008; further explained in section 7.4) can be considered as an extension or an ‘extra layer’ to study multiple innervation of individual neurons. Because three tracers are involved, each with its own particular staining procedural envelope, the staining procedures in multitracing experiments can be complex and laborious.

2.11. ‘Golden rules’ in multiple tracing

A set of ‘golden rules’ should be taken into consideration when selecting the best combination of tracers. This set lists as follows. It does not depend on the number of tracers to be combined in a multiple experimental paradigm.

(i) Whenever possible, all involved tracers should be transported unidirectionally (either anterogradely or retrogradely).

(ii) Only tracers with similar nature can be combined together (avoid combining fluorescent with non-fluorescent tracers).

(iii) Multiple surgical sessions are currently under increased criticism and therefore only tracers requiring a similar survival time should be used (all of them to be injected in a single surgical session). Avoid multiple surgeries.

(iv) Make sure that available antibodies for tracer detection do not cross-react with each other.

(v) It is desirable that the detection of all involved tracers can be accomplished both by multiple immunoperoxidase and immunofluorescence methods.

(vi) It is also worth noting that obtaining the ultrastructural correlate is a desirable option. Experiments should preferably be compatible with electron microscopy procedures and subsequent ultrahigh resolution observation.

Although none of the existing multiple tracing procedures fully satisfies all these demanding criteria, some combinations of tracers produce significant and reproducible results. The involved tracers can therefore be designated as ‘tracers of choice’ when bearing in mind multiple tracing paradigms (Lanciego and Wouterlood, 2006; see also Box #1).

3. Tracing based on infection of living neurons and vectorial spread: viruses

Neurotropic viruses can be exploited as tracing agents. These organisms enter neurons, find their way to the nucleus and replicate. Viruses are self-amplifying tracers, so to speak. Their ability to cross synapses to infect second-order neurons makes them particularly interesting for the study of connectivity in neuronal cascades (e.g., neurons innervating motoneurons). From the laboratory of Krister Kristensson, the tracing pioneer of the 1970’s, one of the first studies originated exploring systematically the tracing properties of a virus (*Herpes simplex*) as a retrograde tracer (Kristensson et al., 1974). The innate characteristic of a virus to replicate inside infected neurons is extremely helpful to maintain a high signal to-noise-ratio across the labeled neuron chain. Viruses also have nasty characteristics that inhibit their popularity as tracers. Viral infections may for instance spread explosively, and viruses may be harmful if not properly handled.

3.1. Herpes simplex, pseudorabies and rabies virus CVS strain

The particular drawback of the 'explosive spread' was eliminated by the introduction of less aggressively spreading strains of virus (Ugolini, 1995; 2008). Good timing remains essential, though. Most important is that the laboratory and the animal housing unit need to be certified biosafety facilities because viruses are notorious biological hazards (Strick and Card, 1992). Since working with viruses implies the possibility of infection, their experimental use requires specific training for the technicians and researchers potentially exposed to infected material and those who take care of the experimental animals. In the case of rabies virus, prior vaccination of personnel is mandatory.

Viruses used as transneuronal tracers are the human alpha-herpes virus, *Herpes simplex* type 1 (HSV 1), the porcine alpha-herpes virus, *Herpes suis* (PrV, also called *pseudorabies*) (Kuypers and Ugolini 1990; Strack and Lowy, 1990; Strick and Card, 1992), and the fixed Challenge Virus Standard (CVS) strain of *Rabies virus* (Ugolini 1995; Kelly and Strick, 2000). Application of the CVS strain of rabies virus (Ugolini, 1995) makes it possible to trace neuronal connections across a practically unlimited number of synapses. For a detailed review of viruses as tracers, see Aston-Jones and Card, 2000; Geerling et al., 2006; Morecraft et al., 2009; Ugolini, 2010. Several new developments promise to open an entire new chapter for viral tracing: double viral retrograde tracing (Jansen et al., 1995); double recombinant viral transsynaptic tracing (Ohara et al., 2009) and the introduction of Brainbow cassette recombined herpesvirus (Card et al., 2011).

3.2. Golgi-like retrograde labeling using rabies virus

A novel application for viruses is to improve the retrograde filling of neurons with label. Although the currently available non-viral retrograde tracers robustly label *perikarya* of neurons and in some cases extend labeling into the primary dendritic trunks, a common drawback with these tracers is their failure to produce in the retrogradely labeled neurons a sufficient and crisp visualization of longer dendrites and especially their failure to label delicate dendritic spines and appendages, and the poor buildup or outright absence of label in distal, mostly thin dendrites. Even with the most sensitive retrograde tracers like FG (Schmued and Fallon, 1986), labeling is often restricted to the cellular perikaryon and to the thickest, main dendrites. Several approaches are possible to circumvent this problem. One convenient, yet labor-consuming choice is to literally introduce extra label via the penetration of individual cell bodies of a retrogradely labeled cells with a sharp micropipette and complete the 'filling' with a dye like Lucifer yellow such that the morphological details of the entire neurons become appreciable (introduced by Buhl and Lübke, 1989; see section 7.4). Another feasible approach for retrograde Golgi-like labeling of striatofugal neurons is

represented by BDA 3 kD, as explained before in section 2.1. Recently, in collaboration with the group of Lydia Kerkerian-Le Goff from the Université de la Méditerranée (Marseille, France), we have introduced another approach to circumvent the back-filling limitation of the current retrograde tracers (Salin et al., 2008; López et al., 2010). This approach is based on retrograde tracing with rabies virus followed by the antibody-based detection of the retrogradely infected neuron. The result of this approach is a sensitive labeling of projection neurons that bears resemblance to Golgi-silver impregnation. With this procedure even the finest post-synaptic elements in the retrogradely labeled cells become visible (Figures 5 and 6). Best results obtained so far is with antibodies directed against the viral phosphoprotein (31G10) (isolated during the fusion experiment described by Raux et al., 1997) rather than using antibodies against virus-specific nucleoproteins. Furthermore, when compared to other neurotropic viruses (for a review, see Kelly and Strick, 2000; Aston-Jones and Card, 2000; Geerling et al., 2006), rabies virus is an RNA virus that exhibits a higher efficiency for retrograde transport than herpes virus together with a lower cytopathogenicity (Ugolini, 1995). Moreover, the lack of viral uptake through fibers of passage by rabies virus is clearly advantageous (Ugolini, 1995; Kelly and Strick, 2000; Nassi and Callaway, 2006).

3.3. Tract-specific intrinsic fluorescence in transgenic mice

The surgical procedure to introduce an exogenous and robust tracer into a specific brain area is complex, time consuming and prone to errors based on individual variability of the experimental animals and the experience of the researcher performing the surgery. What if a label can be introduced by inducing the genome of specific cells to produce an identifying label that tags all the processes belonging to these cells, including the axon and its appendages? This idea has become reality in strains of genetically engineered mice. One recent example is the Thy1-eYFP-H strain of mice (Porreroa et al., 2010). The metabolism of neocortical pyramidal neurons, hippocampal neurons and neurons in the amygdala produces in these mice the red-shifted spectral variant of green fluorescent protein (GFP) named eYFP, and distributes that protein throughout their efferent processes, including the axons. Thus, in Thy1-eYFP-H mice a number of tracts can be studied directly in fluorescence microscope preparations, without additional histological staining or immunohistochemical treatment. GFP can be used as a tool to visualize the morphology of isolated neurons in a Golgi silver-impregnation like way (Chakravarthy et al., 2008; Harvey et al., 2009).

3.4. Retrograde trans-synaptic tracing to visualize interneurons

When it comes to elucidating the architecture of brain microcircuits the unmet desire has existed for a long time to ascertain the number and identity of interneurons that modulate projection neurons innervating a selected target. Since interneurons are local-circuit neurons, their identification has remained elusive by means of tract-tracing approaches. The only available option so far for identifying interneurons was via intracellular filling with an opaque dye after neurophysiological recording (reviewed by Klausberger and Somogyi, 2008) or via the intracellular injection of interneurons in slices of fixed material, poking in the dark and incidentally penetrating an interneuron by sheer luck (e.g., Kajiwara et al., 2008). A third way has opened to trace interneurons by taking advantage of the trans-synaptic spread of rabies virus. Such a trans-synaptic spread requires the presence of a synaptic contact to be established for the virus to spread through and to infect the second-order neuron (a given interneuron). In other words, only interneurons innervating a virus-infected projection neuron (first-order neuron) can be further infected by the trans-synaptic spread of rabies virus. Furthermore, since the virus is detected by immunofluorescence methods, the neurochemical identity of the infected interneuron also can be readily ascertained by using specific antibodies against standard interneuron markers and multicolor fluorescence. Several examples are provided in Figure 7. Further information is available elsewhere (Salin et al., 2008; 2009; López et al., 2010). A parallel novel development is the introducing into neurons of the brainbow cassette trough which second-order infected neurons can be ‘illuminated’ (Lichtman et al., 2008; Kobiler et al., 2010; Card et al., 2011).

4. Tract-tracing goes ‘functional’: Combinations of retrograde tracing and in situ hybridization

Single-, double- or even triple-tracing experiments produce valuable data on the organization of brain regions and neuronal circuits. This type of information can be categorized as ‘structural information’ since the data collected reveal basically a static picture that says little about the dynamism of the circuit’s activity and the role of the neurons in temporal and spatial activity patterns. A long-desired dream is to develop tracing tools that provide the researcher with the functional correlate of the brain pathway under study. A few years ago we conceived that the analysis of changes in gene expression patterns of circuits of interest represents a feasible strategy to fill this pending gap, ultimately resulting in ‘functional’ neuroanatomical tract-tracing (Pérez-Manso et al., 2006). These studies were based on combinations of retrograde tract-tracing (using FG or CTB as retrograde tracers) with non-radioactive in situ hybridization protocols (colorimetric and fluorescent). In other words, the underlying reasoning is somewhat simplistic: efferent neurons projecting to a given brain target of interest are retrogradely traced, then the

expression of a given transcript of interest is detected within the labeled neurons by means of in situ hybridization. With this approach it is possible to disclose functional changes comparing the levels of expression for a given transcript within identified projection neurons in animal models of neurodegenerative diseases (see Figure 8). For instance, increased expression of the mRNA coding the vesicular glutamate transporter 2 (vGlut2) was shown in thalamostriatal-projecting neurons (identified after retrograde labeling with FG) following unilateral dopaminergic depletion in rats (Aymerich et al., 2006), and the same holds true for projection neurons in the subthalamic nucleus innervating the ventral thalamus of Parkinsonian monkeys (Rico et al., 2010). Furthermore, up to two different transcripts could be identified within a single retrogradely-labeled neuron, as shown for the mRNAs coding vesicular glutamate transporters 1 and 2 (vGlut1 and vGlut2) within thalamostriatal-projecting neurons, these neurons being identified by means of the retrograde transport of CTB (Barroso-Chinea et al., 2008a). Similarly, a number of changes in gene expression patterns have been reported in pallidothalamic-projecting neurons in rodents (Barroso-Chinea et al., 2008b). These procedures, although technically very demanding, represent one step over the horizon in the field of tract-tracing (reviewed in Conte-Perales et al., 2010). Finally, it is also worth noting that besides multifluorescence tracing plus in situ hybridization, a number of protocols have been made available combining colorimetric tracing with radioactive in situ hybridization. The data obtained with these protocols seem very reliable and reproducible (Ferré et al., 1994; Orieux et al., 2000; Vázquez-Borsetti et al., 2009).

5. Juxtacellular tracing and labeling of axons following intracellular recording or patch-clamping

One confusing aspects of classical tract-tracing is that most procedures, except for the single-neuron methods, result in ‘mass labeling’ of populations of neurons. These methods were originally designed to study gross fiber connectivity between brain compartments and not for the study of delicate neuronal networks of connectivity, e.g., within cortical layers. Notwithstanding the massive nature of classical labeling with retrograde tracing methods it is possible to single out individual projection neurons. Large injections with anterograde neuroanatomical tracers, on the other hand, result in the indiscriminate labeling of cells belonging to all categories of neuron present in the injection spot: intrinsic (e.g. neurons whose axon remains within a particular cortical layer, local circuit neurons (whose axons span the depth of various cortical layers) and neurons projecting out to different target nuclei. Because there are so many parameters involved, cases with identical stereotaxic injection coordinates may produce qualitatively and quantitatively quite different results in terms of labeled neurons and fibers. As a consequence, most ‘gross’ tracing

studies interpret a number of individual tracing experiments into a generalized connectivity pattern at the neuron population level. Study of microcircuitry (neurons whose axons remain within a nucleus or cortical area) requires a more refined approach with preparations that contain the smallest number of labeled neurons possible. Various strategies are possible here. First, intracellular recording of single neurons followed by labeling these neurons with biocytin (Gauthier et al., 1999), BDA (Prensa and Parent, 2001) makes it possible to trace complete dendritic patterns and follow the complete distribution of axons, axon collaterals and axon terminals of individual neurons. Second, juxtacellular deposition of neurobiotin (Pinault, 1996) or BDA (Parent and Parent, 2007) together with mild local stimulation (Pinault, 1996) results in the labeling of very small populations of neurons or even of single neurons (Wu et al., 2000; Duque and Zaborszky, 2006). A very sophisticated example of microcircuit tracing through small, juxtacellular injections is provided by Parent and Parent, 2007. Finally, the characteristics of Neurobiotin and biocytin (reviewed in section 2.3.1) favor their application for short-distance tracing purposes and single-neuron visualization (e.g. Wouterlood et al., 2004).

6. Note on recent developments: MRI diffusion-weighted 'tract tracing' in human brain

The rapid development in the last decade of diffusion tensor magnetic resonance imaging (DTI) techniques has led to a completely new type of rapid-throughput study of connectivity called 'connectomics' (review in Hagmann et al., 2010). A 'connectome' is the network made up of edges, nodes and connectivity that together form the unique entity called the human brain (Wedeen et al., 2005). Analysis of DTI datasets, through a set of computer algorithms collectively called 'tractography', reveals the trajectories of white matter fiber bundles (Conturo et al., 1999). This is quite some achievement since tract-tracing in humans has traditionally been dominated by manual dissection (Gluhbecovic and Williams, 1980), silver staining in material obtained from patients with brain lesions, or with one of the experimental methods discussed in the next section. Thus, with DTI the large fascicles and tracts in the human brain can be identified and followed to verify which brain areas are connected. No indication is provided with respect to at what end of the fiber tracts the cells of origin are located and where the terminal projection fields. Compared with histological images, those produced with DTI are low-resolution and they provide information about myelinated fiber tracts only. With the rapid advent of MRI technology and in parallel fast progression in the development of computer software, we expect an equally rapid increase of resolution leading to much more detail in the knowledge of fiber connectivity in the human brain.

7. Tracing based on diffusion in fixed or post mortem material

As recently as 1993, Francis Crick and Edward Jones complained about the lack of tract-tracing methods specifically applicable to the study of the structure of the human brain (Crick and Jones, 1993). They expressed their concern before the development of diffusion tensor MRI improved the situation considerably (see previous section). To the limited possibilities to do work on human brain material belongs, surprisingly, experimental tracing based on transport. For this purpose BDA and Neurobiotin can be applied provided that the brain tissue is unfixed and obtained after a relatively short post-mortem delay (3-8 hrs). Slices from the autopsy human brain are first incubated with artificial cerebrospinal fluid following which spot injections can be made with one of the above tracers (Dai et al., 1998a,b). As neurobiotin and BDA rely on active metabolism, these tracers fail to do their work in fixed human brain tissue. In such material, positioning of crystals of the strongly lipophilic carbocyanine dye, DiI, will result in uptake and the exclusive diffusion in myelin sheaths (Mufson et al., 1990, reviewed by Honig, 1993) and thus, after a relatively long diffusion 'spread' time, in labeling of fibers and even cells. The transport of DiI is bidirectional (see also section 7.3). Finally, several investigators have successfully injected Lucifer yellow intracellularly into neurons in slices of fixed human brain (e.g., Einstein, 1988; Belichenko and Dahlström, 1994) but these experiments served primarily for cell identification and not for tracing per sé.

7.1. Golgi silver impregnation

The names of Santiago Ramón y Cajal and Camillo Golgi are indissolubly connected to each other. Golgi became famous because he discovered the *reazione nera,* the formation of a black deposit inside neurons when a piece of brain tissue is immersed in solutions of potassium dichromate and silver nitrate (Golgi, 1873). Ramón y Cajal brought the staining method to its zenith by describing in superb detail neuronal morphology and connectivity in an amazing collection of brain regions (Ramón y Cajal, 1909-1911). Society's reward to both men was a shared Nobel Prize in 1906. Ramón y Cajal's neuron doctrine so to say is based on observations made in pieces of brains of a score of animals and human subjects stained through Golgi's *reazione nera.* The essence of Golgi silver impregnation is that, given the proper sequence of immersion in the inorganic solutions and a little bit of luck a stable, black amorphous deposit forms in individual neurons (Figure 9). This precipitate was identified by Fregerslev et al. (1971) as silver chromate. As the deposit is present throughout an impregnated cell while it does not extend beyond the limiting membrane, the contours of an impregnated neuron represent its true shape. With some chemical modification it is possible to transfer the material to the electron microscope (Blackstad, 1975; Fairén et al., 1977) (reviewed by Wouterlood, 1992; Fairén, 2005). Thus for the first time a reliable correlate was established between

the light microscopic description of an identified neuron and the subsequent electron microscopic study of its cellular details (‘correlative light-electron microscopy’, a term coined by Ingham et al. in 1985). This development was extremely important. Only the electron microscope offers resolution in the nanometer range that is necessary to distinguish the anatomical correlate of synaptic connectivity, i.e. the presynaptic bouton with its population of synaptic vesicles and the pre- and postsynaptic membrane densities that contain the molecular scaffolds and machineries supporting vesicle docking, exocytosis of neurotransmitter, transmitter reception and reuptake.

Golgi silver impregnation can be applied as a tracing tool. In well impregnated neurons the main axon and its ramifications contain the precipitate that identifies these structures as processes belonging to that neuron, even when the axon has progressed far away from the parent cell body. However, in the electron microscope it can be observed that as soon as a myelin sheath develops around an axon the silver chromate precipitate progressively decreases over a short trajectory (Fairén et al., 1977; Wouterlood and Mugnaini, 1984). Golgi silver impregnation therefore only reveals unmyelinated axons. This explains the focusing of Ramón y Cajal on brains of newborn mice and kitten because at such a young age the myelination of the major tracts is about to begin. Axon collaterals can be traced down to their distal axon terminals as long as they haven’t developed a myelin sheath and, of course, as long as they are present in the tissue blocks subjected to the impregnation procedure.

Many Golgi silver impregnation recipes are available. We have used for correlative light-electron microscopy with success on blocks of perfusion-fixed brain the following solutions: mordant consisting of 4% formaldehyde, 3% potassium dichromate and 2% chloral hydrate, 3-4 days followed by 2-3 days in 0.75% silver nitrate (dark conditions) (Wouterlood and Mugnaini, 1984). It is also possible to conduct the impregnation with (thick) sections of brain (Freund and Somogyi, 1983; Gabbott and Somogyi, 1984; Izzo et al., 1987; Dall’Oglio et al., 2010). Gold toning (Fairén et al., 1977) stabilizes the precipitate and makes it easier to prepare ultrasections.

Modeling of 3D reconstructions of Golgi-Cox impregnated material via confocal microscopic imaging has recently been introduced as the so-called ‘reflection method’ (Spiga et al., 2005). This procedure has some advantages over conventional optical microscopy, particularly the rejection of out-of-focus light. Via post-acquisition computer image processing (deconvolution and rendering methods), the background ‘noise’ is greatly reduced and an unprecedented level of rendering is obtained. Most importantly, a procedure enabling the combination of Golgi-impregnated material with immunofluorescence processing to reveal a number of neuronal markers has been developed very recently (Spiga et al., 2011). Examples of Golgi-Cox impregnated material as seen under the confocal microscope are illustrated in Figure 9.

7.2. Golgi silver impregnation combined with anterograde and retrograde tracing

The observation that axons cut off from their parent cell bodies undergo metabolic changes prior to breaking up and removal by reactive glia has been exploited by many in the past to track nerve fiber systems. Lesions can be made in an area known to give rise to a particular projection or in a fiber projection. The axons cut off from their parent cell bodies become engaged sooner or later in an intrinsic sequence including microtubule disassembly, blebbing and increased affection for heavy metal ions collectively known as 'Wallerian' degeneration, named after its pioneer, Waller (1850) (review by Saxena and Carroni, 2007). Within a time frame of hours to days the orphaned portion of the axon is removed by reactive glia (Wiśniewski et al., 1972). The metabolic changes can be visualized either via a histochemical procedure based on increased argyrophilia (e.g. Nauta, 1952; see section 2.3.2), or directly in the electron microscope via increased osmiophilia that renders the 'labeled' fibers electron dense compared with the surrounding, unlesioned fibers. The combination of the anterograde degeneration method with Golgi silver impregnation and electron microscopy was pioneered by Blackstad in 1965 and histotechnically improved by Somogyi et al. (1979) and Frotscher et al. (1981). Somogyi et al. (1985) introduced postembedding neurotransmitter immunocytochemistry in combination with correlative light-electron microscopy of Golgi silver impregnated neurons. A very nice example of this combined technique, dealing with coexistence of GABA and glutamate in identified CA3 pyramidal neuron mossy fibers in the hippocampus of primates was published by Sandler and Smith (1991).

Brain tissue blocks subjected to Golgi silver impregnation can be taken from the brains of animals involved in horseradish peroxidase (HRP) retrograde tracing experiments. The reaction product of the HRP detection histochemistry survives the silver impregnation procedure and thus provides evidence as to which region the Golgi-silver impregnated neurons project to. This combined method was pioneered by Somogyi and Smith in 1979, and it enables the anatomist to study the connectivity of single, morphologically identified neurons.

7.3. Lipophilic carbocyanine dye tracing

One of the methods that bring about labeling of individual neurons is the application of a strongly lipophilic, dialkylcarbocyanine or dialkyl aminostyryl dye (DiI, DiA; Honig and Hume, 1986). These dyes diffuse exclusively along the lipid portions of neuronal membranes and label the involved cells completely including their entire dendritic arborization, and especially including the delicate dendritic appendages. By highlighting the neuron's membraneous envelope, carbocyanine dye labeling resembles Golgi-silver impregnation. The fluorescence provided by carbocyanine dyes is very strong and robust and withstands intense illumination, e.g. in a confocal laser scanning

microscope. Several ‘colors’ (fluorescence emissions) are commercially available: DiI (red – excitation with 488 nm laser light), DiO (green - excitation with 568 nm light), DiD (short infrared - excitation with 647 nm light) and DiR (long infrared - excitation with 750 nm light) (data from the manufacturer, Invitrogen-Molecular Probes). Co-application of DiI, DiO and DiD permits three-channel, multicolor visualization in an appropriately equipped fluorescence microscope. After photoconversion of the carbocyanine dye into an electron dense substance the study of the preparation can be continued in the electron microscope (von Bartheld et al., 1990; Gan et al., 1999). As these dyes are insoluble in water their application can be problematic. Typical means of delivery are placing a solid dye crystal or a small amount of dye paste via a needle into the planned brain area. Another way of delivery is dissolution of carbocyanine dye in an inorganic solvent like dimethylformamide (DMF) (Honig and Hume, 1986) followed by pressure injection (von Bartheld et al., 1990). More exotic means of application include a ‘biolistic’ approach i.e., shooting carbocyanine-coated particles into neurons with a gene gun (Gan et al., 2000; Grutzendler et al., 2003; Neely et al., 2009). Carbocyanine dyes are mostly applied to fixed tissue wherein tracing with transport techniques is not possible or inadequate, e.g. human post mortem brain tissue and embryonic brain tissue. They are also applied to track cells in live cell cultures and cell migration models (Gan et al., 1999, 2000).

Tracing with lipophilic carbocyanine dyes, especially with DiI, is reportedly poorly compatible with immunohistochemical procedures that for antibody penetration purposes require lipid-solubilizing detergents like Triton X-100 (Elberger and Honig, 1990; Holmqvist et al., 1992). The introduction of less aggressive detergents like digitonin may improve this situation (Matsubayashi et al., 2008). In fixed, post mortem material the lipophilic dyes diffuse along lipid membranes with a speed of at most 6 mm/day (Haugland, 1996). Internalization has been reported in living cells, resulting in a granular cytoplasmic distribution of the dye (Holmqvist et al. 1992), presumably effectuated by lipid membrane turnover. Application of carbocyanine dyes for tract-tracing purposes in post mortem human material has been discussed by Molnár et al. (2006).

7.4. Intracellular filling of single neurons in slices of fixed brain

Fibers entering and innervating a particular area may do so in all kinds of ways, from the seemingly chaotic in hypothalamic networks to the near-perfect laminar order of parallel fibers in cerebellar cortex. Independent of the distribution pattern that fibers express in their terminal fields, the field itself always involves a circumscript and discrete tissue volume. Only those neurons whose dendrites extend into that discrete tissue volume are physically available to receive synaptic contacts from the innervating fibers. The cell bodies of the recipient neurons may often be

located external to the tissue volume. Most exemplary in this respect are brain areas wherein the neurons possess long apical dendrites, e.g., in cerebral and cerebellar cortex and in hippocampus where fibers of afferent projections may terminate in a stratified way, far away from the cell bodies of the neurons that receive synaptic contacts. In field CA1 of the hippocampus for example a 500 µm 'gap' exists between stratum lacunosum-moleculare where entorhinal cortical afferents end and stratum pyramidale that host the cell bodies of the CA1 pyramidal neurons (Kajiwara et al., 2008). One way to visualize entire, individual neurons, apart from procedures described in previous sections, is via intracellular injection of a dye in living neurons *in situ* or in vitro slice preparations, or in slices of lightly fixed brain tissue (the latter pioneered in 1986 by Rho and Sidman and refined in 1989 by Buhl and Lübke). Intracellular injection in living neurons is in the neurophysiology realm, outside the scope of this review. We limit this discussion therefore to intracellular injections in slices of lightly fixed brain. We present here an example of the demonstration of striato-mesostriatal neuron connectivity. The substantia nigra pars compacta (SNc) is home to the cell bodies of dopaminergic neurons that innervate the neostriatum while the fibers from striatal neurons that innervate the substantia nigra end in the pars reticulata (SNr) (see Gerfen, 2004). Similar to the hippocampus example above there is a 'gap' between terminal field of the striatal innervation and the area where the cell bodies are located that give rise to the mesencephalic neostriatal projections. Nigrostriatal cells may be involved in various striato-nigro-striatal loops (Gerfen, 2004). The anatomical proof of the existence of such a loop requires: A, labeling of the striatonigral fibers, B, labeling of the mesostriatal projection neurons, and C, proof of the convergence of A and B. Thus we conducted experiments in rats in which an anterograde tracer (BDA) was injected in the neostriatum (in this case, nucleus accumbens) simultaneously with the deposition of a retrograde tracer (FG) in the neostriatum in a different, dorsal location. After 7 days survival the midbrain of the lightly fixed brain was cut into 500 µm thick slices. These slices were inspected in a fluorescence microscope in order to identify retrogradely labeled neurons in the ventral mesencephalon. As we know from anatomical descriptions that the terminal fields of striatonigral fibers do not coincide with the positions of the cell bodies of mesostriatal neurons, our solution to bridge the gap was by intracellular injection of retrogradely labeled SNc cell bodies with a substance that a) completely fills the dendritic trees of the injected neurons, b) can be differentiated both from the label present in the anterogradely labeled fibers of striatal origin and the retrograde tracer, c) is compatible with multichannel confocal laser scanning because the latter technique is by virtue of signal separation, resolution, Z-scanning and associated 3D reconstruction very useful to determine the apposition of small structures each labeled with a different fluorescent marker (Wouterlood et al., 2007) . Several substances fulfilling the above

criteria are available for intracellular injection: Lucifer yellow (LY; Stewart, 1982) and Alexa Fluor™ 555 hydrazide (AF555; Invitrogen-Molecular Probes, Eugene, OR) (Kajiwara et al, 2008). Biocytin and Neurobiotin have been used as well for this purpose (Kita and Armstrong, 1991) (or mixtures of Lucifer Yellow and Neurobiotin to improve visibility during the approach and penetration of single cells). The method of intracellular injection of LY neurons in slices of fixed brain was pioneered by Buhl and Lübke (1989), and we started developing the combination with anterograde tracing in the pre-confocal era (Wouterlood et al., 1992), assisted by the availability of an antibody against LY (Taghert et al., 1982). LY has wide fluorescence absorption (peak at 425 nm) and emission (peak at 528 nm) spectra. Maranto (1082) was the first to publish a photoconversion procedure to convert LY into an electron dense deposit serving subsequent ultrastructural analysis of the LY filled cell in the electron microscope (photoconversion see also Box # 2).
The midbrain slices were rinsed in phosphate buffer and transferred to a small Petri dish mounted in the intracellular injection unit consisting of a fluorescence microscope equipped with a fixed stage and with long-working distance objectives, a micromanipulator and an iontophoretic injection device capable of delivering nA currents (a detailed description of the equipment is provided by Buhl and Lübke, 1989). FG-containing neurons were located and impaled with the micropipette after which we injected a small amount of LY into the cell by applying a nanocurrent to the pipette. The subsequent filling of a neuron takes about 10 minutes and can be monitored visually. Filling was judged to approach the ideal when the finest details became visible like thin distal branches of dendrites far away from their parent cell bodies. In total it was possible to fill 12 to 14 SNc neurons per slice. After filling we transferred the sections to cold phosphate-buffered 4% formaldehyde and post fixed overnight. Next, the slices were transferred to graded cryoprotective solutions with as final composition 20% glycerin and 2% dimethyl sulfoxide (DMSO) in PB (Rosene et al., 1986), frozen on dry ice and resectioned at 40 µm thickness. Subsequently they were rinsed and immunostained with a cocktail of primary antibodies: rabbit anti-LY and goat anti-tyrosine hydroxylase (to determine whether the intracellularly labeled cells are dopaminergic). The next step consisted of incubation with donkey anti-rabbit - AlexaFluor™ 488 in a cocktail with streptavidin-Alexa Fluor™ 546 to detect the LY simultaneously with the anterogradely transported BDA. Donkey anti-goat Alexa™ 633 was included in the cocktail to identify tyrosine hydroxylase immunopositive cells and dendrites which we take for evidence of being dopaminergic. This third marker added even more value by helping us to accurately delineate the SNc at low magnification. The triple-immunofluorescence sections were investigated at high magnification (63x immersion objective) in a three-channel confocal laser scanning microscope equipped wit the appropriate lasers and filtering (details in Kajiwara et al., 2008). A striking example of a contact between a

BDA labeled striatonigral fiber and a LY filled dendrite of a tyrosine hydroxylase positive, FG-labeled nigrostriatal neuron, is shown in Figure 10.

The general definition of a contact is the physical apposition of processes of two different neurons (SNr: varicosity of a BDA labeled fiber with a TH-positive, LY labeled dendrite of a retrogradely labeled SNc neuron). We especially looked for varicosities because fibers and dendrites often are in plain juxtaposition associated with the dense packing of fibers, axons and dendrites in a constrained neuropil compartment. We have good reasons to consider boutons of PHA-L labeled fibers as the light microscopic representations of axon terminals since correlative light and electron microscopy has shown good correlation between such swellings and axon terminals (Wouterlood and Groenewegen, 1985). Boutons are operationally defined by us as any swelling of a fiber in an *en passant* or terminal position with a diameter at least three times that of the fiber giving rise to the swelling.

We employ the intracellular injection technique in three situations. The first is when we suspect that the terminal field of a fiber projection to an area of interest is located at a dendrite's length away (the 'previously discussed 'gap') from the perikarya of the neurons that project out of that area of interest. The second situation occurs when we are interested in the distribution of contacts of afferent fibers on the dendritic tree of neurons of a particular morphological type, and the third situation is when we are interested in the convergence of fibers that originate from two sources onto the dendrites of individual neurons in a particular area (e.g., Kajiwara et al., 2008).

Next to advantages the intracellular injection method has its limitations. The technique is very demanding and requires highly skilled personnel. Furthermore, only a limited number of neurons can be filled intracellularly in each slice and there is always the operator's bias to impale the retrogradely labeled neurons most closely located to the surface of the slice, producing filling of only part of the dendritic tree as well as filling of truncated dendrites. As mentioned above in section 3.2., retrograde Golgi-like labeling using rabies virus can be regarded as a feasible alternative method. Since the visualization of structures displaying viral tracing is made by using a monoclonal antibody against a viral phosphoprotein, this procedure is then fully compatible with existing tools for anterograde tract-tracing such as BDA and PHA-L. The combination of rabies virus with BDA and PHA-L in a multiple tracing paradigm enables the unequivocal identification of the potential convergence of two afferent systems onto a given population of projection neurons (and hence connected interneurons). The subsequent use of high-resolution confocal laser scanning microscopy followed by post-acquisition computer image processing (deconvolution and rendering) resulted in the accurate visualization of the pre- and post-synaptic elements with an unprecedented level of resolution (Salin et al., 2008; López et al., 2010). However, it should be

considered that such a tracer combination has two main inherent caveats: firstly, tracing with rabies virus requires a survival time shorter than the one often used for BDA and PHA-L and therefore a two-step surgical procedure is always required. Secondly, a number of safety concerns should be strictly regarded when manipulating these kinds of viral strains. Illustrative examples of this combination of tracers are supplied in Figure 6.

8. Tips and tricks

BOX #1: Tracer selection is a critical choice

Neuroanatomical tracers can be broadly categorized into anterograde, retrograde and trans-synaptic tracers, depending on the direction in which tracer uptake and transport occurs. In other words, we have at our disposal different tracers for different purposes, and tracer selection always is a difficult choice, mainly depending on the researcher's needs. Below we briefly summarize a number of advantages and disadvantages of the most commonly used neuroanatomical tracers, these ones representing -to our own criteria- the best choices to satisfy almost any experimental design, even when used alone or in combination among themselves. Please also consider the 'golden rules' (section 2.11).

1. Biotinylated dextran amine (BDA, 10kD, Ref: D-1956 from Molecular Probes-Invitrogen)

Type of tracer: Mostly anterograde, with a moderate retrograde transport.

Advantages:

- Immunohistochemistry-independent visualization, making it easy to combine BDA-tracing with other tracing methods and with [additional] immunohistochemistry to detect neuroactive substances.
- BDA can be delivered by both pressure and iontophoresis.
- Compatible with a wide variety of delivery vehicles: distilled water to different phosphate buffers. In our hands, best results were obtained with BDA in 0.01 M phosphate buffer, pH 7.25. Range of concentrations: 5-10%
- Survival time is not critical, ranging from 4 days to 2 months (survival times longer than 2 months were never tested by us).
- Very well suited for ultrastructural studies.
- Efficacy proven in a large number of animal species.
- Golgi-like retrograde labeling being made possible when using BDA 3 kD.

Disadvantages:

- Taken up by fibers of passage, particularly when large volumes are pressure-injected.
- When considering multiple staining paradigms, biotinylated secondary antibodies might crossreact with the BDA during the detection step for the additional markers.

2. *Phaseolus vulgaris*-leucoagglutinin (PHA-L, Ref: L-1110 from Vector Laboratories)

Type of tracer: Exclusively anterograde.

Advantages:

- Two primary antibodies against PHA-L are available, one raised in rabbit (first choice; Ref: AS-2300 from Vector Labs), the other raised in goat (second choice; Ref: AS-2224 from Vector Labs).
- PHA-L requires iontophoretical delivery.
- To be injected as a 2.5% solution in 0.05 M PB, pH 7.4.
- Survival time is not critical, from 7 days to 3 months.
- No uptake by fibers of passage.
- Efficacy proven in a large number of animal species.

Disadvantages:

- Somewhat capricious nature.
- Most successful are small, iontophoretic injections. Coverage of larger areas requires multiple penetrations/small injections.

3. Fluoro-Gold (FG, from Fluorochrome, Inc.)

Type of tracer: Exclusively retrograde

Advantages:

- Direct fluorescent emission in the UV range, highly resistant to fading when compared to other fluorescent tracers.
- A primary antibody against FG raised in rabbit is available from Chemicon (Ref: AB153).
- FG allows pressure and iontophoretical delivery.
- Compatible with a wide variety of delivery vehicles: distilled water, phosphate buffers and cacodylate buffer (the latter one probably is the best choice). In our hands, best results were obtained with FG as a 3% solution in 0.1 M cacodylate buffer, pH 7.3.
- Survival time is not critical, from 2 days to 1 year.
- Efficacy proven in a large number of animal species. It is worth noting that somewhat poor results were obtained in monkeys, probably due to the vehicle used for delivering FG. As

mentioned above, cacodylate buffer in our hands represents a good choice to circumvent these problems.

Disadvantages:

- Taken up by fibers of passage, particularly when large volumes are pressure-injected. It is generally accepted that that the iontophoretical delivery of FG minimizes the uptake by fibers of passage (Divac and Mogensen, 1990; Pieribone and Aston-Jones, 1988; Schmued and Fallon, 1986; Schmued and Heimer, 1990).

4. Cholera toxin, B subunit (CTB, Ref: 104 from List Biological Laboratories)

Type of tracer: Mostly retrograde, with some anterograde transport.

Advantages:

- Well suited when large tracer deposits are required.
- Two primary antibodies against CTB are available, one raised in rabbit (first choice; Ref: 18-272-195906 from GenWay), the other raised in goat (Ref: 703 from List Biologicals).
- CTB allows pressure and iontophoretical delivery (better results obtained with pressure injections).
- CTB is injected as a 2% solution in 0.1 M phosphate buffer, pH 6.0.
- Survival time is not critical, from 4 days to 4 weeks (it is worth noting that anterograde tracing with CTB is enhanced when short survival times are used).
- Efficacy proven in a large number of animal species. In our hands, CTB represents the first choice retrograde tracer for monkey experiments.
- A large number of Alexa™ Fluor conjugates of CTB have been made available recently from Molecular-Probes-Invitrogen. In our hands, all these Alexa™ Fluor -CTB conjugates work similarly to unconjugated CTB. More specific information on these conjugates can be found elsewhere (Conte et al., 2009a,b).

Disadvantages:

- Taken up by fibers of passage.

Box #2: Best ways to visualize labels in multiple tract-tracing paradigms

1. Multiple immunoperoxidase methods (light and electron microscopy)

Detecting up to three neuroanatomical tracers by immunoperoxidase methods is a choice that has been made possible following the introduction of a number of different peroxidase substrates.

Selected chromogens should obviously differ in color or aspect in such a way that unequivocal discrimination is possible. Moreover, whenever possible the selected peroxidase substrates should have their own ultrastructural identity or texture. A brief survey of the most commonly used peroxidase substrates is provided in Cartoon 2.

Option #1: Triple neuroanatomical tracing combining WGA-HRP + PHA-L + biocytin (Smith and Bolam, 1991, 1992). Injected tracers were visualized by using tetramethylbenazine (TMB), nickel-enhanced diaminobenzidine (DAB-Ni) and diaminobenzidine (DAB), respectively.

Option #2: Triple neuroanatomical tracing combining PHA-L + rhodamine-dextran amine + BDA (Dolleman-Van der Weel et al., 1994). Injected tracers were visualized using DAB-Ni, DAB and 1-napthol/azur B, respectively.

Option #3: Combinations of BDA + PHA-L + FG or BDA + CTB + FG. Tracers were sequentially visualized by using DAB-Ni, DAB and V-VIP (see Lanciego et al., 1997; 1998a,b; 2000; Köbbert et al., 2000; Gonzalo et al., 2001). A number of illustrative examples dealing with multiple immunoperoxidase methods are provided in Figures 2, 4, 11, and 12.

At the ultrastructural level the immunoperoxidase detection of an anterogradely transported tracer can be combined with immunoperoxidase-silver enhancement detection of a neuroactive substance present in the structures postsynaptic to tracer-labeled axon terminals. Illustrative in this respect is an electron microscopic study by Omelchenko and Sesack (2009) describing the detection of transported PHA-L via an immunoperoxidase protocol, in combination with pre-embedding immunocytochemistry to detect tyrosine hydroxylase or GABA with a silver enhanced gold-immunoperoxidase procedure. Pre-embedding peroxidase detection of transported PHA-L in combination with postembedding GABA immunocytochemistry to determine the neurotransmitter inside tracer-containing presynaptic axon terminals was pioneered by Freund and Antal (1988).

To the very best of our knowledge, the only attempt successfully combining three different markers was made by Anderson et al. (1994). Each marker was visualized with a different peroxidase substrate, therefore resulting in three different electron dense textures, comprising DAB (flocculent precipitate), silver-intensified immunogold (distinct texture of the precipitate) and benzidine hydrochloride (crystalline texture). In this regard, it is worth noting that the V-VIP peroxidase substrate also has its own characteristic electron dense texture (granular appearance), easily distinguishable from other commonly used peroxidase substrates in pre-embedding procedures, such as DAB. Illustrative examples comparing the ultrastructural precipitates of DAB and V-VIP when combined together in double pre-embedding methods are provided in Figure 11.

2. Multiple immunofluorescence methods

The availability of an expanding number of fluorochrome-conjugated secondary antibodies together with the standardization of confocal microscopy has boosted the implementation of a great number of multiple fluorescence labeling strategies (see also Cartoon 3). Since there is no longer a need for achieving a permanent detection through the use of different peroxidase substrates, multi-fluorescence scenarios have made multitracing studies easier than ever (see examples provided in Figures 3, 4, 6 and 7). Overall, the same considerations that apply to tracer selection for combined paradigms should also be regarded when considering multiple fluorescence visualization, as stated above in section 2.10 (“multitracing experiments with various anterograde and retrograde tracers”). Drawbacks include fading of the fluorescence signal over time or following repetitive exposure and the danger of unnoticed fluorescence signal crosstalk in an inappropriately configured or operated confocal instrument. Several examples comparing multiple immunoperoxidase vs. multiple immunofluorescence are provided in Figure 4. Fluorescent labels can via strong UV illumination in the presence of DAB be ‘photoconverted’ into an electron dense label (Maranto, 1982; Buhl and Lübke, 1989; Bentivoglio and Su, 1990; Lübke, 1993; Kacza et al., 1997).

BOX #3: Co-injecting tracers to visualize reciprocally-connected brain areas

A number of techniques are available for the analysis of reciprocally-interconnected brain areas. Procedures are based on preparing a variety of cocktails of neuroanatomical tracers that basically mix together one anterograde tracer with a given retrograde tracer. By taking advantage of these combinations, it is possible to simultaneously elucidate both afferent and efferent connections from a single injection site. In other words, a single cocktail injection allows visualizing the efferent axons arising from as well as the afferent neurons projecting to the injected brain area. For these purposes, the most reliable alternatives include the combination of BDA + CTB (Coolen et al., 1999) as well as combinations of either PHA-L+CTB or BDA+FG (Thompson and Swanson, 2010). Besides the use of cocktails of tracers, it is also worth noting that BDA labeling of axon collaterals could be used for the analysis of reciprocal connections between functionally-related neuronal groups (Shink et al., 1996).

BOX #4: Be aware of fluorescent conjugates of CTB

The retrograde tracer cholera toxin B subunit (CTB) has been broadly used as an excellent retrograde tracer. Most often, CTB is used as an unconjugated preparation, to be detected via an immunoperoxidase procedure (Luppi et al., 1990). More recently, a large variety of Alexa™ Fluor-conjugates of CTB have been made available by Molecular Probes-Invitrogen, including CTB Alexa™ Fluor 488, 555, 594 and 647 (Refs: C-34775, C-34776, C-34777 and C-34778, respectively). The combined use of these conjugates allows sensitive multiple retrograde tracing paradigms to be easily implemented (Conte et al., 2009a,b). Furthermore, when considering permanent visualization of Alexa™ Fluor conjugates of CTB, it is worth mentioning that a reliable rabbit anti- Alexa™ Fluor 488 antibody is also available from Molecular Probes-Invitrogen (Ref: A-11094), and therefore Alexa™ Fluor 488-conjugated CTB (CTB488) can be converted into a permanent precipitate by immunoperoxidase methods. The manufacturer claims that the CTB488 is not detected with standard anti-CTB antibodies. This feature would enable the implementation of a dual retrograde immunoperoxidase labeling paradigm including the combination of unconjugated CTB (to be detected with anti-CTB antibodies) with CTB488 (to be detected with the anti- Alexa™ Fluor 488 antibody). However, we empirically found that this claim is not realistic (Figure 13).

In summary, although Alexa™ Fluor conjugates of CTB are very good choices for multiple retrograde tracing (here we have successfully tested CTB488, CTB555 and CTB647; see also Conte et al., 2009a,b) the combination of unconjugated CTB and CTB488 is a poor choice for dual labeling experiments. Therefore, retrograde tracers other than unconjugated CTB (we propagate here selecting Fluoro-Gold) should be used in multiple retrograde tracing when combined with Alexa Fluor™ conjugates of CTB. Finally, single retrograde tracing with CTB488 is a good choice when bearing in mind the permanent detection of CTB488-labeled neurons via immunoperoxidase methods by using the available anti-Alexa™ Fluor 488 antibody.

9. Acknowledgements

We like to acknowledge the continuous and generous support provided by technicians who skillfully assisted us in the past: Barbara Jorritsma-Byham, Annaatje Pattiselanno, Peter Goede, Amber Boekel and Ainhoa Moreno, as well as the professional support of the current generation of technical assistants: Elvira Roda at Pamplona and Angela Engel in Amsterdam. Their skills and enthusiasms always made our daily work much easier. Moreover, we also want to recognize the know-how, technical skills and “savoir faire” received from our former mentors, Dr. Enrico Mugnaini (FGW) and Dr. Francisco Collía (JLL). All experiments dealing with tract-tracing using rabies viruses are part of an ongoing collaboration with Lydia Kerkerian-Le Goff, Pascal Salin, Philippe Kachidian and Patrice Coulon from the Institut de Biologie du Développement de Marseille Luminy UMR 6216 (France). Funding to JLL comes from the Spanish Ministry of Science and Innovation (ref: BFU2006-06744 and BFU2009-08351), Ciberned (ref: CB06/05/08351), Departamento de Salud del Gobierno de Navarra and by the UTE project/Foundation for Applied Medical Research. Funding to FGW comes from the VU Medical Center, Amsterdam.

10. Figure Legends

CARTOON 1: Chemical formulation of Fluoro-Gold (hydroxystilbamidine).

CARTOON 2: Overview of peroxidase substrates currently available.

CARTOON 3: Absorption (excitation and emission spectra for the most commonly used Alexa™ Fluor conjugates, together with standard band-pass (BP) and long-pass (LP) filters commonly implemented to avoid cross-talk phenomena.

FIGURE 1: Multiple retrograde fluorescence tracing viewed under epifluorescence illumination. The retrograde tracers Fluoro-Gold (FG; yellow-labeled neurons), Fast Blue (FB; blue-labeled neurons) and Alexa™ Fluor 555-conjugated cholera toxin (CTB555, red-labeled neuron) have been injected in different cortical areas of the rat to further identify basal forebrain neurons innervating the cerebral cortex. Neurons innervating two different cortical areas by means of axon collaterals are double labeled with FB and CTB555 (arrow). Scale bar is 150 μm.

FIGURE 2: Multiple colorimetric tract tracing in a primate, combining dual retrograde tracing with Fluoro-Gold (FG; injected in the putamen) and cholera toxin (CTB; injected in the caudate nucleus), together with anterograde tracing with biotinylated dextran amine (BDA; injected in the external division of the globus pallidus). Transported BDA is firstly visualized using a nickel-enhanced DAB solution (black product), followed by CTB visualization using a regular DAB solution (brown-labeled neurons). Finally, neurons containing transported FG are finally stained in purple using the V-VIP substrate. (A-C) Photomicrographs taken at the level of the substantia nigra illustrating structures displaying labeling for each of the transported tracers.

FIGURE 3: Multiple fluorescence tract tracing combining dual retrograde tracing with Fluoro-Gold (FG; injected in the rat entopeduncular nucleus) and cholera toxin (CTB; injected in the substantia nigra pars reticulata), together with anterograde tracing with biotinylated dextran amine (BDA; injected in the parafascicular nucleus of the thalamus). Sections were first incubated in a cocktail solution of primary antisera comprising 1:2000 rabbit-anti FG (Chemicon) and 1:2000 goat anti-CTB (List Biologicals), followed by a second cocktail solution of antisera comprising 1:200 Alexa488-conjugated donkey anti-rabbit IgG (Molecular Probes-Invitrogen) and 1:200 Alexa564-conjugated donkey anti-goat IgG (Molecular Probes-Invitrogen). Transported BDA was next visualized using an Alexa633-conjugated

streptavidin (1:100; Molecular Probes-Invitrogen). FG was visualized in green, CTB was color-coded in light blue, and BDA in red color. Scale bar is 50 μm.

FIGURE 4: Brightfield microscopy compared with fluorescence confocal microscopy in multiple tracing paradigms. (A) BDA-labeled thalamostriatal projections are stained in black with DAB-Ni; CTB (DAB peroxidase substrate, brown) was used to disclose striatonigral-projecting neurons, whereas FG-labeled striatopallidal neurons are seen in purple with V-VIP substrate. Scale bar: 30 μm (B) An adjacent section containing the same combination of tracers was visualized under the confocal microscope. In this case, BDA-labeled fibers are color-coded in red, CTB-containing neurons in light blue, and neurons labeled with FG are visualized in green. Scale bar: 40 μm (C) Inset taken from B at higher magnification. Scale bar: 20 μm (D) Shows a combination of BDA-labeled thalamostriatal projections (stained in black with DAB-Ni), striatal cholinergic interneurons (DAB peroxidase substrate, brown) and FG-labeled striatopallidal neurons (V-VIP, purple reaction color). Scale bar: 15 μm (E) The same combination of markers as seen in an adjacent section by means of confocal laser-scanning microscopy. Scale bar: 40 μm (F) Inset taken from E at higher magnification. Scale bar: 20 μm (G) Anterograde tracing of thalamostriatal fibers (BDA-labeled, black reaction color, DAB-Ni substrate) combined with the immunocytochemical detection of striatal interneurons positive for parvalbumin (brown color, DAB peroxidase substrate) and with FG tracing to identify striatopallidal-projecting neurons (purple-stained neurons, V-VIP reaction product). Scale bar: 30 μm (H) The same combination of markers in an adjacent section seen with confocal laser-scanning microscopy. Scale bar: 40 μm (I) Inset taken from E at higher magnification. Scale bar: 20 μm. Triple immunoperoxidase methods using three different peroxidase chromogens (DAB-Ni, DAB and V-VIP) allow the permanent visualization of three markers in the same histological section. Although multiple immunofluorescent stains suffer from inherent fading problems over time, it is worth summarizing several advantages: firstly, the histological processing is less demanding than multiple immunoperoxidase methods; secondly, laser zooming with the confocal microscope enhances the visualization of cellular details and finally, the confocal microscope allows the unequivocal identification of colocalizing markers.

FIGURE 5: Golgi-like retrograde tracing of striatonigral neurons using rabies virus. Application of a monoclonal antibody raised against a soluble viral phosphoprotein produces a very high degree of detail, even the thinnest dendrites as well as small cellular processes like dendritic spines. Scale bar: 30 μm in panel A and 7.5 μm in panel B.

FIGURE 6: Dual anterograde tracing with BDA and PHA-L combined with retrograde tracing using rabies virus. Striatonigral neurons were retrogradely labeled following an injection of rabies virus in the substantia nigra pars reticulata (color-coded in green). The anterograde tracer PHA-L was injected in the thalamic parafascicular nucleus to further identify thalamostriatal projections (color-coded in blue). In the same surgical session, the anterograde tracer BDA was delivered into primary motor cortex to label corticostriatal projections (color coded in red). Through post-acquisition deconvolution followed by volumetric rendering a final resolution is obtained high enough to disclose potential contacts between pre- and post-synaptic elements. Scale bar are 40 μm (A), 20 μm (B) and 3 μm (C).

FIGURE 7: Trans-synaptic tracing with rabies virus (RV) to identify interneurons innervating projection neurons. (A) Thalamostriatal projections labeled with PHA-L. (B) Cholinergic striatal interneurons. (C) Striatal neurons labeled following a deposit of RV into the substantia nigra pars reticulata. Up to two different types of neurons were identified, one type comprising striatonigral-projecting neurons (first-order neurons, asterisk), the other one consisting of a cholinergic interneuron infected with rabies virus (second-order neuron, arrowhead). (D) Only cholinergic interneurons innervating striatonigral neurons were secondarily infected with rabies virus (arrowhead), whereas cholinergic interneurons innervating striatofugal neurons other than the ones projecting to the substantia nigra remained unlabeled with rabies virus (arrow). Scale bar is 40 μm in all panels.

FIGURE 8: “Functional” neuroanatomical tract-tracing. Combination of retrograde tracing with cholera toxin together with dual fluorescence in situ hybridization to further assess the expression levels for the transcripts of interest (GAD56 mRNA and vGlut2 mRNA). (A) the retrograde tracer CTB was pressure-injected into the ventral anterior and ventral lateral thalamic nuclei, resulting in a large number of CTB-positive neurons being identified a the level of the internal division of the globus pallidus (B&C). Scale bars are 3,500 μm in A, 500 μm in B and 100 μm in C. (D) Pallidothalamic-projecting neurons showing CTB retrograde labeling. (E) Expression of GAD65 mRNA. (F) Expression of vGlut2 mRNA. (G) Merged image showing that all pallidothalamic-projecting neurons contains transcripts for GAD65 and vGlut2 mRNA. Scale bar is 30 μm in panels D-G.

FIGURE 9: Layer V pyramidal neurons of the rat auditory cortex. (A) Golgi-Colonnier stain, brightfield illumination. (B) Golgi-Cox stain, visualized in the confocal laser-scanning microscope, using reflection mode. Scale bar is 80 μm in panel A and 40 μm in panel B.

FIGURE 10: Combination of anterograde tracing (BDA injected ventrally in the striatum of a rat), retrograde tracing (FG injected dorsally in the striatum), and intracellular Lucifer yellow injection (LY) of FG-labeled neurons in the mesencephalon, in slices of fixed brain. A. low-magnification view of the mesencephalon showing the LY injected neuron (circled), TH-positive, in the ventral tegmental area (VTA). Blue immunofluorescence represents tyrosine hydroxylase. SNc and SNr = substantia nigra, pars compacta and reticulata. MB = mamillary body, P = cerebal peduncle. Bar = 250 µm. B High magnification confocal image showing LY (488 nm excitation, green), BDA (543 nm, red) and TH (633 nm, blue). Most contacts of BDA fibers are on TH+ (dopaminergic) neurons. bar = 50 µm. C, A complicated contact, far away from the cell body of a FG labeled, LY injected cell, between a BDA-labeled fiber and the LY-containing dendrite of a FG-positive, TH-positive and LY filled neuron. Green: dendrite of LY injected neuron, red, BDA. the arrow indicates the contact. bar = 10 µm. D, Screenshot of a computer 3D reconstruction of this dendrite (green), the BDA-labeled fiber (red) and the contact. This fiber spirals around a spine on the dendrite while being in contact. Bar = 2 µm. All images for this purpose enhanced with computer software (Photoshop).

FIGURE 11: (A) Multiple colorimetric detection of (i) BDA-labeled perirhinal afferents reaching the entorhinal cortex (DAB-Ni substrate), (ii) FG-labeled layer II neurons of the entorhinal cortex projecting to the hippocampus (brown-labeled with DAB) and (iii) parvalbumin-immunoreactive layer III interneurons (purple-labeled with V-VIP substrate). Presumptive contacts between anterogradely-labeled terminals and parvalbumin neurons are marked with blue arrowheads. (B & C). Asymmetric synapses formed by BDA-labeled terminals (DAB flocculent reaction product) onto parvalbumin-positive dendrites (granular V-VIP precipitate). Besides the usefulness of V-VIP substrate for multiple colorimetric paradigms, one of the main advantages of this substrate is represented by its own ultrastructural texture, which makes this peroxidase chromogen very suitable for double pre-embedding methods in ultrastructural studies. Scale bar is 100 µm.

FIGURE 12: Multiple colorimetric detection of (i) thalamostriatal axons, labeled with BDA and stained in brown with DAB, (ii) striatonigral-projecting neurons, retrogradely labeled with FG and stained in purple with V-VIP substrate and (iii) NADPH-d striatal interneurons, stained with nitroblue tetrazolium (blue reaction product). Scale bar is 100 µm

FIGURE 13: The combination of Alexa™ Fluor 488-conjugated CTB (CTB488) with unconjugated CTB (CTB) is not a good choice for their combined use. Antibodies against the unconjugated form of CTB also recognize CTB488. One monkey received one injection of CTB488 in the GPi nucleus (panel A)

and one injection of unconjugated CTB in the thalamic ventral nuclei VA/VL (not shown). Single immunoperoxidase detection of transported CTB488 (by using an anti- Alexa™ Fluor 488 antibody) revealed both the injection site (GPi nucleus, panel A) as well as the expected retrograde labeling observed in the striatum (striatopallidal-projecting neurons, panel A'). However, the same pattern of labeling was noticed when detecting the unconjugated form of CTB with antibodies against CTB (panels B & B'). Both the injection site of CTB488 as well as CTB488-containing striatopallidal-projecting neurons was observed, according to a pattern that fully mimics the one that accounts for CTB488 tracing. In other words, since there is no "striato-thalamic pathway", these results demonstrate the presence of cross-reactivity between the anti-CTB antibody and the Alexa™ Fluor 488-conjugated CTB. Scale bar is 2,000 μm for panels A & B, and 100 μm in insets.

11. Literature references

Anderson KD, Karle EJ, Reiner A. 1994. A pre-embedding triple-label microscopic immunohistochemical method as applied to the study of multiple inputs to defined nigral neurons. J Histochem Cytochem 42:49-56.

Aston-Jones G. Card JP. 2000. Use of pseudorabies virus to delineate multisynaptic circuits in brain: opportunities and limitations. J Neurosci Meth 103:51-61.

Aymerich MS, Barroso-Chinea P, Pérez-Manso M, Muñoz-Patiño AM, Moreno-Igoa M, González-Hernández T, Lanciego JL. 2006. Consequences of unilateral nigrostriatal denervation on the thalamostriatal pathway in rats. Eur J Neurosci 23:2099-2108.

Baba Y. 2000. New methods of dye application for staining motor neurons in an insect. J Neurosci Meth 98:165-169.

Bachmann L, Salpeter MM. 1969. Resolution in electron microscope radioautography. J Cell Biol. 41:1-32.

Bácskai T, Veress G, Halasi G, Matesz C. 2010. Crossing dendrites of the hypoglossal motoneurons: possible morphological substrate of coordinated and synchronized tongue movements of the frog, Rana esculenta. Brain Res 1313:89-96.

Barbas-Henry HA, Wouterlood FG. 1986. Synaptic connections between primary trigeminal afferents and accessory abducens motoneurons in the monitor lizard, *Varanus exanthematicus*. J Comp Neurol 267:387-397.

Barroso-Chinea P, Castle M, Aymerich MS, Lanciego JL. 2008a. Expression of vesicular glutamate transporters 1 and 2 in the cells of origin of the rat thalamostriatal pathway. J Chem Neuroanat 35:101-107.

Barroso-Chinea P, Rico AJ, Pérez-Manso M, Roda E, López IP, Luis-Ravelo D, Lanciego JL. 2008b. Glutamatergic pallidothalamic projections and their implications in the pathophysiology of Parkinson's disease. Neurobiol Dis 31:422-432.

Basbaum AI, Menetrey D. 1987. Wheat germ agglutinin–apoHRP gold: a new retrograde tracer for light- and electron-microscopic single and double-label studies. J Comp Neurol 261:306–318.

Bazer GT, Ebbesson SO. 1984. A simplified cobalt-lysine method for tracing axon trajectories in the central nervous system of vertebrates. Neurosci Lett. 51:315-318.

Becker H. 1952. Retrograde und transneuronale degeneration der Neurone. Abh. Math-Naturwiss Klasse, nr. 10: 3-162.

Belichenko PV, Dahlström A. 1994. Dual channel confocal laser scanning microscopy of lucifer yellow-microinjected human brain cells combined with Texas red immunofluorescence. J Neurosci Meth 52:111-8.

Bentivoglio M, Kuypers HG, Castman-Berrevoets CE, Dann O. 1979. Fluorescent retrograde neuronal labeling in rat by means of substances binding specifically to adenine-thymine rich DNA. Neurosci Lett 12:235-240.

Bentivoglio M, Kuypers HG, Castman-Berrevoets CE, Loewe H, Dann O. 1980. Two new fluorescent retrograde neuronal tracers which are transported over long distances. Neurosci Lett 18:25-30.

Bentivoglio M, Su H-S 1990. Photoconversion of fluorescent retrograde tracers. Neurosci Lett 113:127-133.

Bharali DJ, Klejbor I, Stachowiak EK, Dutta P, Roy I, Kaur N, Bergey EJ, Prasad PN, Stachowiak MK. 2005. Organically modified silica nanoparticles: A nonviral vector for in vivo gene delivery and expression in the brain. PNAS 102:11539-11544

Björklund A, Skagerberg G. 1979. Simultaneous use of retrograde fluorescent tracers and fluorescence histochemistry for convenient and precise mapping of monoaminergic projections and collateral arrangements in the CNS. J Neurosci Meth 1:261-277

Blackstad TW. 1965. Mapping of experimental axon degeneration by electron microscopy of Golgi preparations. Z Zellforsch Mikrosk Anat 67: 819–834.

Blackstad TW. 1975. Electron microscopy of experimental axonal degeneration in photochemically modified Golgi preparations: a procedure for precise mapping of nervous connections. Brain Res 95:191-210.

Boesten AJP, Voogd J. 1985. Hypertrophy of neurons in the inferior olive after cerebellar ablations in the cat. Neurosci Lett 61:49-54.

Cowan WM, Gottlieb DI, Hendrickson AE, Price JL, Woolsey TA.1972. The autoradiographic demonstration of axonal connections in the central nervous system. Brain Res. 37:21-51.

Cowan WM, Cuénod M. 1975. The use of axonal transport for the study of neural connections: a retrospective survey. In The Use of Axonal Transport for Studies of Neuronal Connectivity. (eds Cowan MW, Cuénod M. Elsevier, Amsterdam, p 1.

Buhl EH, Lübke J. 1989. Intracellular lucifer yellow injection in fixed brain slices combined with retrograde tracing, light and electron microscopy. Neuroscience 28:3-16.

Card JP, Kobiler O, McCambridge J, Ebdlahad S, Shan Z, Raizada MK, Sved AF, Enquist LW. 2011. Microdissection of neural networks by conditional reporter expression from a Brainbow herpesvirus. Proc Natl Acad Sci USA, Feb 3 (Epub ahead of print).

Chakravarthy S, Keck T, Roelandse M, Hartman R, Jeromin A, Perry S, Hofer SB, Mrsic-Flogel T, Levelt CN. 2008. Cre-dependent expression of multiple transgenes in isolated neurons of the adult forebrain. PLoS One 3:e3059.

Chang HT. 1991. Anterograde transport of Lucifer yellow-dextran conjugate. Brain Res Bull 26:813-816.

Chang HT, Kuo H, Whittaker JA, Cooper NG. 1990. Light and electron microscopic analysis of projection neurons retrogradely labeled with Fluoro-Gold: notes on the application of antibodies to Fluoro-Gold. J Neurosci Meth 35:31-37.

Chase R, Tolloczko B. 1993. Tracing neural pathways in snail olfaction: from the tip of the tentacles to the brain and beyond. Microsc Res Tech. 24:214-230.

Chen S, Aston-Jones G. 1997. Axonal collateral-collateral transport of tract tracers in brain neurons: false anterograde labelling and useful tool. Neuroscience 82:1151-1163.

Conte WL, Kamishina H, Reep RL. 2009a. The efficacy of the fluorescent conjugates of cholera toxin subunit B for multiple retrograde tracing in the central nervous system. Brain Struct Funct 213:3667-3673.

Conte WL, Kamishina H, Reep RL. 2009b. Multiple neuroanatomical tract-tracing using fluorescent Alexa Fluor conjugates of cholera toxin subunit B in rats. Nature Prot 4:1158-1166

Conte-Perales L, Barroso-Chinea P, Rico AJ, Gómez-Bautista V, López IP, Roda E, Wouterlood FG, Lanciego JL. 2010. Neuroanatomical tracing combined with in situ hybridization: Analysis of gene expression patterns within brain circuits of interest. J Neurosci Meth 194:28-33.

Conturo TE, Lori NF, Cull TS, Akbudak E, Snyder AZ, Shimony JS, McKinstry RC, Burton H, Raichle ME. 1999. Tracking neuronal fiber pathways in the living human brain. Proc Natl Acad Sci USA 96:10422-10427.

Coolen LM, Jansen HT, Goodman RL, Wood RI, Lehman MN. 1999. A new method sor simultaneous demonstration of anterograde and retrograde connections in the brain: co-injections of biotinylated dextran amine and the beta subunit of cholera toxin. J Neurosci Meth 91:1-8.

Cowan RL, Sesack SR, Van Bockstaele EJ, Branchereau P, Chain J, Pickel VM. 1994. Analysis of synaptic inputs and targets of physiologically characterized neurons in rat frontal cortex: combined in vivo intracellular recording and immunolabeling. Synapse 17:101-114.

Cragg BG. 1970. What is the signal for chromatolysis? Brain Res 23:1-21.

Crick F, Jones E. 1993. Backwardness of human neuroanatomy. Nature. 361:109-110.

Dai J, Swaab DF, Buijs RM. 1998a. Recovery of axonal transport in "dead neurons". Lancet 351:499-500.

Dai J, Van Der Vliet J, Swaab DF, Buijs RM. 1998b. Postmortem anterograde tracing of intrahypothalamic projections of the human dorsomedial nucleus of the hypothalamus. J Comp Neurol401:16-33.
shown by radioautography. J Comp Neurol. 121:325-346.

Dall'Oglio A, Ferme D, Brusco J, Moreira JE, Rasia-Filho AA. 2010. The "single-section" Golgi method adapted for formalin-fixed human brain and light microscopy.J Neurosci Meth. 189:51-55.

Deller T, Naumann T, Frotscher M. 2000. Retrograde and anterograde tracing combined with transmitter identification and electron microscopy. J Neurosci Meth 103:117-126.

Divac I, Mogensen J. 1990. Long-term retrograde labeling of neurons. Brain Res 524:339-341.

Dolleman-Van der Weel MJ, Wouterlood FG, Witter MP. 1994. Multiple anterograde tracing, combining Phaseolus vulgaris leucoagglutinin with rhodamine- and biotin-conjugated dextran amine. J Neurosci Meth 51:9-21.

Droz B, Leblond CP. 1962. Migration of proteins along the axons of the sciatic nerve. Science 137:1047-1048.

Droz B, Leblond CP. 1963. Axonal migration of proteins in the central nervous system and peripheral nerves as shown by radioautography. J Comp Neurol 121:325-46.

Duque A, Zaborszky L. 2006. Juxtacellular labeling of individual neurons in vivo: from electrophysiology to synaptology. In: Zaborszky L, Wouterlood FG, Lanciego JL (Eds) Neuroanatomical Tract-Tracing 3: Molecules, Neurons, and Systems, New York: Springer, pp. 197-236.

Egensperger R, Holländer H. 1988. Electron microscopic visualization of fluorescent microspheres used as a neuronal tracer. J Neurosci Meth 23:181-186.

Einstein G. 1993. Intracellular injection of lucifer yellow into cortical neurons in lightly fixed sections and its application to human autopsy material. J Neurosci Meth 26:95-103.

Elberger AJ, Honig MG.1990. Double-labeling of tissue containing the carbocyanine dye DiI for immunocytochemistry. J Histochem Cytochem. 38:735-739.

Fairén A. 2005. Pioneering a golden age of cerebral microcircuits: The births of the combined Golgi–electron microscope methods. Neuroscience 136:607-614.

Fairén A, Peters A, Saldanha J. 1977. A new procedure for examining Golgi impregnated neurons by light and electron microscopy. J Neurocytol. 6:311-337.

Fan RJ, Marin-Burgin A, French KA, Otto Friesen W. 2005. A dye mixture (Neurobiotin and Alexa 488) reveals extensive dye-coupling among neurons in leeches; physiology confirms the connections. J Comp Physiol A 191:1157-1171.

Ferré S, Cortés R, Artigas F. 1994. Dopaminergic regulation of the serotoninergic raphe-striatal pathway: microdialysis studies in freely-moving rats. J Neurosci 14:4839-4846.

Ferreira-Gomes J, Adães S, Sarkander J, Castro-Lopes JM. 2010. Phenotypic alterations of neurons that innervate osteoarthritic joints in rats. Arthritis Rheum 62:3677-3685.

Fink RP, Heimer L. 1967. Two methods for selective silver impregnation of degenerating axons and their synaptic endings in the central nervous system. Brain Research 4:369-374.

Foster M, Sherrington CS.1897. A Textbook of Physiology. Macmillan, New York. 1252 pp. Online at www.archive.org/stream/textbookofphysio1897fost#page/n5/mode/2up

Fregerslev S, Blackstad TW, Fredens K, Holm MJ. 1971. Golgi potassium-dichromate silver-nitrate impregnation. Nature of the precipitate studied by x-ray powder diffraction methods. Histochemie 26:289-304.

Freund TF, Antal M. 1988. GABA-containing neurons in the septum control inhibitory interneurons in the hippocampus. Nature 336:170-173.

Freund TF, Somogyi P. 1983. The section-Golgi impregnation procedure. 1. Description of the method and its combination with histochemistry after intracellular iontophoresis or retrograde transport of horseradish peroxidase. Neuroscience 9:463-474.

Fritszch B, Wilm C. 1990. Dextran amines in neuronal tracing. TINS 13:14.

Frotscher M, Rinne U, Hassler R, Wagner A. 1981. Termination of cortical afferents on identified neurons in the caudate nucleus of the cat. A combined Golgi-EM degeneration study. Exp Brain Res 41:329-337.

Fuller PM, Prior DJ.1975. Cobalt iontophoresis techniques for tracing afferent and efferent connections in the vertebrate CNS. Brain Res 88:211-220.

Gabbott PL, Somogyi J. 1984. The 'single' section Golgi-impregnation procedure: methodological description. J Neurosci Meth 11:221-230.

Gan WB, Bishop D, Turney SG, Lichtman JW. 1999. Vital imaging and ultrastructural analysis of individual axon terminals labeled by iontophoretic application of lipophilic dye. J Neurosci Meth 93:13–20.

Gan WB, Grutzendler J, Wong WT, Wong RO, Lichtman JW. 2000. Multicolor "DiOlistic" labeling of the nervous system using lipophilic dye combinations. Neuron. 27:219-225.

Geerling JC, Mettenleiter TC, Loewy AD. 2006. Viral tracers for the analysis of neural circuits, in Neuroanatomical Tract-Tracing 3 (Zaborszky L, Wouterlood FG, Lanciego JL, Eds), pp. 263-303, Springer, NY, USA.

Gerfen, CR. 2004. Basal Ganglia. In Paxinos G (ed) The rat nervous system, Elsevier Academic Press. 3rd Edition, pp. 455-508.

Gerfen CR, Sawchenko PE.1984. An anterograde neuroanatomical tracing method that shows the detailed morphology of neurons, their axons and terminals: immunohistochemical localization of an axonally transported plant lectin, *Phaseolus vulgaris* leucoagglutinin (PHA-L). Brain Res 290:219-238.

Gerfen CR, Sawchenko PE. 1985. A method for anterograde axonal tracing of chemically specified circuits in the central nervous system: combined *Phaseolus vulgaris*-leucoagglutinin (PHA-L) tract tracing and immunohistochemistry. Brain Res 343:144-150.

Glover JC, Petursdottir G, Jansen JKS. 1986. Fluorescent dextran amines used as axonal tracers in the nervous system of chicken embryo. J. Neurosci. Methods 18: 243–254.

Gluhbecovic N, Williams TH 1980. The human brainA a photographic guide. Harper & Row Hagerstown, MD. 176 pp.

Godschalk M, Lemon RN, Kuypers HG, Ronday HK. 1984. Cortical afferents and efferents of monkey postarcuate area: an anatomical and electrophysiological study. Exp Brain Res 56:410-424.

Golgi C. 1873. Sulla struttura della sostanza grigia del cervello (Comunicazione preventiva). *Gazzetta Medica Italiana, Lombardia* **33**:244–246.

Gonatas NK, Harper C, Mizutani T, Gonatas JO. 1979. Superior sensitivity of conjugates of horseradish peroxidase with wheat germ agglutinin for studies of retrograde axonal transport. J Histochem Cytochem 27:728-734.

Gonzalo N, Moreno A, Erdozain MA, García P, Vázquez A, Castle M, Lanciego JL. 2001. A sequential protocol combining dual neuroanatomical tract-tracing with the visualization of local circuit neurons within the striatum. J Neurosci Meth. 111:59-66.

Graham RC Jr, Karnovsky MJ. 1965. The histochemical demonstration of monoamine oxidase activity by coupled peroxidatic oxidation. J Histochem Cytochem 13:604-605.

Grutzendler J, Tsai J, Gan WB. 2003. Rapid labeling of neuronal populations by ballistic delivery of fluorescent dyes. Methods 30:79-85.

Hackney CM, Altman JS. 1982. Cobalt mapping of the nervous system: how to avoid artifacts. J. Neurobiol 13:403-411.

Hagmann P, Cammoun L, Gigandet X, Gerhard S, Ellen Grant P, Wedeen V, Meuli R, Thiran JP, Honey CJ, Sporns O. 2010. MR connectomics: Principles and challenges. J Neurosci Meth 194:34-45.

Hancock MB.1986. Two-color immunoperoxidase staining: visualization of anatomic relationships between immunoreactive neural elements. Am J Anat. 175:343-352.

Harvey AR, Ehlert E, de Wit J, Drummond ES, Pollett MA, Ruitenberg MJ, Plant GW, Verhaagen J, Levelt CN. 2009. Use of GFP to Analyze Morphology, Connectivity, and Function of Cells in the Central Nervous System. in: Hicks BW (Ed) Methods in Molecular Biology, Viral Applications of Green Fluorescent Protein, vol. 515:63-95. Humana Press.

Haugland RP 1996. Handbook of fluorescent probes and research chemicals. Molecular Probes, Eurgene, OR.

Hayes NL, Rustioni A. 1979. Dual projections of single neurons are visualized simultaneously: use of enzymatically inactive [^{3}H]HRP. Brain Res 165:321-326.

Herrera M, Hurtado-García JF, Collia F, Lanciego J. 1994. Projections from the primary auditory cortex onto the dorsal cortex of the inferior colliculus in albino rats. Arch Ital Biol. 132:147-164.

Hendrickson AE. 1982. The orthograde axoplamic transport autoradiographic tracing technique and its implications for additional neuroanatomical analysis of the striate cortex. In: Cytochemical methods in neuroanatomy. Eds. Chan-Palay V, Palay SL. Alan R. Liss, New York, pp. 1-16

Holmqvist BI, Ostholm T, Ekström P.1992. DiI tracing in combination with immunocytochemistry for analysis of connectivities and chemoarchitectonics of specific neural systems in a teleost, the Atlantic salmon. J Neurosci Meth 42:45-63.

Holstege JC, Kuypers HG. 1987. Brainstem projections to lumbar motoneurons in rat--I. An ultrastructural study using autoradiography and the combination of autoradiography and horseradish peroxidase histochemistry. Neuroscience 21:345-367.

Honig M. 1993. DiI labelling. Neurosci Prot 93-050-16-01- 20.
Honig MG, Hume RI. 1986. Fluorescent carbocyanine dyes allow living neurons of identified origin to be studied in long-term cultures. J Cell Biol 103:171–187.

Horikawa K, Armstrong WE. 1988. A versatile means of intracellular labeling: injection of biocytin and its detection with avidin conjugates. J Neurosci Meth 25:1-11.

Huisman AM, Ververs B, Cavada C, Kuypers HG. 1984. Collateralization of brainstem pathways in the spinal ventral horn in rat as demonstrated with the retrograde fluorescent double-labeling technique. Brain res 3000:362-367.

Hultström D, Malmgren L, Gilstring D, Olsson Y. 1983. FITC-Dextrans as tracers for macromolecular movements in the nervous system. A freeze-drying method for dextrans of various molecular sizes injected into normal animals. Acta Neuropathol 59:53-62.

Ingham CA, Bolam JP, Wainer BH, Smith AD. 1985. A correlated light and electron microscopic study of identified cholinergic basal forebrain neurons that project to the cortex in the rat. J Comp Neurol 239:176-192.

Izzo PN, Graybiel AM, Bolam JP. 1987. Characterization of substance P- and [Met]enkephalin-immunoreactive neurons in the caudate nucleus of cat and ferret by a single section Golgi procedure. Neuroscience 20:577–587.

Jansen AS, Nguyen XV, Karpitskiy V, Mettenleiter TC, Loewy AD. 1995. Central command neurons of the sympathetic nervous system: basis of the fight-or-flight response. Science 270:644-646.

Jongen-Rêlo AL, Amaral DG. 2000. A double labeling technique using WGA-apoHRP-gold as a retrograde tracer and non-isotopic in situ hybridization histochemistry for the detection of mRNA.
J Neurosci Meth 101:9-17.

Kacza J, Härtig W, Seeger J. 1997. Oxygen-enriched photoconversion of fluorescent dyes by means of a closed conversion chamber. J Neurosci Meth 71:225-232.

Kajiwara R, Wouterlood FG, Sah A, Boekel AJ, Baks-te Bulte LTG, Witter MP. 2008. Convergence of entorhinal and CA3 inputs onto pyramidal neurons and interneurons in hippocampal area CA1. An anatomical study in the rat. Hippocampus 18:266-280.

Katz LC, Burkhalter A, Dreyer WJ. 1984. Fluorescent latex microspheres as a retrograde neuronal marker for in vivo and in vitro studies of visual cortex. Nature 310:498-500.

Katz LC, Iarovici DM. 1990. Green fluorescent latex microspheres: a new retrograde tracer. Neuroscience 34:511-520.

Keizer K, Kuypers HG. 1989. Distribution of corticospinal neurons with collaterals to the lower brain stem reticular formation in monkey (Macaca fascicularis). Exp Brain Res 74:311-318.

Keizer K, Kuypers HG, Huisman AM, Dann O. 1983. Diamidino yellow dihydrochloride (DY 2HCl); a new fluorescent retrograde neuronal tracer, which migrates only very slowly out of the cell. Exp Brain res 51:179-191.

Kelly RM, Strick P. 2000. Rabies as a transneuronal tracer of circuits in the central nervous system. J Neurosci Meth 103:63-72.

King MA, Louis PM, Hunter BE, Walker DW. 1989. Biocytin: a versatile anterograde neuroanatomical tract-tracing alternative. Brain Res 497:361-367.

Kita H, Armstrong W. 1991. A biotin-containing compound N-(2-aminoethyl)biotinamide for intracellular labeling and neuronal tracing studies: comparison with biocytin. J Neurosci Meth. 37:141-150.

Klausberger T, Somogyi P. 2008. Neuronal diversity and temporal dynamics: the unity of hippocampal circuit operations. Science 321:53-57.

Köbbert C, Apps R, Bechmann I, Lanciego JL, Mey J, Thanos S. 2000. Current concepts in neuroanatomical tracing. Prog Neurobiol 62:327-351.

Kobiler O, Lipman Y, Therkelsen K, Daubechies I, Enquist LW. 2010. Herpesviruses carrying a Brainbow cassette reveal replication and expression of limited numbers of incoming genomes. Nat Commun 1:146.

Kristensson K. 1970. Transport of fluorescent protein in peripheral nerves. Acta Neuropatol. 16:293-300.

Kristensson K, Olsson Y. 1971a. Uptake and retrograde transport of peroxidase in hypoglossal neurons. Electron microscopical localization in the neuronal perikaryon. Acta Neuropathol. 19:1–9.

Kristensson K, Olsson Y. 1971b. Retrograde axonal transport of protein. Brain Res 29:363-365.

Kristensson K, Olsson Y, Sjöstrand J.1971. Axonal uptake and retrograde transport of exogenous proteins in the hypoglossal nerve. Brain Res 32:399-406.

Kristensson K, Ghetti B, Wiśniewski HM. 1974. Study on the propagation of herpex simplex virus (type 2) into the brain after intraocular injection, Brain Res 69:189-201.

Kuypers HG, Bentivoglio M, van der Kooy D, Castman-Berrevoets CE. 1979. Retrograde transport of bisbenzimide and propidium iodide through axons to their parent cell bodies. Neurosci Lett 12:1-7.

Kuypers HG, Bentivoglio M, Castman-Berreveoets CE, Bharos AT. 1980. Double retrograde neuronal labeling through divergent axon collaterals, using two fluorescent tracers with the same excitation wavelength which label different features of the cell. Exp Brain Res 40:383-392.

Kuypers HG. Ugolini G. (1990) Viruses as transneuronal tracers. Trends Neurosci 13:71–75 .

Lakos S, Basbaum AI. 1986. Benzidine dihydrochloride as a chromogen for single- and double-label light and electron microscopic immunocytochemical studies. J Histochem Cytochem 34:1047-1056.

Lanciego JL, Wouterlood FG. 1994. Dual anterograde axonal tracing with *Phaseolus vulgaris* leucoagglutinin (PHA-L) and biotinylated dextran amine (BDA). Neurosci Prot 94-050-06-01-13.

Lanciego JL, Wouterlood FG. 2006. Multiple neuroanatomical tract-tracing: approaches for multiple tract tracing. In: Zaborszky L, Wouterlood FG, Lanciego JL (Eds) Neuroanatomical Tract-Tracing 3: Molecules, Neurons, and Systems, New York: Springer, pp. 336-365.

Lanciego JL, Goede PH, Witter MP, Wouterlood FG. 1997. Use of peroxidase substrate Vector VIP for multiple staining in light microscopy. J Neurosci Meth 74:1-7.

Lanciego JL, Wouterlood FG, Erro E, Giménez-Amaya JM. 1998a. Multiple axonal tracing: simultaneous detection of three tracers in the same section. Histochem Cell Biol. 110:509-515.

Lanciego JL, Luquin MR, Guillén J, Giménez-Amaya JM. 1998b. Multiple neuroanatomical tracing in primates. Brain Res Prot 2:323-332.

Lanciego JL, Wouterlood FG, Erro E, Arribas J, Gonzalo N, Urra X, Cervantes S, Giménez-Amaya JM. 2000. Complex brain circuits studied via simultaneous and permanente detection of three transported neuroanatomical tracers in the same histological section. J Neurosci Meth 103:127-135.

Lanciego JL, Gonzalo N, Castle M, Sánchez-Escobar C, Aymerich MS, Obeso JA. 2004. Thalamic innervation of striatal and subthalamic neurons projecting to the rat entopeduncular nucleus. Eur J Neurosci 19:1267-1277.

Lapper SR, Bolam JP. 1991. The anterograde and retrograde transport of neurobiotin in the central nervous system of the rat: comparison with biocytin. J Neurosci Meth 39:163-174.

LaVail JH, LaVail MM. 1972. Retrograde axonal transport in the central nervous system. Science 176:1416-1417.

Lázár G. 1978. Application of cobalt-filling technique to show retinal projections in the frog. Neuroscience 3:725-736.

Lei W, Jiao Y, Del Mar N, Reiner A. 2004. Evidence for differential cortical input to direct pathway versus indirect pathway striatal projection neurons in rats. J Neurosci 24:8289-8299.

Li D, Seeley PJ, Bliss TVP, Raisman G. 1990. Intracellular injection of biocytin into fixed tissue and its detection with avidin-HRP. Neurosci Lett Suppl 38:581.

Lichtman JW, Livet J, Sanes JR. 2008. A technicolour approach to the connectome. Nat. Rev. Neurosci. 9: 417–422.

Liu WL, Behbehani MM, Shipley MT. 1993. Intracellular filling in fixed brain slices using Miniruby, a fluorescent biocytin compound. Brain Res 608:78-86.

Ljungdahl A, Hökfelt T, Goldstein M, Park D. 1975. Retrograde peroxidase tracing of neurons combined with transmitter histochemistry. Brain Res 84:313-319.

López lP, Salin P, Kachidian P, Barroso-Chinea P, Rico AJ, Gómez-Bautista V, Conte-Perales L, Coulon P, Kerkerian-Le Goff L, Lanciego JL. 2010. The added value of rabies virus as a retrograde tracer when combined with dual anterograde tract-tracing. J Neurosci Meth 194:21-27.

Lübke J. 1993. Photoconversion of diaminobenzidine with different fluorescent neuronal markers into a light and electron microscopic dense reaction product. Microsc Res Tech 24: 2–14.

Luppi PH, Fort P, Jouvet M. 1990. Iontophoretic application of unconjugated choleratoxin B subunit (CTB) combined with immunohistochemistry of neurochemical substances: a method for transmitter identification of retrogradely labeled neurons. Brain Res 534:209-224.

Lyckman AW, Fan G, Rios M, Jaenisch R, Sur M. 2005. Normal eye-specific patterning of retinal inputs to murine subcortical visual nuclei in the absence of brain-derived neurotrophic factor. Vis Neurosci 22:27-36.

Maranto A. 1982. Neuronal mapping: a photooxidation reaction makes Lucifer Yellow useful for electron microscopy. Science 217: 953–955.

Matesz C. 1994. Synaptic relations of the trigeminal motoneurons in a frog (Rana esculenta). Eur J Morphol 32:117-121.

Matsubayashia Y, Iwai L, Kawasakia H. 2008. Fluorescent double-labeling with carbocyanine neuronal tracing and immunohistochemistry using a cholesterol-specific detergent digitonin. J Neurosci Meth 174:71-81.

Mauro A, Germano I, Giaccone G, Giordana MT, Schiffer D. 1985. 1-Naphthol basic dye (1-NBD), an alternative to diaminobenzidine (DAB) in immunoperoxidase techniques. Histochemistry 83:97-102.

Mesulam, MM. 1982. Principles of horseradish peroxidase neurochemistry and their applications for tracing neural pathways-axonal transport, enzyme histochemistry and light microscopic analysis In Mesulam MM, Ed., Tracing Neural Connections with Horseradish Peroxidase; IBRO Handbook Series: Methods in the Neurosciences, pp. 1-551, Wiley, NY, USA.

Mesulam MM, Mufson EJ. 1982. The rapid anterograde transport of horseradish peroxidase. Neuroscience 5:1277-1286.

Molnár Z, Blakey DL, Bystron I, Carney RSE. 2006. Tract-tracing in developing systems and in postmortem human material using carbocyanine dyes. In: Zaborszky L, Wouterlood FG, Lanciego JL (Eds) Neuroanatomical Tract-Tracing 3: Molecules, Neurons, and Systems, New York: Springer, pp. 366-393.

Morecraft RJ, Herrick JL, Stilwell-Morecraft KS, Louie JL, Schroeder CM, Ottenbacher JG, Schoolfield MW. 2002. Localization of arm representation in the corona radiata and internal capsule in the non-human primate. Brain 125:176-198.

Morecraft RJ, Ugolini G, Lanciego JL Wouterlood FG, Pandya DN. 2009. Classic and contemporary neural tract tracing techniques. In: Johansen-Berg H, Behrens T. (eds) Diffusion MRI: from quantitative measurement to in-vivo neuroanatomy. Oxford University Press., p. 273-308.

Mufson EJ, Brady DR, Kordower JH. 1990. Tracing neuronal connections in postmortem human hippocampal complex with the carbocyanine dye DiI. Neurobiol Aging 11:649-653.

Nance DM, Burns J. 1990. Fluorescent dextrans as sensitive anterograde neuroanatomical tracers: applications and pitfalls. Brain Res Bull 25:139-145.

Nassi JJ, Callaway EM. 2006. Specialized circuits relying primate parallel visual pathways to the middle temporal area. J Neurosci 26:12789-12798.

Nauta WJ.1952. Selective silver impregnation of degenerating axons in the central nervous system. Stain Technol. 27:175-179.

Neely MD, Stanwood GD, Deutch AY. 2009. Combination of diOlistic labeling with retrograde tract tracing and immunohistochemistry. J Neurosci Meth 184:332-336.

Ohara S, Inoue K, Witter MP, Iijima T. 2009. Untangling neural networks with dual retrograde transsynaptic viral infection. Front Neurosci. 15:344-349.

Olsson Y, Svensjö E, Arfors KE, Hultström D. 1975. Fluorescein labelled dextrans as tracers for vascular permeability studies in the nervous system. Acta Neuropathol. 33:45-50.

Omelchenko N, Sesack SR. 2009. Ultrastructural analysis of local collaterals of rat ventral tegmental area neurons: GABA phenotype and synapses onto dopamine and GABA cells. Synapse 63:895-906.

Orieux G, François C, Féger J, Yelnik J, Vila M, Ruberg M, Agid Y, Hirsch EC. 2000. Metabolic activity of excitatory parafascicular and pedunculopontine inputs to the subthalamic nucleus in a rat model of Parkinson's disease. Neuroscience 97:79-88.

Parent M, Parent A. 2007. The microcircuitry of primate subthalamic nucleus. Parkinsonism Relat Disord 13, Suppl 3:S292-5.

Pérez-Manso M, Barroso-Chinea P, Aymerich MS, Lanciego JL. 2006. "Functional" neuroanatomical tract-tracing: análisis of changes in gene expresión of brain circuits of interest. Brain Res 1072:91-98.

Pieribone VA, Aston-Jones G. 1988. The iontophoretic application of Fluoro-Gold for the study of afferents to deep brain nuclei. Brain Res 475:259-271.

Pinault D. 1996. A novel single-cell staining procedure performed in vivo under electrophysiological control: morpho-functional features of juxtacellularly labeled thalamic cells and other central neurons with biocytin or Neurobiotin. J Neurosci Meth 65:113-136.

Pitman RM, Tweedle CD, Cohen MJ. 1972. Branching of central neurons; ntracellular cobalt injection for light and electron-microscopy. Science 176:412-414.

Porreroa C, Rubio-Garridoa P, Avendañoa C, Clascá F. 2010. Mapping of fluorescent protein-expressing neurons and axon pathways in adult and developing Thy1-eYFP-H transgenic mice. Brain Research 1345:59-72.

Prensa L, Parent A. 2001.The nigrostriatal pathway in the rat: A single-axon study of the relationship between dorsal and ventral tier nigral neurons and the striosome/matrix striatal compartments. J Neurosci 21:7247-7260.

Ramón y Cajal, S. 1909-1911. Histologie du système nerveux de l'Homme et des vertébrés. 2 volumes. Maloine, Paris (facsimile reprint, 1972).

Raux H, Iseni F, Lafay F, Blondel D. 1997. Mapping of monoclonal antibody epitopes of the rabies virus P protein. J Gen Virol 78:119-124.

Reep RL, Baccala MJ, Booth MP, Goodwin GS. 1988. Combined retrograde and anterograde tracing of neuronal connections: Fluoro-Gold and autoradiography. J Neurosci Meth 23:1-5.

Reiner A, Honig MG. 2006. Dextran amines: versatile tools for anterograde and retrograde studies of nervous system connectivity. In: Zaborszky L, Wouterlood FG, Lanciego JL (Eds) Neuroanatomical Tract-Tracing 3: Molecules, Neurons, and Systems, New York: Springer, pp. 304-335.

Reiner A, Veenman CL, Honig MG (1993) Anterograde tracing using biotinylated dextran amine. Neurosci. Prot. 93, section 050-14.

Reiner A, Veenman CL, Medina L, Jiao Y, Del Mar N, Honig MG. 2000. Pathway tracing using biotinylated dextran amines. J Neurosci Meth 103:23-37.

Rho JH, Sidman RL. 1986. Intracellular injection of lucifer yellow into lightly fixed cerebellar neurons. Neurosci Lett 72:21-24.

Rice CD, Weber SA, Waggoner AL, Jessell ME, Yates BJ. 2010. Mapping of neural pathways that influence diaphragm activity and project to the lumbar spinal cord in cats. Exp Brain Res 203:205-211.

Richmond FJ, Gladdy R, Creasy JL, Kitamura S, Smits E, Thomson DB. 1994. Efficacy of seven retrograde tracers, compared in multiple-labelling studies of feline motoneurones. J Neurosci Meth 53:35-46.

Rico AJ, Barroso-Chinea P, Conte-Perales L, Roda E, Gómez-Bautista V, Gendive M, Obeso JA, Lanciego JL. 2010. A direct projection from the subthalamic nucleus to the ventral thalamus in monkeys. Neurobiol Dis 39:381-392.

Robertson B, Arvidsson J. 1985. Transganglionic transport of wheat germ agglutinin-HRP and choleragenoid-HRP in rat trigeminal primary sensory neurons. Brain Res 348:44-51.

Robertson B, Grant G. 1985. A comparison between wheat germ agglutinin- and choleragenoid-horseradish peroxidase as anterogradely transported markers in central branches of primary sensory neurons in the rat with some observations in the cat. Neuroscience 14:895-905.

Rooney D, Døving KB, Ravaille-Veron M, Szabo T. 1992. The central connections of the olfactory bulbs in cod, *Gadus morhua L*. J Hirnforsch 33:63-75.

Rosene DL, Roy NJ, Davis BJ. 1986. A cryoprotection method that facilitates cutting frozen sections of whole monkey brains for histological and histochemical processing without freezing artifact. J Histochem Cytochem. 34:1301-1315.

Roy I, Ohulchanskyy TY, Pudavar HE, Bergey EJ, Oseroff AR, Morgan J, Dougherty TJ, Prasad PN. 2003. Ceramic-based nanoparticles entrapping water-insoluble photosensitizing anticancer drugs: a novel drug-carrier system for photodynamic therapy. J Am Chem Soc. 125:7860-7865.

Ruigrok TJ, Hensbroek RA, Simpson JI. 2011. Spontaneous activity signatures of morphologically identified interneurons in the vestibulocerebellum. J Neurosci 31:712-224.

Salin P, Castle M, Kachidian P, Barroso-Chinea P, López IP, Rico AJ, Kerkerian-Le Goff L, Coulon P, Lanciego JL. 2008. High-resolution neuroanatomical tract-tracing for the analysis of striatal microcircuits.. Brain Res 1221:49-58.

Salin P, López IP, Kachidian P, Barroso-Chinea P, Rico AJ, Gómez-Bautista V, Coulon P, Kerkerian-Le Goff L, Lanciego JL. 2009. Changes to interneuron-driven striatal microcircuits in a rat model of Parkinson's disease. Neurobiol Dis 34:545-552.

Sandler R, Smith AD. 1991. Coexistence of GABA and glutamate in mossy fiber terminals of the primate hippocampus: an ultrastructural study. J Comp Neurol 303:177-192.

Saxena S, Caroni P. 2007. Mechanisms of axon degeneration: From development to disease. Progr Neurobiol 83:174–191.

Schmued LC, Fallon JH. 1986. Fluoro-Gold: a new fluorescent retrograde axonal tracer with numerous unique properties. Brain Res 377:147-54.

Schmued LC, Heimer L. 1990. Iontophoretic injection of Fluoro-Gold and other fluorescent tracers. J Histochem Cytochem 38:721-723.

Schmued L, Kyriakidis K, Heimer L. 1990. In vivo anterograde and retrograde axonal transport of the fluorescent rhodamine-dextran-amine, Fluoro-Ruby, within the CNS. Brain Res 526:127-134.

Schwab ME, Javoy-Agid F, Agid Y. 1978. Labeled wheat germ agglutinin (WGA) as a new, highly sensitive retrograde tracer in the rat hippocampal system. Brain res 152:145-150.

Schwab ME, Agid I. 1979. Labeled wheat germ agglutinin and tetanus toxin as highly sensitive retrograde tracers in the CNS: the afferent fiber connections of the rat nucleus accumbens. Int J Neurol 13:117-126.

Shink E, Bevan MD, Bolam JP, Smith Y. 1996. The subthalamic nucleus and the external pallidum: two tightly interconnected structures that control the output of the basal ganglia in the monkey. Neuroscience 73:335-357.

Sidibé M, Smith Y. 1996. Differential synaptic innervation of striatofugal neurons projecting to the internal or external segments of the globus pallidus by thalamic afferents in the squirrel monkey. J Comp Neurol 365:445-465.

Skirboll L, Hökfelt T, Norell G, Phillipson O, Kuypers HG, Bentivoglio M, Catsman-Berrevoets CE, Visser TJ, Steinbusch H, Verhofstad A, et al. 1984. A method for specific transmitter identification of retrogradely labelled neurons: immunofluorescence combined with fluorescence tracing. Brain Res 320:99-127.

Smith Y, Bolam JP. 1991. Convergence of synaptic inputs from the striatum and the globus pallidus onto identified nigrocollicular cells in the rat: a double anterograde labeling study. Neuroscience 44:45-73.

Smith Y, Bolam JP. 1992. Combined approaches to experimental neuroanatomy: combined tracing and immunocytochemical techniques for the study of neuronal microcircuits. In: Bolam JP, Ed. Experimental Neuroanatomy, A Practical Approach, pp. 239-266, Oxford University Press, Oxford, UK.

Somogyi P, Smith AD. 1979. Projection of neostriatal spiny neurons to the substantia nigra. Application of a combined Golgi-staining and horseradish peroxidase transport procedure at both light and electron microscopic levels. Brain Res. 178:3-15.

Somogyi P, Hodgson AJ, Smith AD. 1979. An approach to tracing neuron networks in the cerebral cortex and basal ganglia. Combination of Golgi staining, retrograde transport of horseradish peroxidase and anterograde degeneration of synaptic boutons in the same material. Neuroscience. 4:1805-1852.

Somogyi P, Freund TF, Hodgson AJ, Somogyi J, Beroukas D, Chubb IW. 1985. Identified axo-axonic cells are immunoreactive for GABA in the hippocampus and visual cortex of the cat. Brain Res 332:143-149.

Spiga S, Puddu MC, Pisano M, Diana M. 2005. Morphine withdrawal-induced morphological changes in the nucleus accumbens. Eur J Neurosci 22:2332-2340.

Spiga S, Acquas E, Puddu MC, Mulas G, Lintas A, Diana M. 2011. Simultaneous Golgi-Cox and immunofluorescence using confocal microscopy. Brain Struct Funct, *in press*.

Stewart WW. 1982. Lucifer dyes-highly fluorescent dyes for biological tracing. Nature 292:17-21.

Strack AM, Loewy AD. 1990. Pseudorabies virus: a highly specific transneuronal cell body marker in the sympathetic nervous system. J Neurosci 10:2139-2147.

Strick Pl, Card JP. 1992. Transneuronal mapping of neural circuits with alpha herpesviruses. in: Bolam JP (Ed) Experimental neuroanatomy, a practicakl approach. oxford University press, pp 81-101.

Swanson LW. 1981. Tracing central pathways with the autoradiographic method. J Histochem Cytochem 29:117-124

Szabadics J, Varga C, Brunner J, Chen K, Soltesz I. 2010. Granule cells in the CA3 area. J Neurosci. 30:8296-8307.

Taghert PH, Bastiani MJ, Ho RK, Goodman CS. 1982. Guidance of pioneer growth cones: filopodial contacts and coupling revealed with an antibody to Lucifer Yellow. Dev Biol 94:391-399.

Taverna S, van Dongen YC, Groenewegen HJ, Pennartz CM. 2004. Direct physiological evidence for synaptic connectivity between medium-sized spiny neurons in rat nucleus accumbens in situ. J Neurophysiol 91:1111-1121.

Thomas MA, Lemmer B. 2005. HistoGreen: a new alternative to 3.3'-diaminobenzidine-tetrahydrochloride-dihydrate (DAB) as a peroxidase substrate in immunohistochemistry? Brain Res Prot 14:107-118.

Thompson RH, Swanson LW. 2010. Hypothesis-driven structural connectivity: analysis supports network over hierachical model of brain architecture. Proc Natl Acad Sci 34:15235-15239.

Tóth P, Lázár G, Wang SR, Li TB, Xu J, Pál E, Straznicky C. 1994. The contralaterally projecting neurons of the isthmic nucleus in five anuran species: a retrograde tracing study with HRP and cobalt. J Comp Neurol 346:306-320.

Trojanowski JQ, Gonatas JO, Gonatas NK. 1981. Conjugates of horseradish peroxidase (HRP) with cholera toxin and wheat germ agglutinin are superior to free HRP as orthograde transported markers. Brain res 223:381-385.

Trojanowski JQ, Gonatas JO, Steiber A, Gonatas NK. 1982. Horseradish peroxsidase (HRP) conjugates of cholera toxin and lectins are more sensitive retrograde transported markers than free HRP. Brain res 231:33-50.

Trojanowski JQ. 1983. Native and derivatized lectins for in vivo studies of neuronal connectivity and neuronal cell biology. J Neurosci Meth 9:185-204.

Ugolini G. 1995. Specificity of rabies virus as a transneuronal tracer of motor networks: transfer from hypoglossal motoneurons to connected second-order and higher order central nervous system cell groups. J Comp Neurol 356:457-480.

Ugolini G (2008) Use of rabies virus as a transneuronal tracer of neuronal connections: implications for the understanding of rabies pathogenesis. In: Dev Biol (Cazel) (Dodet B, Hooks AR, M ü ller T, Tordo N, Scientific & Technical Department of the OIE, eds), pp. 493 — 506. Basel: Karger.

Ugolini G. 2010. Advances in viral transneuronal tracing. J Neurosci Meth 194:2-20.

Ugolini G, Kuypers HG. 1986. Collaterals of corticospinal and pyramidal fibers to the pontine gray demonstrated by a new application of the fluorescent fibre labeling technique. Brain Res 365:211-227.

van der Kooy D, Steinbusch HWM. 1980. Simultaneous fluorescent retrograde axonal tracing and immunofluorescent characterization of neurons. J Neurosci Res 5:479–484.

Vázquez-Borsetti P, Cortés R, Artigas F. 2009. Pyramidal neurons in rat prefrontal cortex projecting to ventral tegmental area and dorsal raphe nuclei express 5-HT2A receptors. Cereb Cortex 19:1678-1686.

Veenman CL, Reiner A, Honig MG. 1992. Biotinylated dextran amine as an anterograde tracer for single- and double-label studies. J Neurosci Meth 41:239-254.

von Bartheld CS, Cunningham DE, Rubel EW. 1990. Neuronal tracing with DiI: decalcification, cryosectioning, and photoconversion for light and electron microscopic analysis. J Histochem Cytochem 38:725-733.

von Monakow C. 1897. Gehirnpathologie. A. Hölder, Vienna.

von Waldeyer-Hartz HWG 1891. Ueber einige neuere Forschungen im Gebiete der Anatomie des Centralnervensystems. Deutsche medizinische Wochenschrift, Berlin, 17: 1213-1218, 1244-1246, 1287-1289, 1331-1332, 1350-1356.

Waller A. 1850. Experiments on the sections of glossopharyngeal and hypoglossal nerves of the frog and observations of the alterations produced thereby in the structure of their primitive fibers. Phil Trans R Soc Lond 140, 423–429.

Wan XS, Trojanowski JQ, Gonatas JO, Liu CN. 1982. Cytoarchitecture of the extranuclear and commissural dendrites of hypoglossal nucleus neurons as revealed by conjugates of horseradish peroxidase with cholera toxin. Exp Neurol 78:167-175.

Wedeen VJ, Hagmann P, Tseng WY, Reese TG, Weisskoff RM. 2005. Mapping complex tissue architecture with diffusion spectrum magnetic resonance imaging. Magn Reson Med 54:1377-1386.

Wessendorf MW. 1990 Characterization and use of multi-color fluorescence microscopic techniques. In: Handbook of Chemical Neuroanatomy, vol. 8 (Eds A. Björklund, T Hökfelt, FG Wouterlood, AN van der Pol), pp.1-45. Amsterdam, Elsevier.

Wiesendanger M. 2006. Constantin von Monakow (1853–1930): A pioneer in interdisciplinary brain research and a humanist. C. R. Biol.329:406–418.

Wiśniewski HM, Ghetti B, Horoupian DS. 1972. The fate of synaptic membranes of degenerating optic nerve terminals, and their role in the mechanism of trans-synaptic changes. J Neurocytol 1:297-310.

Wouterlood FG. 1992. Techniques for converting Golgi precipitate in CNS neurons into stable electron microscopic markers. Microsc Res Tech. 23:275-288.

Wouterlood FG, Mugnaini E. 1984. Cartwheel neurons of the dorsal cochlear nucleus. A Golgi electron microscopic study in the rat. J Comp Neurol 227:136-157.

Wouterlood FG, Groenewegen HJ. 1985. Neuroanatomical tracing by use of *Phaseolus vulgaris*-leucoagglutinin (PHA L): Electron microscopy of PHA L filled Neuronal Somata, Dendrites, Axons and Axon Terminals. Brain Research 326:188 191.

Wouterlood FG, Jorritsma-Byham B. 1993. The anterograde neuroanatomical tracer biotinylated dextran amine: comparison with the tracer PHA-L in preparations for electron microscopy. J Neurosci Meth 48:75-87.

Wouterlood FG, Bol JGJM, Steinbusch HWM. 1987. Double- label immunocytochemistry: Combination of anterograde neuroanatomical tracing with *Phaseolus vulgaris*-leucoagglutinin and enzyme immunocytochemistry of target neurons. J. Histochem. Cytochem. 35: 817-823.

Wouterlood FG, Goede PH, Arts MPM, Groenewegen HJ. 1992. Simultaneous characterization of efferent and afferent connectivity, neuroactive substances and morphology of neurons. J. Histochem. Cytochem. 40:457-465.

Wouterlood FG, van Haeften T, Eijkhoudt M, Baks-te-Bulte L, Goede PH, Witter MP. (2004) Input from the presubiculum to dendrites of layer-V neurons of the medial entorhinal cortex of the rat. Brain Res1013:1-12.

Wouterlood FG, Boekel AJ, Meijer GA, Beliën JAM. 2007. Computer assisted estimation in the CNS of 3D multimarker overlap or touch at the level of individual nerve endings. A confocal laser scanning microscope application. J. Neurosci. Res. 85:1215-1228.

Wouterlood FG, Boekel AJ, Kajiwara R, Beliën JAM. 2008. Counting contacts between neurons in 3D in confocal laser scanning images. J. Neurosci Meth.171:296-308.

Wu Y, Richard S, Parent A. 2000. The organization of the striatal output system: a single-cell juxtacellular labeling study in the rat. Neurosci Res 38:49-62.

Zhang J, Zhang AJ, Wu SM. 2006. Immunocytochemical analysis of GABA-positive and calretinin-positive horizontal cells in the tiger salamander retina. J. Comp. Neurol. 499:432-441.

Zhou M, Grofova I. 1995. The use of peroxidase substrate Vector VIP in electron microscopic single and double antigen localization. J Neurosci Meth 62:149-158.

***Detailed Response to Reviewers**

REVIEWER #1:

- Boxes 2-4 were somewhat reduced to emphasize strengths/weaknesses/characteristics

REVIEWER #2:

- Issues dealing with the retrograde transport of BDA 3 kD are now better documented in section 2.1. as well as throughout the manuscript.
- The same also applies to the advantages of collateral transport of BDA
- Minor issues all fixed
- The accompanying cartoon in Fig. 2 has been removed and the figure legend changed accordingly.

REVIEWER #3:

- Reference of Skirboll et al. (1984) now added

Cartoon 1

Click here to download high resolution image

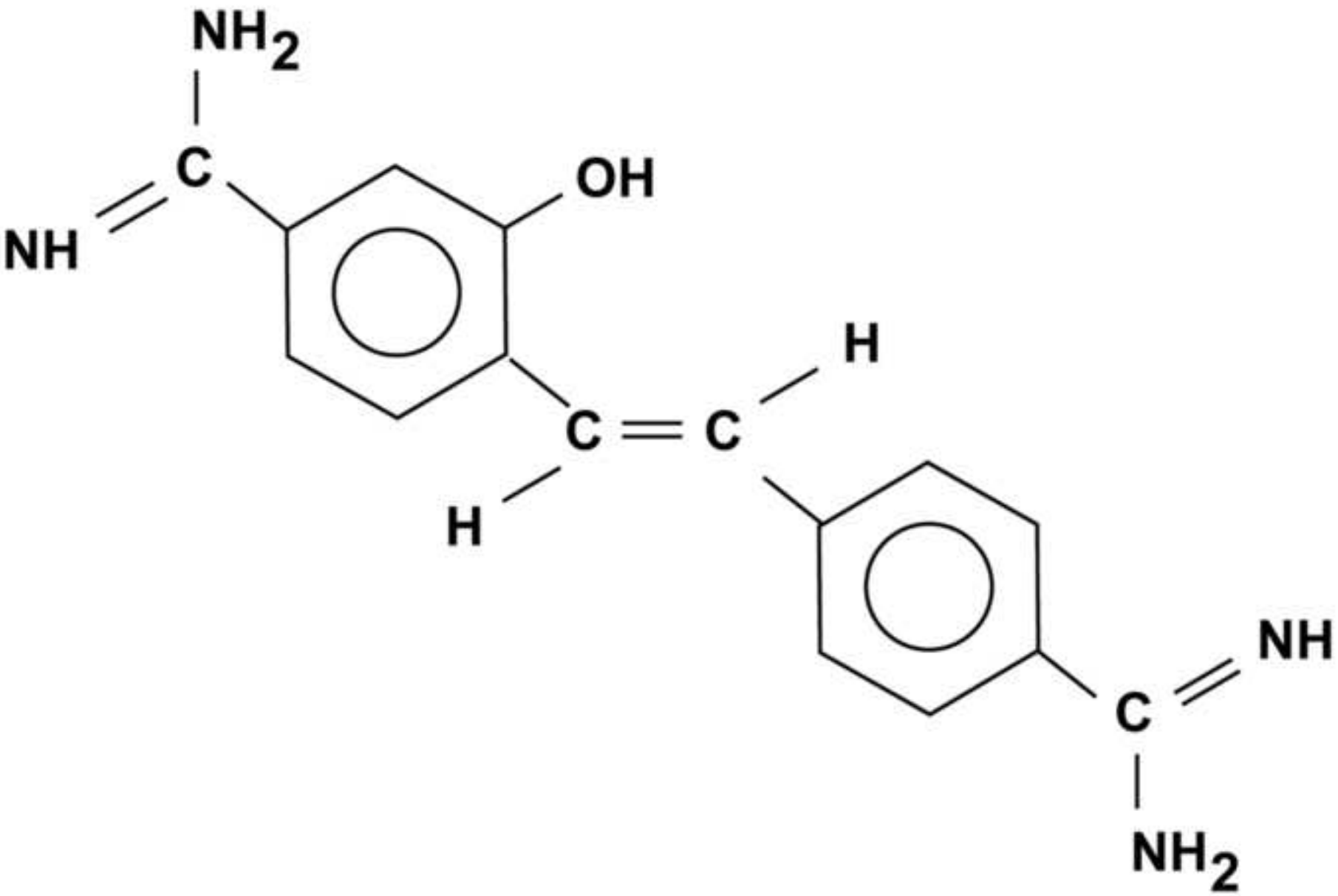

Cartoon 2

Click here to download high resolution image

Peroxidase substrate	Color	Comments
Tetramethylbenzidine (TMB)	Dark blue	Own electron-dense texture Difficult to combine with other chromogens Presumed carcinogenic
Diaminobenzidine (DAB)	Brown	Incubation time of 10-40 min Own electron-dense texture Presumed carcinogenic Compatible with DAB-Ni, BHDC, V-VIP and HGR
Nickel-enhanced DAB (DAB-Ni)	Black	Incubation time of 5-10 min Strongest chromogen Presumed carcinogenic Compatible with DAB, BHDC, V-VIP and HGR
Benzidine dihydrochloride (BHDC)	Blue	Own electron-dense texture Presumed carcinogenic Compatible with DAB-Ni and DAB
Vector very intense purple (V-VIP)	Purple	Incubation time of 3-5 min Own electron-dense texture (see Figure 4) Presumed non-carcinogenic Compatible with DAB-Ni and DAB Soluble in ethanol
1-Naphthol/azur B	Blue-green	Non electron-dense Compatible with DAB-Ni and DAB Fading over time
HistoGreen (HGR)	Green	Incubation time of 1-5 min Presumed non-carcinogenic Soluble in ethanol Compatible with DAB-Ni and DAB So far, electron-dense texture not reported

Cartoon 3

Click here to download high resolution image

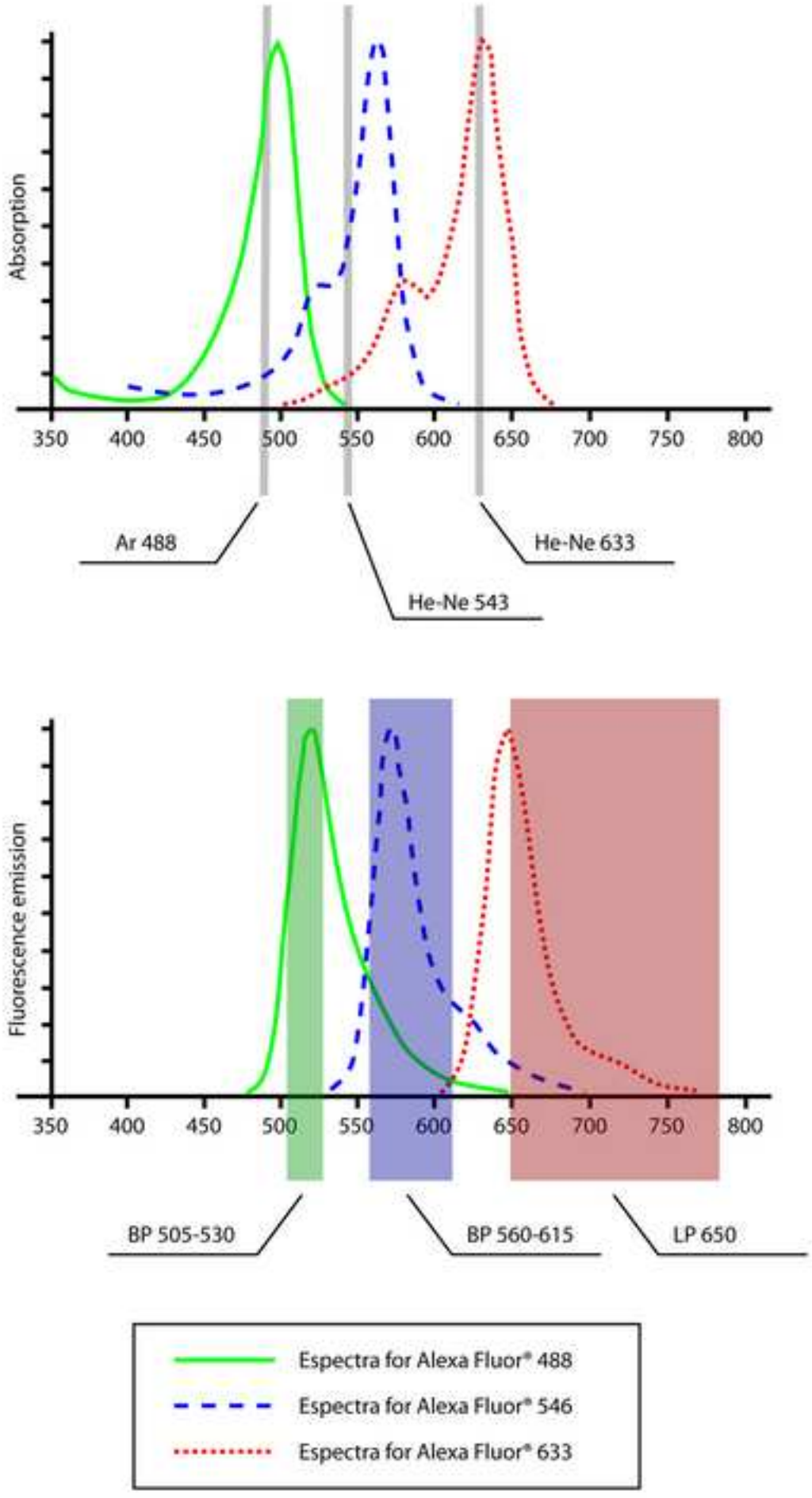

Figure 1

Click here to download high resolution image

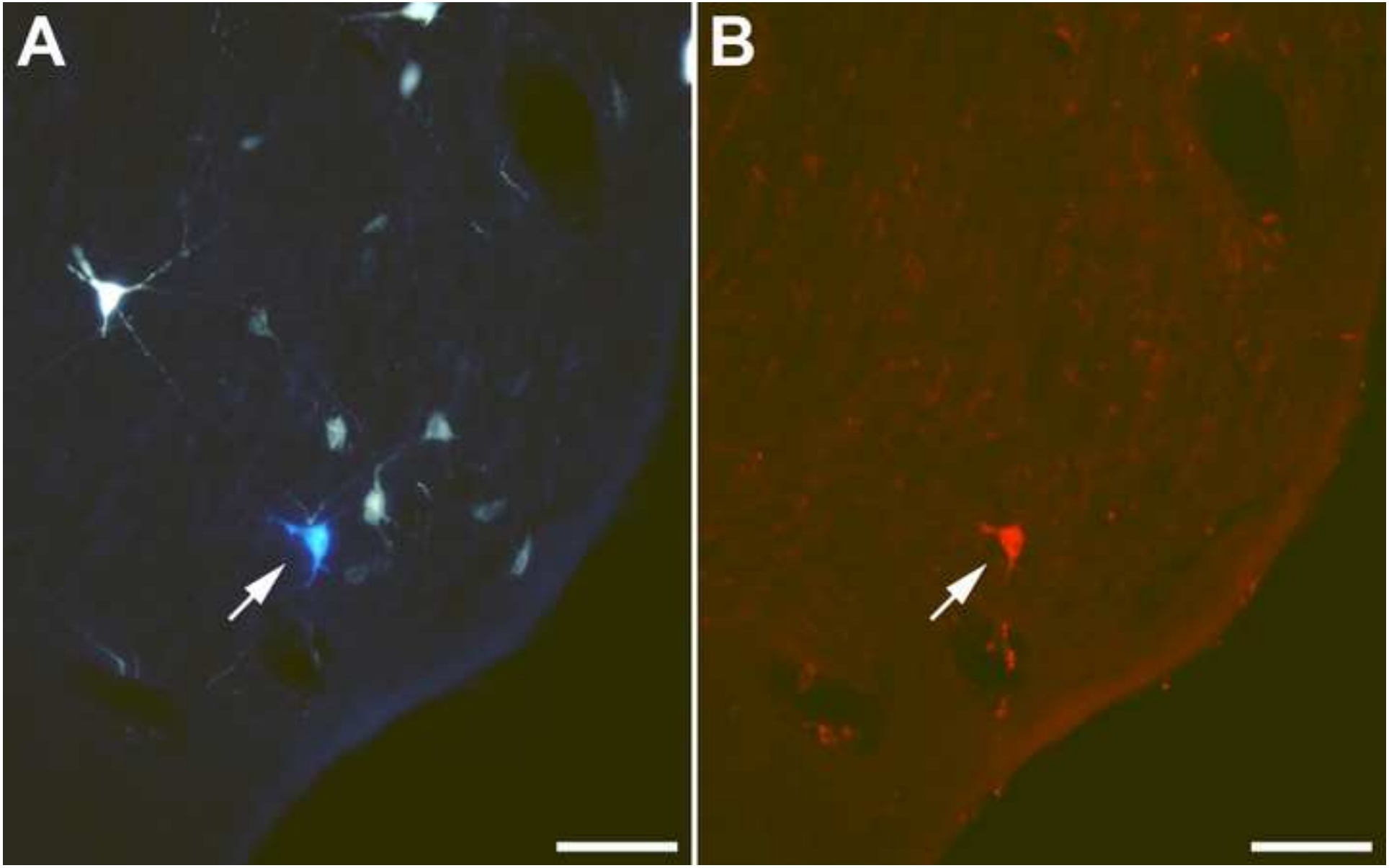

Figure(s)

Click here to download high resolution image

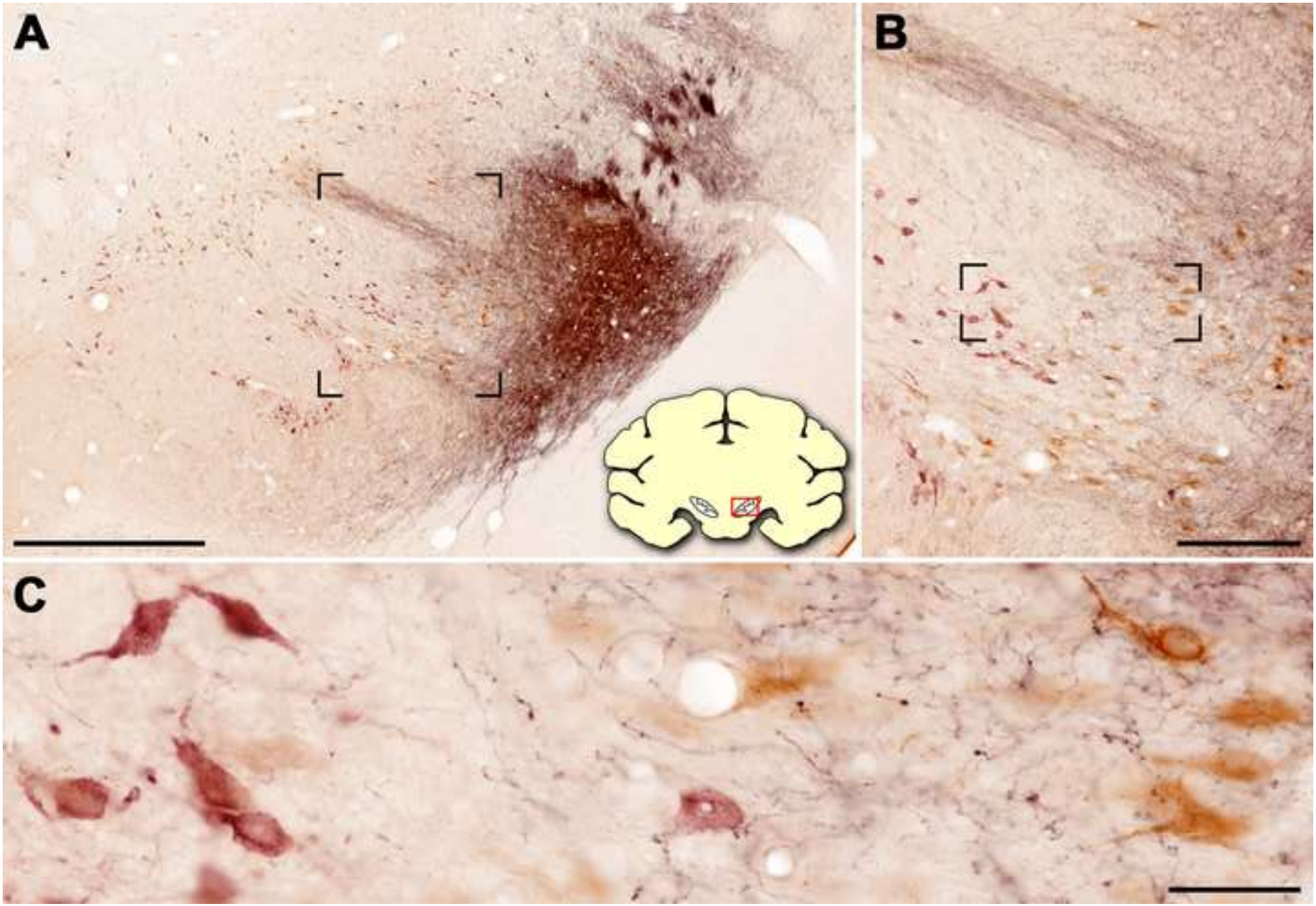

Figure 3

Click here to download high resolution image

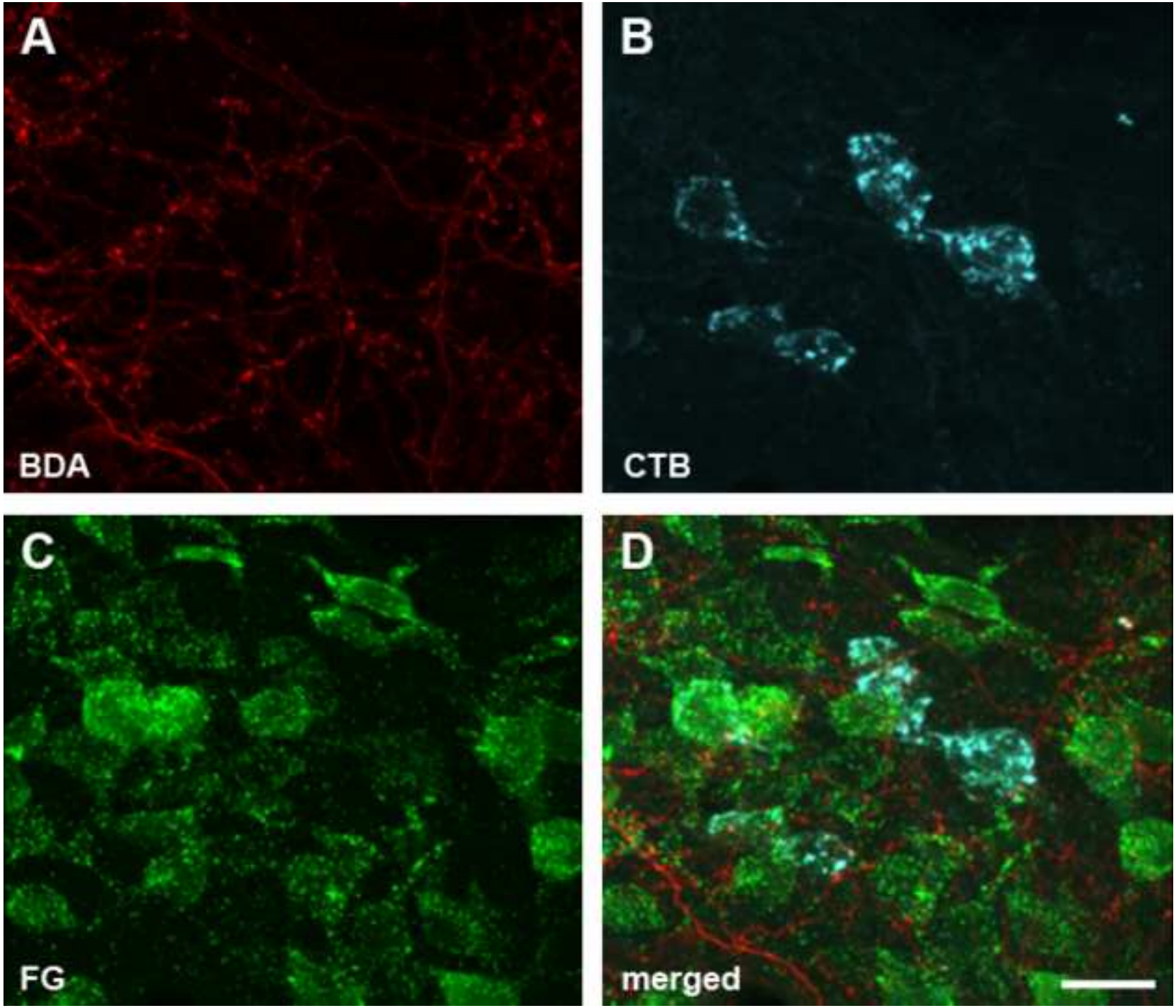

Figure 4

Click here to download high resolution image

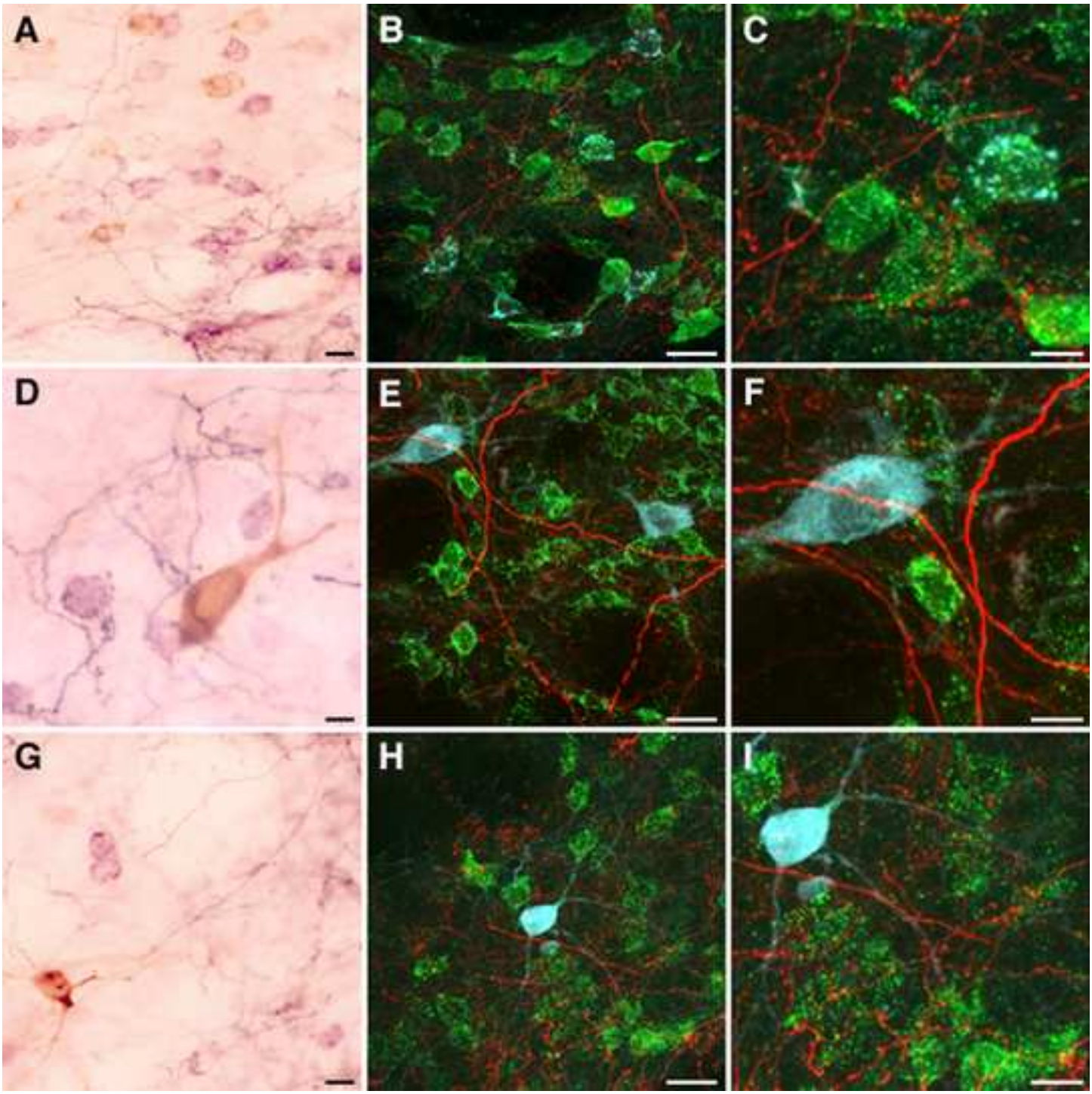

Figure 5

Click here to download high resolution image

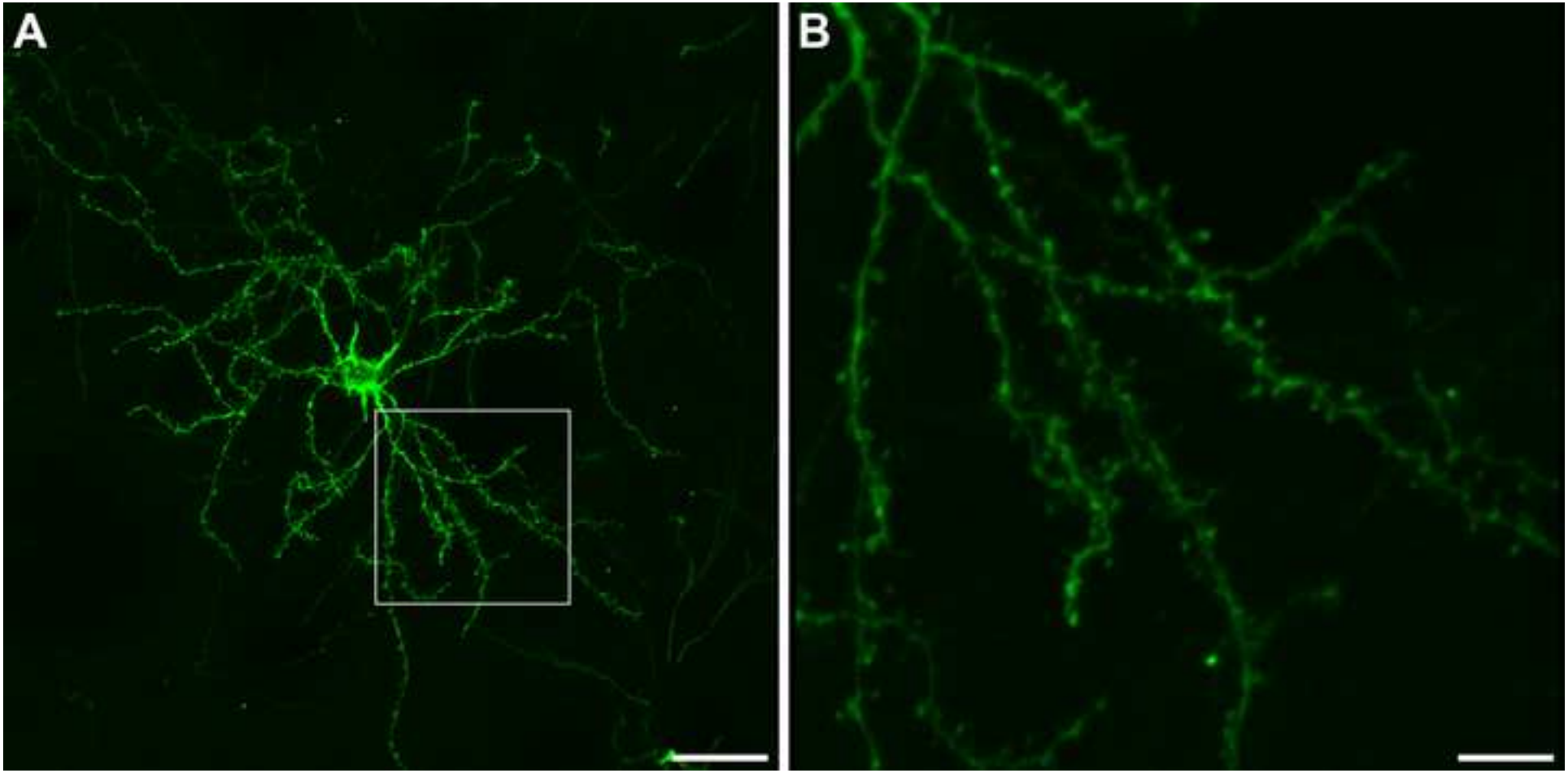

Figure 6

Click here to download high resolution image

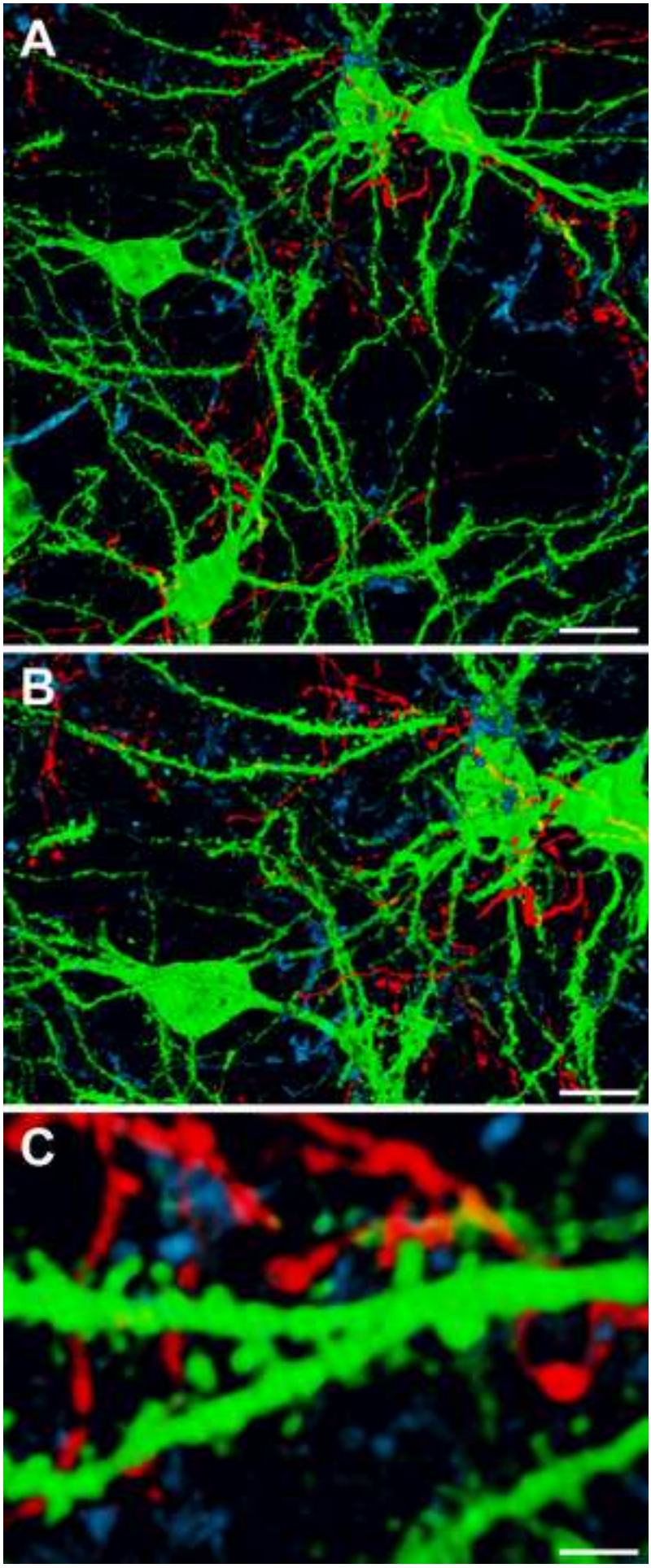

Figure 7

Click here to download high resolution image

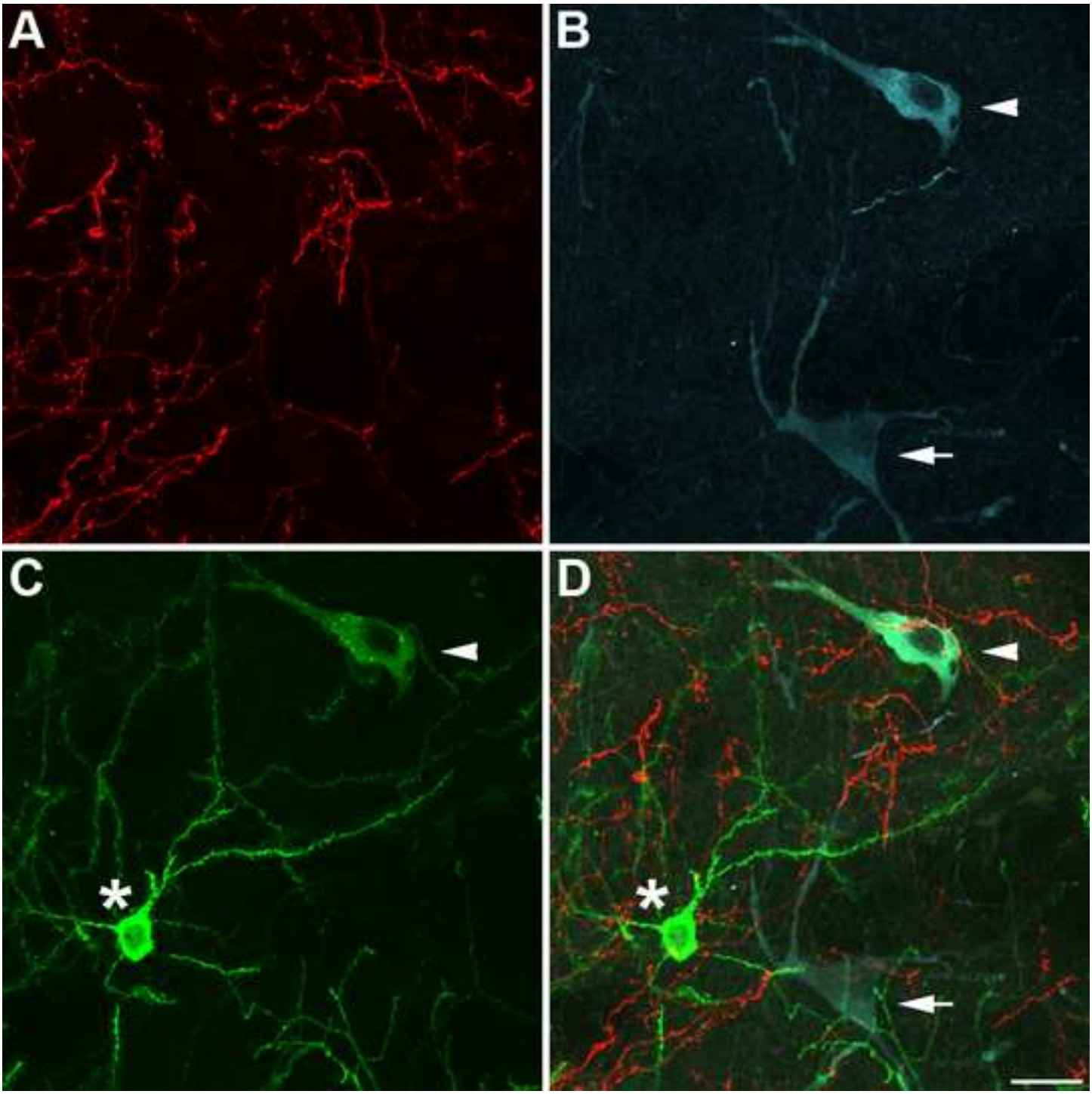

Figure 8

Click here to download high resolution image

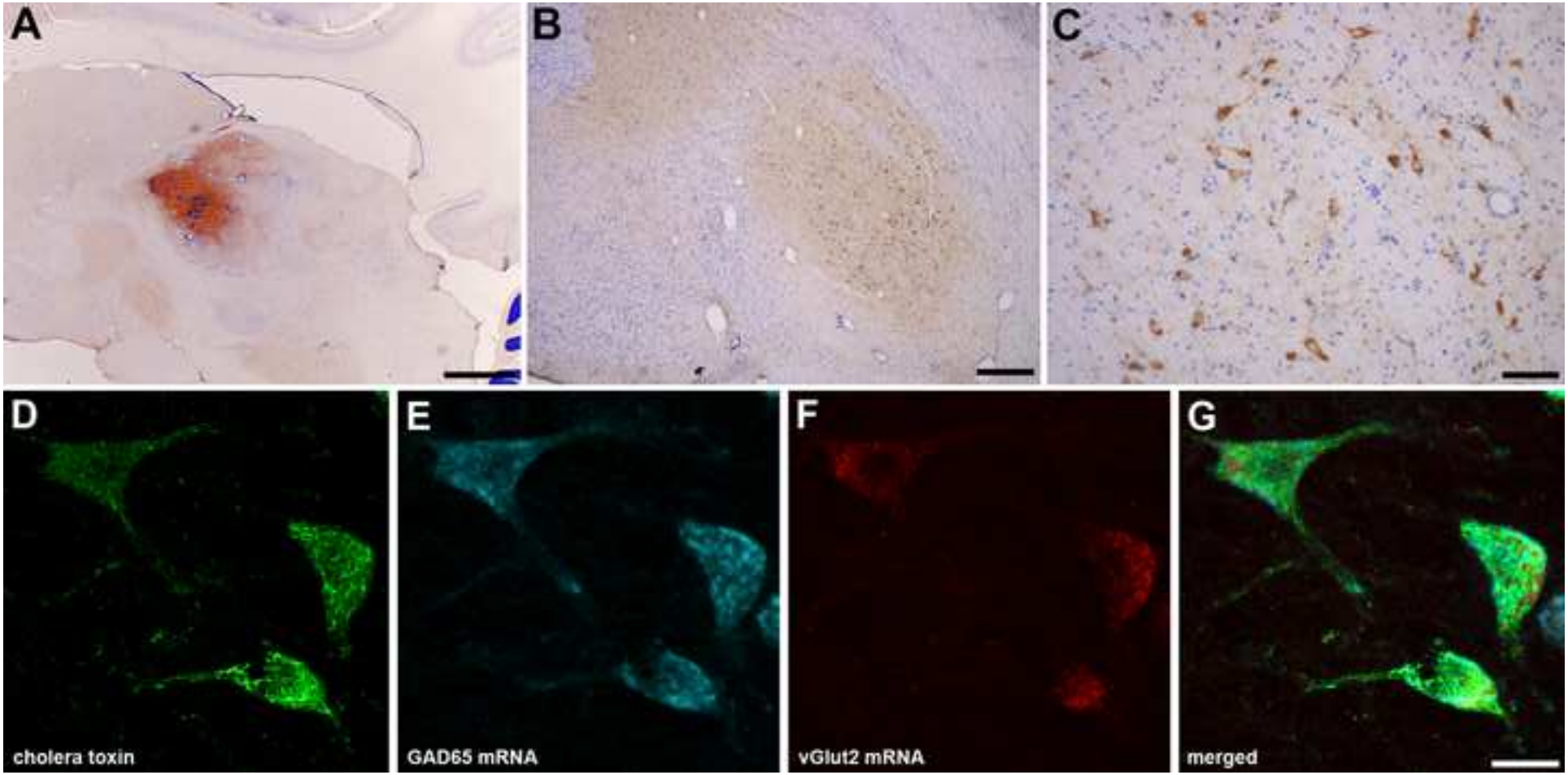

Figure 9

Click here to download high resolution image

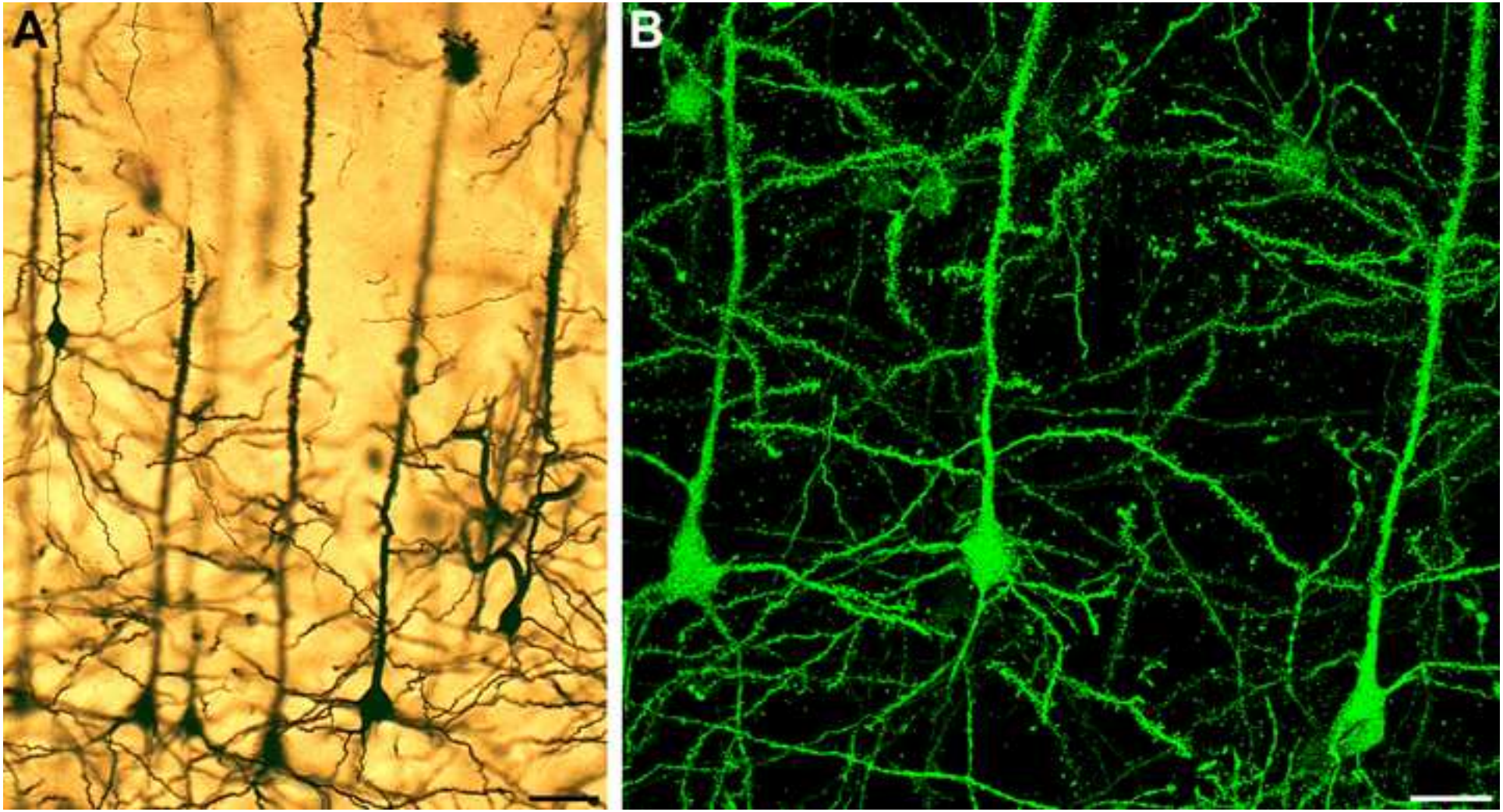

Figure 10

Click here to download high resolution image

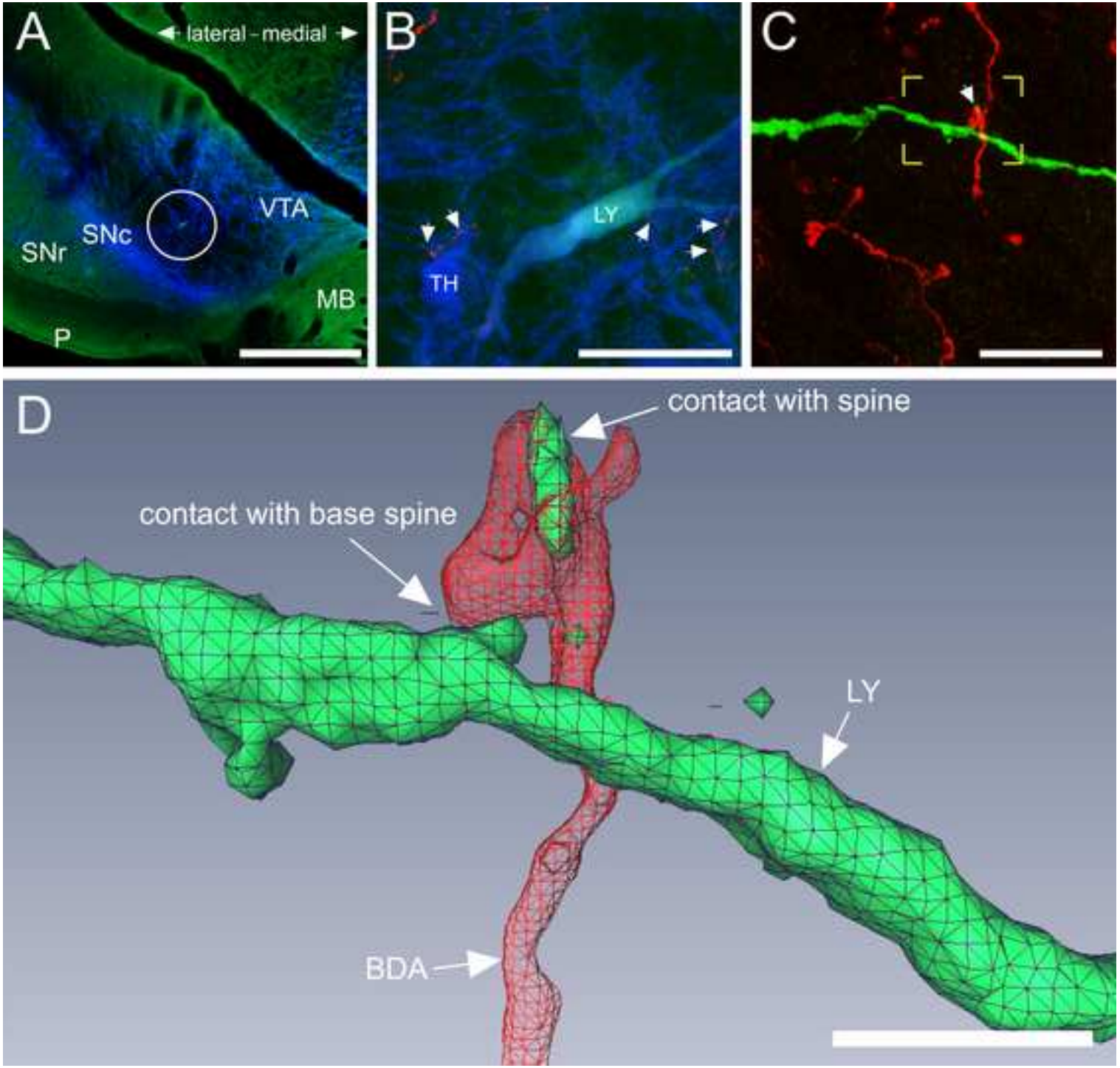

Figure 11

Click here to download high resolution image

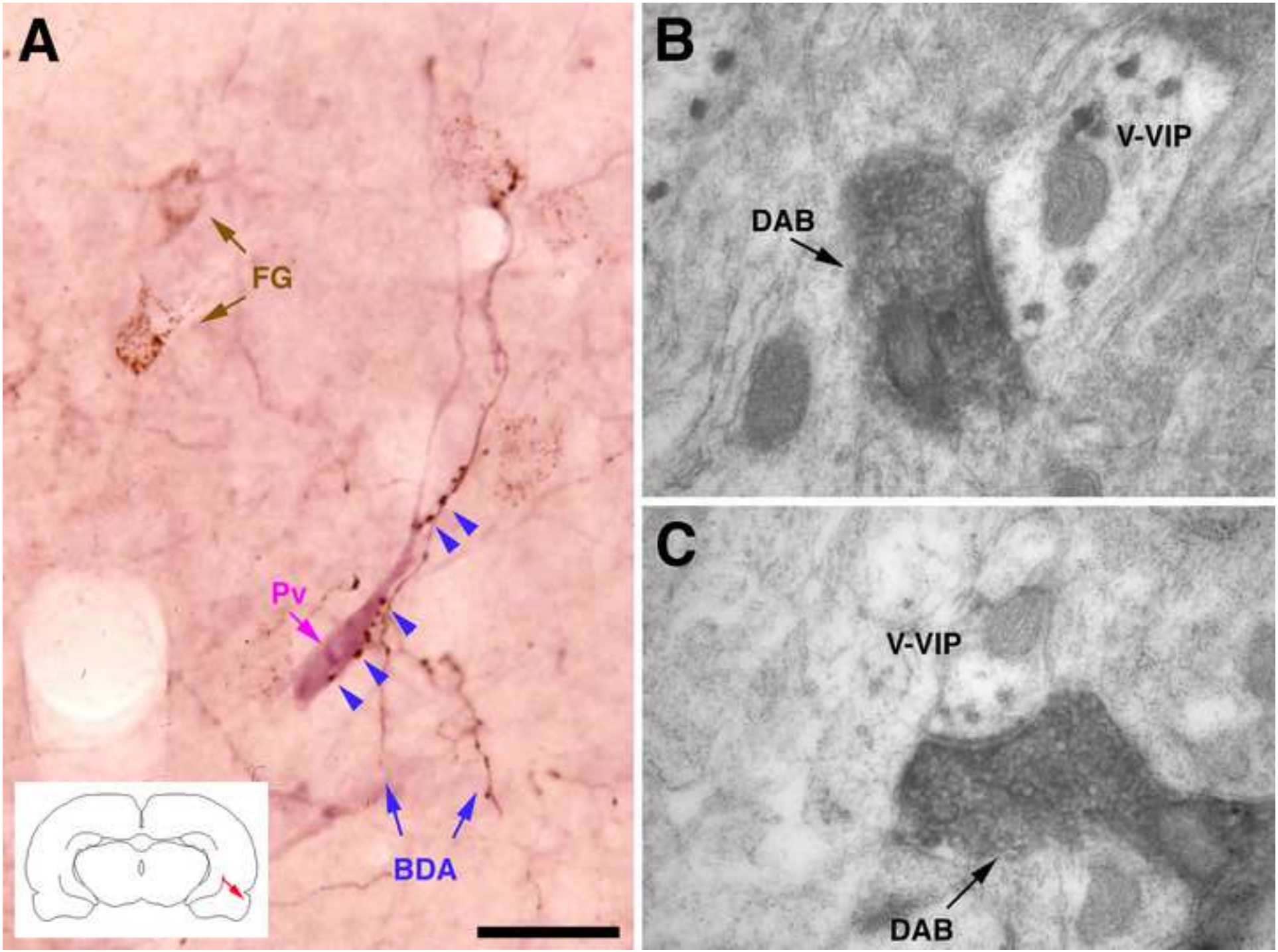

Figure 12

Click here to download high resolution image

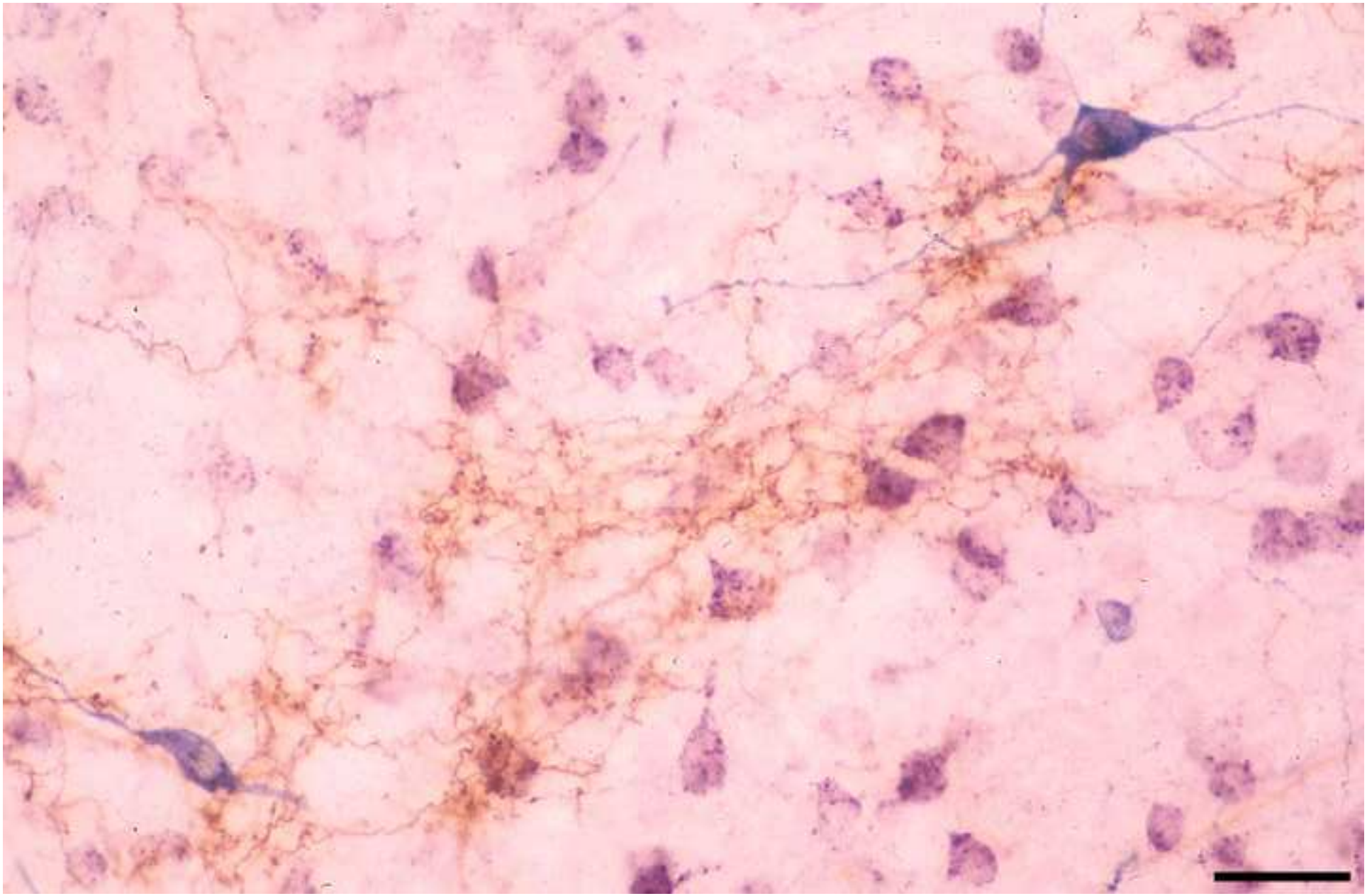

Figure 13

Click here to download high resolution image

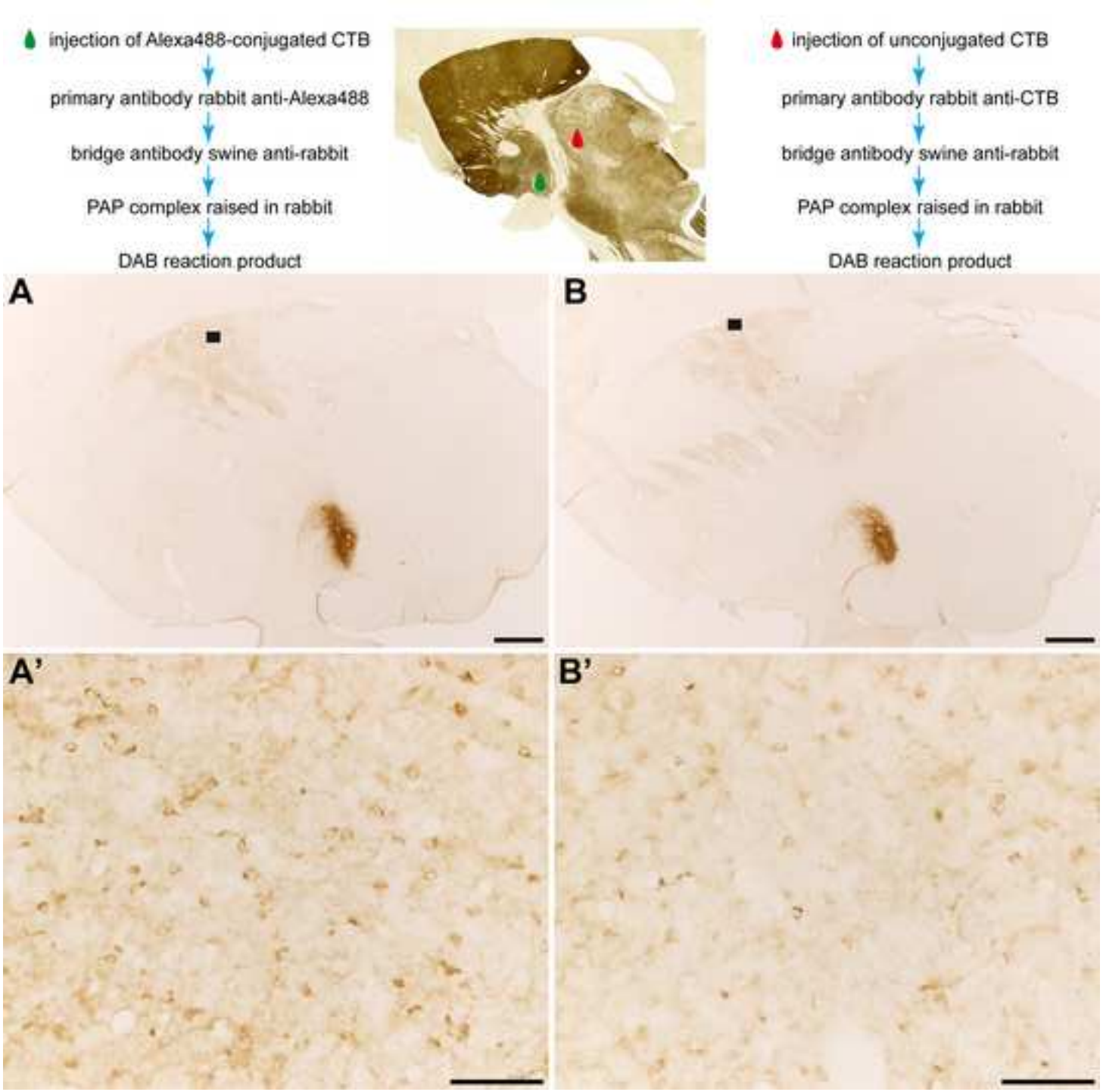

***Author Agreement**

We the undersigned declare that this manuscript is original, has not been published before and is not currently being considered for publication elsewhere.

We confirm that the manuscript has been read and approved by all named authors and that there are no other persons who satisfied the criteria for authorship but are not listed. We further confirm that the order of authors listed in the manuscript has been approved by all of us.

We understand that the Corresponding Author is the sole contact for the Editorial process. He/she is responsible for communicating with the other authors about progress, submissions of revisions and final approval of proofs.

Signed by all authors as follows:

Floris G Wouterlood (corresponding author)
José L. Lanciego (co-author)